Differential Effects of Niacin on Adipose Tissue Inflammation, Hepatic Function, and Gut Microbiota Composition in C57BL/6J and B6129SF2/J Mice

by

Han Fang

A dissertation submitted to the Graduate Faculty of
Auburn University
in partial fulfillment of the
requirements for the Degree of
Doctor of Philosophy

Auburn, Alabama
August 3, 2019

Keywords: Obesity, Adipose tissue inflammation, Nonalcoholic fatty liver disease, Mouse strains, Gut microbiota

Approved by

Robert L. Judd, Chair, Professor of Anatomy, Physiology, and Pharmacology
Ya-Xiong Tao, Professor of Anatomy, Physiology, and Pharmacology
Satyanarayana R. Pondugula, Associate Professor of Anatomy, Physiology, and Pharmacology
Michael W. Greene, Associate Professor of Nutrition, Dietetics, and Hospitality Management

Abstract

Background. Obesity is associated with adipose tissue inflammation, development of nonalcoholic fatty liver disease (NAFLD) and altered gut microbiota composition. Niacin is beneficial in inhibiting obesity-associated adipose tissue inflammation, decreasing hepatic triglyceride content in NAFLD and suppressing colitis and colorectal cancer. B6129SF2/J (B6129) mice have emerged in recent years to meet the need for better appropriate controls for genetically engineered strains maintained on a mixed B6;129 background. However, a limited number of studies have characterized the physiological and metabolic changes which occur in B6129 mice during diet-induced obesity compared with that of C57BL/6J (B6) mice. **Objectives.** Therefore, the objectives of this dissertation are to comparatively assess the impact of high-fat diet (HFD) and niacin on 1) adipose tissue inflammation, 2) NAFLD development, and 3) gut microbiota composition in B6 and B6129 mice. **Method.** Three-week old male B6 (n=32) and B6129 (n=32) mice were maintained on a chow (10% fat) or HFD (60% fat) for 20 weeks. Niacin (360 mg/kg/day) or vehicle was added to the drinking water from week 5 until the end of the study. **Results.** Adipose tissue inflammation was increased in HFD-fed mice of both strains, but it was more advanced in B6 mice. Niacin decreased adipose tissue inflammation in HFD-fed B6129 but not B6 mice. Both strains of mice fed a HFD developed NAFLD with increased histological score. Surprisingly, niacin treatment increased normalized liver weight, hepatic triglyceride content and histological score in HFD-fed B6129 mice but had no impact on B6 mice. Metabolomic analysis revealed that niacin affected a greater number of metabolites in

HFD-fed B6129 than B6 mice. In HFD-fed B6 mice, no specific pathway was identified as impacted by niacin. However, 5 pathways were impacted by niacin in HFD-fed B6129 mice. Of the metabolites that were changed in these pathways, 4-HPP did not change with HFD feeding but significantly decreased with niacin treatment. Decreased 4-HPP by niacin is associated with decreased β-oxidation in the liver. Lipidomic analysis suggested different hepatic lipid profiles with HFD feeding and niacin treatment in B6129 mice. The abundance of phosphocholine (PC), which is critical for very low-density lipoprotein (VLDL) triglyceride production and secretion, was not changed in B6 mice with either HFD feeding or niacin treatment. In contrast, PC was increased in HFD-fed B6129 mice, and decreased with niacin treatment.

Utilizing a live bacteria culture technique to evaluate microbiota composition, we observed that the anaerobes/aerobes ratio dramatically decreased in HFD-fed B6129 mice. *Firmicutes/Bacteroidetes* ratio remained relatively consistent in B6 mice, whereas it was increased in HFD-fed B6129 mice, which was reversed by niacin treatment. HFD remarkably increased the proportion of hemolytic bacteria and decreased proportion of *Bifidobacterium* and *Bacteroides* in B6129 mice, which was reversed by niacin treatment. In B6 mice, HFD and niacin had minor impact on gut microbiota composition. Colon length did not change in B6 mice but increased in HFD-fed B6129 mice treated with niacin. Goblet and Paneth cell number did not change in B6 mice. In contrast, goblet cell number was increased in HFD-fed B6129 mice. Paneth cell number was increased in HFD-fed B6129 mice treated with niacin. **Conclusions.** In conclusion, both B6 and B6129 mice developed adipose tissue inflammation and NAFLD after HFD feeding, but to a lesser degree in B6129 mice. Niacin had no impact on NAFLD development in B6 mice but potentiated hepatic steatosis in HFD-fed B6129 mice. Metabolomics and lipidomics analysis revealed that the mechanisms of niacin-induced hepatic

steatosis in HFD-fed B6129 mice involved decreased β-oxidation and VLDL triglyceride production and secretion. B6 mice were more resistant to HFD and niacin-induced alterations in gut microbiota composition and histological changes of small intestine than B6129 mice. Niacin improved gut microbiota composition and small intestine histology in HFD-fed B6129 mice.

Acknowledgments

First of all, I would like to express my deepest and sincere gratitude to my supervisor, Dr. Robert Judd, who accepted me to study and do research under his guidance and provided me endless support and encouragement throughout my dissertation work. This dissertation would not be possible without his help and great advice. I would also like to acknowledge my committee members, Dr. Ya-Xiong Tao, Dr. Satyanarayana Pondugula and Dr. Michael Greene, for their guidance and distinguished expertise along the way. I am also thankful to my university reader, Dr. Douglas White, for his careful review of my dissertation and valuable comments. I would also like to thank Dr. Iryna Sorokulova, Ludmila Globa and Dr. Henri Giblot Ducray, for their collaboration with the gut project. Special thanks also to my lab colleagues and alumni, Zhuoyue Li, Kayleen McCafferty and Dr. Emily Graff, for their precious assistance and suggestions. Finally, I would like to acknowledge with gratitude and unconditional love of my family-my parents, Xianxiang Fang and Chunxian Liu; my husband, Wei Wang; my son, Leo Wang and my parents-in-law. I could not complete my study without their tremendous support and help.

Table of Contents

List of Tables

List of Figures

List of Abbreviations

ABCA-1	ATP binding cassette A-1
ABCG-1	ATP-binding cassette sub-family G member 1
ACC	Acetyl-CoA carboxylase
AcCa	Acyl Carnitine
AdipoR1	Adiponectin receptor 1
AdipoR2	Adiponectin receptor 2
Aldh1a	Aldehyde dehydrogenase 1 family, member A1
Ang1	Angiopoietin-1
ANOVA	Analysis of variance
ApoB	Apolipoprotein B
ASO	Antisense oligonucleotides
B6	C57BL/6J
B6129	B6129SF2/J
BMI	Body mass index
Cav-1	Caveolin-1
CD36	Cluster of differentiation 36
CDD	Compositionally defined diet
CEPT	Choline/ethanolamine phosphotransferase
CerP	Ceramides phosphate

CETP	Cholesterol ester transfer protein
CFU	Colony-forming units
ChREBP	Carbohydrate-responsive element binding protein
CL	Cardiolipin
CLS	Crown-like structure
Cox-1	Cyclooxygenase-1
CPT	Carnitine palmitoyltransferase
DG	Diglyceride
DGAT	Diacylglycerol acyl transferase
DGDG	Digalactosyldiacylglycerol
DNL	*de novo* lipogenesis
ECT	CTP: phosphoethanolamine cytidylyltransferase
ER	Extended-release
eNOS	Endothelial nitric oxide synthase
eWAT	Epididymal white adipose tissue
FA	Fatty acids
FABP	Fatty acid-binding protein
FABPpm	Plasma membrane fatty acid-binding protein
FABPc	Cytoplasmic fatty acid-binding protein
FAS	Fatty acid synthase
FATP	Fatty acid transport protein
FFA	Free fatty acids
FMT	Fecal microbiota transplantation

FXR	Farnesoid X receptor
HCA_2	Hydroxycarboxylic acid receptor 2
HDL	High-density lipoprotein
H&E	Hematoxylin and eosin
HFD	High-fat diet
HMW	High molecular weight
HO-1	Heme oxygenase-1
HOMA-IR	Homeostatic model assessment of insulin resistance
4-HPP	Hydroxyphenylpyruvate
IKK-β	Inhibitor of nuclear factor kappa-B kinase subunit beta
IL	Interleukin
IL-1R1	Interleukin-1 receptor 1
IR	Immediate-release
KO	Knockout
LCAD	Long-chain acyl-CoA dehydrogenase
LDL	Low-density lipoprotein
LdMePE	Lysodimethylphosphatidylethanolamine
L-FABP	Liver-type fatty acid-binding protein
5LOX	5-lipoxygenase
LPS	Lipopolysaccharide
LXR	Liver X receptor
MCAD	Medium-chain acyl-CoA dehydrogenase
MCP-1	Monocyte chemotactic protein-1

MePC	Methyl phosphatidylcholine
MGDG	Monogalactosyldiacylglycerol
MTBE	Methyl tert-butyl ether
MTP	Microsomal triglyceride transfer protein
NAFLD	Nonalcoholic fatty liver disease
NASH	Nonalcoholic steatohepatitis
NCD	Normal chow diet
NEFA	Non-esterified fatty acids
NFE2L2	Nuclear factor erythroid 2-related factor 2
NF-κB	Nuclear factor kappa-light-chain-enhancer of activated B cells
PAI-1	Plasminogen activator inhibitor-1
PC	Phosphatidylcholine
PD	Parkinson's disease
PE	Phosphatidylethanolamine
PEMT	Phosphatidylethanolamine N-methyltransferase
PEt	Phosphatidylethanol
PGD_2	Prostaglandin D2
PIP	Phosphatidylinositol
PKA	Protein kinase A
PPARα	Peroxisome proliferator-activated receptor alpha
PPARγ	Peroxisome proliferator-activated receptor gamma
PS	Phosphatidylserine
PSD	Phosphatidylserine decarboxylase

PXR	Pregnane X receptor
SAM	S-adenosylmethionine
SCAD	Short-chain acyl-CoA dehydrogenase
SCD1	Stearoyl-CoA desaturase 1
SCFA	Short chain fatty acid
SR	Sustained-release
SR-B1	Scavenger receptor class B type 1
SREBPs	Sterol regulatory element binding proteins
T2D	Type 2 diabetes
TACE	Tumor necrosis factor-alpha-converting enzyme
TG	Triglyceride
TGF-β	Transforming growth factor-beta
TNF-α	Tumor necrosis factor-alpha
TNFR1/2	Tumor necrosis factor receptor 1/2
VCAM-1	Vascular cells adhesion molecule-1
VEGF	Vascular endothelial growth factor
VLCAD	Very long-chain acyl-CoA dehydrogenase
VLDL	Very low-density lipoprotein
WAT	White adipose tissue
WHO	World health organization

Chapter 1

Review of the Literature

Obesity

The World Health Organization (WHO) defines overweight and obesity based on body mass index (BMI), a mathematical calculation of a person's weight in kilograms divided by the square of their height in meters. For adults, a BMI greater than or equal to 25 is considered overweight. BMI greater than or equal to 30 is considered obese. However, this definition is not suitable for children and teenagers even though the calculation of BMI is the same as for adults. The interpretation of BMI for children is age and sex dependent. For children age 5 through 19, overweight is defined as BMI-for-age greater than 1 standard deviation above the WHO growth reference median. If it is greater than 2 standard deviations, the child is considered obese. Clinically, obesity is a complex disorder involving an excessive amount of body fat due to an imbalanced energy intake and expenditure. Diet, environment, genetics and their interactions contribute to the pathogenesis of obesity [1]. According to the WHO, 39% of the adult population worldwide were overweight in 2016. The prevalence of obesity in adults was 13% which was tripled in the past 40 years. In addition, the number of overweight and obese children is also increasing dramatically in both developed and developing countries. Obesity is not just a weight problem but has become a serious global health issue that causes 3.4 million deaths worldwide in 2010 [2]. Obesity is associated with an increased risk for various disease

conditions, including type 2 diabetes (T2D), cardiovascular disease, nonalcoholic fatty liver disease (NAFLD) and certain types of cancer [3-5]. Obesity produces dysfunction in multiple organs due to abnormal fat accumulation and obesity-associated inflammation and metabolic disorders. This review focuses on the physiological and metabolic changes in adipose tissue, liver and gut that occur in obesity.

Obesity and Adipose Tissue

There are two types of adipose tissue in our body, white adipose tissue (WAT) and brown adipose tissue (BAT). WAT primarily functions as a reservoir for energy storage and an insulator for maintaining body temperature. Recently, WAT has also been recognized as an endocrine organ that regulates whole body energy homeostasis through secretion of a large number of adipokines [6]. Adipose tissue communicates with other organs through adipokines and their receptors to influence critical metabolic processes.

Leptin was the first adipokine identified, with its primary function to decrease food intake and increase energy expenditure through a direct effect on the hypothalamus [7]. Plasma levels of leptin are positively correlated with body fat content [8]. Leptin is thought to be a feedback signal from fat that lets the brain know how much fat is in the body. Due to a mutation in the gene coding leptin, the *ob/ob* mice cannot produce leptin, resulting in hyperphagia and a significantly obese and diabetic phenotype. Reduced food intake and body weight is observed in these mice when treated with leptin injections [8]. *Db/db* mice and *fa/fa* rats, which have mutations in the gene coding leptin receptor, are also extremely obese, similar to the *ob/ob* mice [9, 10]. Leptin concentrations are elevated in most obese patients due to the large amount of adipose tissue [11]. Chronic elevation in leptin concentrations leads to leptin resistance in target

cells, which makes the role of leptin in regulating body weight more complex. Therefore, numerous studies have attempted to reveal the underlying mechanisms of leptin resistance, which has been suggested to be initiated by activation of the inflammatory signaling pathway [12]. Inflammatory factors, including tumor necrosis factor-alpha (TNF-α), interleukin (IL) 1-alpha and lipopolysaccharide (LPS), increase circulating leptin concentrations in rodents and humans [13-15], suggesting that these molecules may be involved in hyperleptinemia and the development of leptin resistance.

Adiponectin, another important adipokine secreted from adipocyte, was discovered a year after leptin [16]. It is a 30-kDa monomeric glycoprotein [17] that circulates in mammals in a low molecular weight form (trimer), middle molecular weight form (hexamer) and high molecular weight form (HMW, 12-18 monomers), which is the most bioactive form of adiponectin. Adiponectin is present at high levels in plasma, typically up to 30 μg/mL in healthy individuals [18], but decreases in obese patients as well as individuals with metabolic syndrome, atherosclerosis, and T2D. Interestingly, the reduction in adiponectin appears to precede the development of insulin resistance [18-20]. Adiponectin is an insulin-sensitizing hormone, which possesses anti-inflammatory, anti-atherosclerotic, anti-fibrotic and anti-apoptotic properties. Two adiponectin receptors, AdipoR1 and AdipoR2, mediate adiponectin's effect in different tissues. AdipoR1 is primarily expressed in the skeletal muscle, while AdipoR2 is preferentially expressed in liver [21]. T-cadherin, an atypical glycosylphosphatidylinositol-anchored cadherin cell surface glycoprotein, also binds to the HMW and hexameric forms of adiponectin [22], where it mediates the vascular and cardioprotective effects of adiponectin [23].

WAT is unique in its plasticity, adapting quickly to nutrient deprivation and overnutrition conditions. The expansion of adipose tissue is mainly through adipocyte hypertrophy (increasing

in size) and hyperplasia (increasing in number). Preadipocytes within adipose tissue can differentiate into mature adipocytes throughout life, enabling the hyperplastic expansion of adipose tissue when increased storage requirements are needed [24]. In obese individuals, the adipocyte reaches a size limit where it cannot expand anymore, resulting in increased ectopic fat deposition in other tissues, such as liver and skeletal muscle. Based on the anatomical location, WAT can be classified into subcutaneous and visceral fat. Visceral fat that surrounds internal organs is highly metabolic and largely contributes to adipokine secretion, while subcutaneous fat is located beneath the skin and less involved in obesity-related pathologies. Different fat depots expand via different mechanisms [25]. Scherer *et al.* demonstrated that during high-fat diet (HFD) feeding, the subcutaneous fat expands mainly by hypertrophy, whereas the epididymal fat, representing of visceral fat, undergoes hyperplasia shortly after HFD feeding [26]. WAT expansion through different depots also has different metabolic outcomes. A number of clinical studies have described that, in contrast to "metabolically unhealthy obese" individuals, "metabolically healthy obese" individuals preferentially store the excess fat in subcutaneous depots rather than visceral depots [27]. In addition, surgical removal of visceral fat leads to improvements in oral glucose tolerance, insulin sensitivity and fasting glucose and insulin [28]. However, removal of subcutaneous fat by liposuction does not affect insulin sensitivity and risk factors for coronary heart disease [29].

As the adipocyte progressively enlarges, the expression, production and secretion of various cytokines and adipokines dramatically changes. In obese patients, there is an increase in the production of proinflammatory cytokines, including TNF-α, IL-6, monocyte chemotactic protein-1 (MCP-1) and IL-1β [30]. Circulating monocytes recruited by MCP-1 infiltrate into adipose tissue and polarize to pro-inflammatory M1 "classically activated" macrophages instead

of anti-inflammatory M2 “alternatively activated” macrophages. Therefore, M1 macrophage populations increase in adipose tissue with obesity and are responsible for most of the cytokine production in obese adipose tissue [31]. Macrophages surround and engulf the dead or dying adipocytes to form crown-like structures (CLS), which are hallmark characteristics of adipose tissue inflammation [32].

Adipocyte-derived cytokines and macrophages are associated with obesity-induced inflammation, which plays an important role in the development of obesity-related complications. Nuclear factor kappa-light-chain-enhancer of activated B cells (NF-κB) activity is increased in obese animals. When obese animals are treated with pharmacological inhibitors of nuclear factor kappa-B kinase subunit beta (IKK-β) or subjected to genetic deletion of IKK-β, obesity-induced insulin resistance improves [33]. More studies suggest that the suppression of IKK-β/NF-κB-dependent inflammation improves insulin resistance and T2D in animal models as well as in humans [34]. The inflammasome has also been suggested to play a role in obesity-induced inflammation. The main function of the inflammasome is to induce the maturation of IL-1β and IL-18, two members of the pro-inflammatory IL-1 cytokine superfamily. The major cellular sources of IL-1β and IL-18 are monocytes and macrophages [35]. TNF-α is a classic potent pro-inflammatory cytokine, primarily secreted from monocytes and macrophages via activation of mitogen-activated protein kinase and NF-κB signaling pathways, resulting in the release of other inflammatory cytokines such as IL-1β and IL-6 [36]. Non-obese healthy subjects have normal circulating IL-6 and TNF-α levels, which are elevated in individuals with normal weight but increased whole fat mass. The increases of IL-6 and TNF-α levels are related to excessive fat content and distribution [37]. On the other hand, IL-10 is a classical anti-inflammatory cytokine, expressed by T regulatory cell at high levels but also expressed by

macrophages and other cells. IL-10 may play a protective role in obesity-induced metabolic dysregulation and insulin resistance. IL-10 levels are attenuated in T2D [38] and weight loss enhances WAT IL-10 expression, which coincidents with reduced pro-inflammatory gene expression [39].

Obesity and Liver

Increased adiposity is associated with chronic obesity, resulting in ectopic accumulation of fat in other tissues, including the liver. NAFLD is a group of conditions where there is an accumulation of excess fat in the liver of individuals who drink little or no alcohol. NAFLD encompasses multiple pathogenic states ranging from simple steatosis to steatohepatitis, which can progress to irreversible cirrhosis and liver failure [40]. The estimated prevalence of NAFLD is one billion globally. In the United States, over 80 million individuals (20-30% of Americans) develop NAFLD and a quarter of these people progress to nonalcoholic steatohepatitis (NASH) [41]. NAFLD is strongly linked with obesity, with NAFLD and NASH presenting in about 90% of the obese population [42]. In addition, NAFLD is also highly associated with cardiovascular diseases and T2D. To date, there is no effective pharmacotherapy for treating NAFLD. Lifestyle modifications, including exercise and eating a healthy diet (e.g. Mediterranean diet), are the only clinically recommended interventions for NAFLD.

Recently, a multiple hit hypothesis has been proposed for the development of NAFLD [43]. In this hypothesis, multiple factors have been suggested to contribute to the pathogenesis of NAFLD, including obesity, insulin resistance, alteration in gut microbiome composition and genetic and epigenetic factors. All of these factors contribute to the synthesis and accumulation of triglycerides and inflammation in the liver, two hallmark characteristics of NAFLD

development. The metabolism of fatty acids (FA), the major source of hepatic triglyceride synthesis, is tightly related to the lipid content in the liver [44]. Increased triglycerides in the livers of NAFLD patients are due to one or more of the following events: 1) increase in FA uptake, 2) increase in *de novo* lipogenesis (DNL), 3) decrease in FA oxidation, and/or 4) decrease in lipid secretion.

FA can enter the hepatocyte by direct diffusion across the phospholipid bilayer of the cell membrane [45]. However, long chain FA uptake is facilitated by various plasma membrane-mediated proteins, including CD36, FA-binding protein (FABP), and FA transport protein (FATP) [46, 47]. CD36 is a membrane glycoprotein, also known as FA translocase. It was originally discovered to be a transporter for long chain FA in rat adipocytes [48]. CD36 is expressed in a number of cell types, including monocytes, macrophages, microvascular endothelial cells, adipocytes, muscle cells, enterocytes and hepatocytes [49]. The hepatic expression of CD36 is low in rodents under normal conditions, indicating a limited function of CD36 for FA uptake [49]. However, both rodent and human studies have suggested a positive correlation between the level of CD36 and hepatic triglyceride content [50-52]. In genetic and HFD-induced models of hepatic steatosis, liver-specific deletion of CD36 decreases liver lipid content, including triglycerides, diglycerides and cholesterol ester, and improves insulin sensitivity [53]. This suggests an important role of CD36 in regulating hepatic FA uptake under elevated FA conditions. In addition, CD36 is a target of several lipogenic transcription factors, including liver X receptor (LXR), pregnane X receptor (PXR) and peroxisome proliferator-activated receptor gamma (PPARγ) [54, 55]. The regulation of CD36 by these factors is liver specific. Deletion of CD36 significantly attenuates LXR agonists-induced hepatic steatosis [55], suggesting a critical role of CD36 in regulating lipogenesis as well.

FABPs are a family of transport proteins for long chain FA, which are abundantly expressed in various tissues actively involved in lipid metabolism [56, 57]. Based on their location, the FABPs can be divided into two groups: plasma membrane FA-binding proteins (FABPpm) and cytoplasmic FA-binding proteins (FABPc) [56]. FABPpm are expressed in several tissues, including liver, heart, skeletal muscle, adipose tissue and intestine [56]. In *ob/ob* mouse liver, FABPpm mRNA level is twofold higher than their control littermate [58]. It is proposed that the upregulation of FABPpm may lead to an increase in FA uptake, and subsequent increase in triglyceride synthesis. FABPc function as lipid chaperones escorting FA to specific cell compartments for different purposes, such as lipid droplets for storage, endoplasmic reticulum for signaling, trafficking and membrane synthesis, mitochondria or peroxisomes for oxidation and nucleus for transcriptional regulation [57].

FATPs, also known as very-long-chain acyl-CoA synthesis, are a family of FA transport proteins with six members (FATP1-6). FATP2 and FATP5 are expressed in the liver [59, 60]. Liver-specific knockdown of FATP2 reduces hepatic steatosis in mice fed a HFD [59]. In line with this, overexpression of FATP2 increases FA uptake in human hepatoma cells [61]. Similarly, deletion of FATP5 results in reduced long chain FA uptake, decreased hepatic triglyceride synthesis and protection against diet-induced NAFLD [60, 62]. Overexpression of FATP5 in mammalian cells also increases FA uptake [60]. Even though FATP4 is not substantially expressed in liver under normal conditions [63], its expression is increased in fatty livers, which induces hepatocellular apoptosis [64].

Adipose tissue inflammation is a key feature of obesity, with inflamed adipose tissue being insulin resistant, leading to increased efflux of FA to the liver. The excess flow of FA promotes the synthesis of intrahepatic triglycerides, resulting in the development of hepatic

steatosis. Therefore, targeting the FA transporters to reduce FA uptake may represent a potential therapy for treating NAFLD in obese patients.

The second source of FA for hepatic triglyceride synthesis is DNL. In general, DNL is a process that converts dietary carbohydrates into fat. The synthesis of FA from glucose is controlled by several rate-limiting enzymes and transcriptional factors, including acetyl-CoA carboxylase (ACC), FA synthase (FAS), stearoyl-CoA desaturase 1 (SCD1), diacylglycerol acyltransferase (DGAT), sterol regulatory element binding proteins (SREBPs), carbohydrate-responsive element binding protein (ChREBP), LXR and farnesoid X receptor (FXR) [65].

ACC is an enzyme that converts the acetyl-CoA to malonyl-CoA. There are two isoforms of ACC in rodents and humans. ACC1 is a cytosolic protein expressed mainly in the liver and adipose tissue, whereas ACC2 is a mitochondrial-associated protein expressed in the heart, skeletal muscle and liver [66]. The cellular location of ACC1 and ACC2 plays an important role in their physiological functions. Malonyl-CoA synthesized by ACC1 is utilized in FA synthesis, whereas the malonyl-CoA generated by ACC2 inhibits carnitine palmitoyltransferase I (CPT1) activity and therefore reduces fatty acid oxidation [66]. Global knockout (KO) of ACC1 in mice results in embryonic lethality, while liver-specific KO mice have decreased malonyl-CoA and hepatic triglyceride levels [67, 68]. When liver-specific ACC1 KO mice are fed a fat-free diet, even though their lipogenic enzymes are up-regulated, *de novo* FA synthesis and triglyceride content in the liver is decreased [67]. ACC2 deficient mice have a lifespan equal to WT mice, but with a higher FA oxidation rate and lower hepatic triglyceride content [69]. When challenged with high-fat/high-carbohydrate diet, ACC2 mutant mice exhibit less body weight, fat mass, and normal levels of insulin and glucose due to increased FA oxidation in muscle and liver [70]. Thus, inhibition of ACC1 and ACC2 may be efficient

mechanisms which protect against diet-induced hepatic steatosis. Indeed, suppression of both ACC1 and ACC2 with a single antisense oligonucleotide (ASO) significantly lowers malonyl-CoA and hepatic lipids and improves hepatic insulin sensitivity [71]. In a randomized clinical trial, a single dose of NDI-010976, an inhibitor of ACC1 and ACC2, profoundly decreases hepatic DNL in overweight subjects [72]. However, further investigation is needed to evaluate the efficacy and safety of this inhibitor in treating NAFLD.

FAS is an enzyme that primarily catalyzes the biosynthesis of palmitate from acetyl-CoA and malonyl-CoA. Whole-body KO of FAS leads to embryonic lethality in mice, which is similar to ACC1 global KO mice [73]. Unexpectedly, on a fat-free diet, liver-specific FAS KO mice develop hypoglycemia and fatty liver [74]. This phenotype can be corrected by a peroxisome proliferator-activated receptor alpha (PPARα) agonist, suggesting that the newly synthesized FA via FAS activates PPARα to ensure normal glucose and lipid homeostasis [74]. Increased enzyme activity of FAS has been reported in animal models of obesity, including Zucker rats and *ob/ob* mice [75, 76].

SCD1 is an enzyme attached to the endoplasmic reticulum that converts saturated FA to monounsaturated FA, especially oleate and palmitoleate, two major components of triglyceride. In humans, SCD1 is mainly expressed in adipose tissue and liver [77]. In mice, in addition to adipose tissue and liver, SCD1 is also highly expressed in lung and skin [77]. SCD1 whole-body KO mice are protected from overnutrition-induced adiposity, hepatic steatosis and insulin resistance [78-80]. In line with this, mice treated with SCD1 ASO inhibitors are also protected against diet-induced obesity and steatosis due to a decrease in DNL and expression of lipogenic genes and an increase in FA oxidation [81]. Liver-specific SCD1 KO mice are protected from obesity and hepatic steatosis induced by high-carbohydrate diet but not HFD [82]. Together

these results lead to the hypothesis that hepatic SCD1 is necessary for carbohydrate-induced obesity, while SCD1 deficiency in tissues other than liver is required for resisting HFD-induced obesity and steatosis. Moreover, the hepatic mRNA levels of SCD1 are increased more than twofold in obesity-prone C57BL/6 mice fed a HFD, but do not change in obesity-resistant FVB mice [83]. Targeting SCD1 expression and activity may be a potential treatment for obesity and obesity-associated hepatic steatosis. However, in obese humans, the hepatic SCD1 activity is negatively correlated with liver fat [84]. Thus, the exact role of SCD1 in the development of obesity and hepatic steatosis needs to be addressed in future studies.

DGAT is a microsomal enzyme that catalyzes the final step of triglyceride synthesis from diglyceride. There are two isoforms of DGAT, DGAT1 and DGAT2. DGAT1 is predominantly expressed in small intestine, whereas DGAT2 primarily presents in adipose tissue and liver [85, 86]. Smith *et al.* generated DGAT1-deficient mice which are viable and obesity resistant due to increased energy expenditure [87]. Mice lacking DGAT1 also have increased insulin and leptin sensitivity when fed a Western-type diet [88]. However, these KO mice could still synthesize triglycerides. Thus, it was believed that multiple DGATs may exist, which was confirmed later with the cloning of *DGAT2* [85]. DGAT2 seems to be more critical than DGAT1 for triglyceride synthesis and survival. DGAT2-deficient mice have growth retardation and die shortly after birth, primarily due to substantial substrate shortage for energy metabolism and impaired barrier permeability function in the skin [89]. The fact that DGAT1 does not compensate for the loss of DGAT2 indicates the different roles of these two enzymes in triglyceride synthesis. Furthermore, diet-induced hepatic steatosis and insulin resistance is reversed by suppression of DGAT2 but not DGAT1 with ASO [90, 91]. Together, these data suggest that pharmacological inhibition of DGAT1 or DGAT2 are beneficial for treating obesity, insulin resistance and hepatic

steatosis. Indeed, a number of DGAT inhibitors from different origins have been discovered, most of which are DGAT1 inhibitors [92]. However, suppression of DGAT may be useful for treating hepatic steatosis but not insulin resistance as evidenced by normal insulin and glucose intolerance in mice overexpressing DGAT [93]. In addition, inhibition of DGAT2 suppresses very low-density lipoprotein (VLDL) triglyceride secretion in rodents but has no effect in plasma triglycerides or VLDL-apolipoprotein B (ApoB) levels in non-human primates [94]. Therefore, the therapeutic potential of DGAT inhibitors in treating obesity and metabolic syndrome needs to be studied more carefully.

SREBPs are transcription factors that control cellular lipid metabolism and homeostasis. Three SREBPs (SREBP1a, SREBP1c and SREBP2) has been identified so far with distinct tissue distributions and physiological roles in lipid synthesis [95, 96]. Both SREBP1a and SREBP2 are involved in cholesterol synthesis [96]. However, overexpression of hepatic SREBP1c has no impact on cholesterol biosynthesis genes [97]. Liver-specific deletion of SREBP1c results in reduced mRNAs of enzymes in FA and triglyceride synthesis, including ACC and FAS [98]. The transcriptional regulation of SREBP1c can be modulated by various factors, including nutritional status (fasting or high carbohydrate diet), insulin, LXR, oxidative stress and polyunsaturated FA [96]. Increased SREBP1c protein levels are observed in fatty livers of diabetic mice with insulin resistance and hyperinsulinemia [99]. In line with this, the expression of SREBP1c is fivefold greater in NAFLD patients than their controls [100]. Furthermore, SREBP1c deficiency decreases lipid biosynthesis and ameliorates diet-induced hepatic steatosis and hypertriglyceridemia but not insulin resistance [101, 102].

In addition to SREBPs, ChREBP is another transcription factor that regulates lipid biosynthesis by controlling the expression of ACC and FAS. In 2004, Iizuka *et al.* generated

ChREBP KO mice, which are viable and have a normal life span [103]. These KO mice display a 65% reduction in FA synthesis rates and a 40% increase in liver weight, which is most likely due to increased glycogen storage. In addition, liver-specific suppression of ChREBP ameliorates hepatic steatosis and insulin resistance in *ob/ob* mice [75, 104]. However, mice with hepatic overexpression of ChREBP have exacerbated hepatic steatosis but are still insulin sensitive, which again dissociates hepatic steatosis from insulin resistance [105].

LXRs and FXR are nuclear receptors that function as transcription factors in response to sterols and bile acids, respectively. LXR plays an important role in regulating hepatic fat metabolism through activation of a set of lipogenic genes, including SREBP1c, ACC, FAS, and SCD1 [106-108]. LXR null mice are resistant to high-fat and high-cholesterol diet-induced obesity due to abnormal energy dissipation [109]. Interestingly, the obesity-resistant phenotype of the LXR null mice is dependent on the cholesterol component in the diet. Pharmacological agonists of LXR show beneficial effects of lowering cholesterol by activating ATP-binding cassette transporters. However, LXR agonists have detrimental effects, such as increasing hepatic steatosis and VLDL triglyceride, through activation of SREBP1c pathway [110]. Deletion of FXR in mice results in elevated serum bile acid, cholesterol, triglycerides and a proatherogenic serum lipoprotein profile [111]. The mechanisms involved in the beneficial effects of FXR activation may include suppression of hepatic SREBP1c expression, modulation of apolipoproteins, increase in FA oxidation and induction of peroxisome proliferator activated receptor gamma coactivator 1 alpha [112].

In normal subjects, the contribution of DNL to hepatic triglycerides secreted via VLDL is less than 5%, but this number is greater than 20% in obese subjects with NAFLD [44, 113]. In addition, carbohydrate metabolism shifts from glycogen storage towards DNL in NAFLD

patients with insulin resistance [114]. Therefore, targeting the enzymes and transcription factors involved in DNL has great potential in treating diet-induced hepatic steatosis.

A third mechanism of hepatic triglyceride accumulation is decreased FA oxidation. FA oxidation is the process that breaks down FA into acetyl-CoA, which then either enters into the citric acid cycle or is utilized in the formation of ketone bodies (acetoacetate, acetone, and β-hydroxybutyrate). There are three FA oxidation pathways: mitochondrial β-oxidation, peroxisomal β-oxidation, and microsomal ω-oxidation [65]. The majority of FA are oxidized through mitochondrial β-oxidation. Short- and medium-chain FA can across the inner membrane of mitochondria through simple diffusion, whereas transport of long-chain FA into the mitochondrial matrix is facilitated sequentially by CPT1, carnitine acylcarnitine translocase and CPT2 [115]. The initial step of each cycle of mitochondrial β-oxidation is the dehydrogenation of the acyl-CoA ester by chain-length specific acyl-CoA dehydrogenases, including SCAD (short-chain), MCAD (medium-chain), LCAD (long-chain), and VLCAD (very-long-chain) [65]. A number of animal studies have demonstrated that inhibition or activation of mitochondrial β-oxidation can regulate hepatic triglyceride content [116-118]. Deficiency of MCAD and LCAD results in decreased β-oxidation and leads to hepatic steatosis and insulin resistance in mice [116, 117]. Enhanced FA transportation into the mitochondrial matrix through overexpression of CPT1A increases the rate of the β-oxidation and reduces hepatic triglyceride accumulation by ~35% [118]. Initial human studies in NASH or obesity have demonstrated that hepatic FA oxidation is increased compared with their controls [119, 120]. However, in a more recent study using magnetic resonance spectroscopy, Peterson *et al.* demonstrated in humans that hepatic mitochondrial oxidation and pyruvate cycling are not altered in NAFLD, which suggests that there must be another mechanism responsible for the

hepatic fat accumulation in NAFLD [121]. Thus, a more precise role of β-oxidation in the development of obesity and NAFLD, especially in human subjects, needs further investigation.

Triglyceride secretion via VLDL is responsible for exporting FA from the liver. VLDL particles contain triglycerides esterified from FA, an ApoB-100, and cholesterol esters. Microsomal triglyceride transfer protein (MTP) facilitates triglycerides to infuse into ApoB-100 [122]. MTP liver-specific KO in mice induces hepatic steatosis and reduction in VLDL triglycerides and VLDL/low-density lipoprotein (LDL) levels [123]. In addition, inhibition of MTP in patients with familial hypercholesterolemia results in a reduction of LDL cholesterol levels, accompanied with hepatic fat accumulation [124]. These studies support an important role of MTP in VLDL synthesis and secretion.

Phospholipids, which form a monolayer surrounding a lipid core of triglyceride and cholesterol esters, are also required for the assembly and secretion of VLDL. The most abundant phospholipids in all mammalian cells are phosphatidylcholine (PC) and phosphatidylethanolamine (PE). In general, PC and PE comprise 40-50% and 40% of total cellular phospholipids, respectively. PC is synthesized from choline via the CDP-choline pathway in all nucleated mammalian cells. In the liver, there is an additional pathway for PC synthesis, in which phosphatidylethanolamine N-methyltransferase (PEMT) converts PE to PC via 3 methylation reactions. S-adenosylmethionine (SAM) is the methyl group donor for these methylation reactions. The levels of PC can be regulated by these two pathways. PEMT-deficient mice have an approximately 50% decrease in hepatic PC levels and develop NASH compared with control mice when fed a choline-deficient diet [125]. However, even when fed a diet with choline supplementation, these KO mice still develop hepatic steatosis and have increased apoptotic activity [126]. Furthermore, when PEMT KO mice are challenged with

HFD, the VLDL triglyceride production rate is reduced by 70% compared with control mice [127]. In addition, deficiency in SAM, a substrate for PC synthesis, also leads to a decrease in triglyceride secretion in VLDL [128]. Together, these findings indicate that a reduction in PC synthesis impairs the secretion of VLDL triglyceride, which leads to liver lipid accumulation and consequently hepatic steatosis.

PE may also play a role in VLDL assembly and secretion. There are two separate pathways responsible for biosynthesis of PE. In the CDP-ethanolamine pathway, ethanolamine is phosphorylated to phosphoethanolamine by ethanolamine kinase. Phosphoethanolamine is then converted to CDP-ethanolamine by CTP: phosphoethanolamine cytidylyltransferase (ECT). The final step is the transfer of phosphoethanolamine to diacylglycerol to generate PE in the endoplasmic reticulum catalyzed by choline/ethanolamine phosphotransferase (CEPT). The other pathway is the phosphatidylserine decarboxylase (PSD) pathway, in which phosphatidylserine (PS) is concerted to PE by PSD in the mitochondria. Hepatocyte-specific deletion of ECT leads to a tenfold increase in triacylglycerols and liver steatosis [129]. Interestingly, the nascent VLDL particles have higher PE content than circulating VLDL [130]. Moreover, blockade of plasma lipoprotein lipolysis results in a similar high composition of PE in circulating and hepatic VLDL [131]. These findings suggest an important role of PE in the secretion of VLDL particles. In addition, an appropriate hepatic PC/PE ratio is also critical for VLDL secretion and NAFLD development. PC/PE ratio is significantly increased in *ob/ob* mice compared with controls [132]. In mouse models lacking key enzymes for PC biosynthesis, the PC/PE ratios is inversely correlated with the development of steatosis [133]. When hepatic PC/PE ratio falls below the threshold of ~1, PEMT deficient mice develop liver failure [134].

Increased VLDL secretion is observed in nondiabetic obese NAFLD patients compared with control subjects [135]. This increase may be a compensatory mechanism to combat the excess fat in the liver. However, the capacity for increasing VLDL synthesis and secretion is limited in nondiabetic obese subjects [136]. In addition, increased VLDL secretion is associated with increased risk of atherosclerosis. Therefore, whether increases in VLDL secretion can be used as a target for treating fatty liver disease is not warranted.

The liver has a large population of resident macrophages, known as Kupffer cells. Unlike adipose tissue, macrophages do not infiltrate into the liver during the development of obesity but are activated without altering the total Kupffer cell number [137, 138]. Activation of Kupffer cells is associated with hepatic insulin resistance and the production of inflammatory mediators including TNF-α [139]. TNF-α signaling through activation of Kupffer cells leads to histological changes commonly observed in NASH [140]. Similar to macrophages in adipose tissue, Kupffer cells present immense plasticity and can alter between a pro-inflammatory M1 and anti-inflammatory M2 phenotype in response to their specific environment [141]. Inflammation not only affects liver lipogenesis, but also activates a secretory response involving inflammatory mediators and acute-phase reactants. In obese animals and humans, serum levels of cytokines such as serum amyloid A and IL-6 produced by the liver are increased compare with lean controls [142]. In addition, hepatic NF-kB pathway activation is also observed in NASH patients [143].

Obesity and Gut

In addition to adipose tissue and liver, obesity also has significant impact on microbiota composition and physiological functions of the gut. Gut microbiota is a group of

microorganisms, mainly bacteria, which reside in the human gastrointestinal tract. The number of gut microbiota exponentially increases from proximal to distal gut. Previous studies in adult humans have estimated that there are approximately ten times more microbial cells than human cells. However, a more recent study done by Sender *et al.* re-estimated the ratio of bacterial and human cells, which is very close to 1:1 [144]. The whole gut microbiota can weigh up to 2 kg. The two major microbial phyla in humans are *Bacteroidetes* and *Firmicutes*, which together represent over 90% of the bacterial composition of gut microbiota. Proteobacteria, Actinobacteria and Verrucomicrobia are also present in the gut microbiota, but in a relatively smaller proportion compared with *Bacteroidetes* and *Firmicutes*. In addition, the human gut microbiota can be classified into three major enterotypes: *Bacteroides*, *Prevotella*, and *Ruminococcus*, which are not nation or continent specific [145]. The relationship between gut microbiota and host is considered as mutual, meaning both organisms benefit from each other's existence. Each person has an individualized gut microbiota, which is as unique as their fingerprints. The gut microbiota possesses many functions, including metabolism of nutrients (e.g. indigestive fiber), modulation of host immunity, removal of harmful and toxic compounds, maintenance of gut barrier integrity and protection against pathogens [146]. Disruption of gut microbiota leads to an array of disease conditions, including inflammatory bowel disease, allergies, asthma, metabolic disease and even cancer [147].

Humans start to acquire microorganisms right after birth. Several factors influence the composition of the gut microbiota at early age of human life, including the mode of delivery (vaginal vs. caesarian section) [148], feeding option (breast feeding vs. formula feeding) [149], and the introduction of solid food [150]. Once the gut microbiota reaches a relatively stable state

at the age of 3, other factors play a more important role in shaping the gut microbiota, such as diet, disease state, medications and host genetics [151].

Recent years, numerous studies have suggested a strong link between obesity and gut microbiota. Compared with normal chow diet-fed mice, abundance and diversity of the gut microbiota is significantly reduced in HFD-induced obese C57BL/6J mice, which is completely recovered after switching to normal chow diet for 10 weeks [152]. More specifically, the abundance of *Bacteroidetes* is decreased with a proportional increase in *Firmicutes* during HFD feeding [152]. A lower *Bacteroidetes/Firmicutes* ratio is also observed in genetically obese *ob/ob* mice [153] and obese humans [154]. Similar to the effects of normal chow diet in mice, low-calorie diet leads to weight loss and an increase in *Bacteroidetes* richness in humans [154]. In addition, decreased *Lactobacillus* and increased *Clostridium subcluster XIVa* has also been observed in mice receiving HFD [155]. Data from studies of germ-free mice have suggested that altered gut microbiota is a cause rather than a consequence of the development of obesity. Compared with mice that have living microorganisms in their gut, germ-free mice are protected against diet-induced obesity, evidenced by lower body weight when fed with a Western diet [156]. When conventionalization of germ-free mice with a normal microbiota, even with reduced food intake, an increase in body fat content and insulin resistance is observed, indicating an important role of the normal gut microbiota in energy harvest from the diet and energy storage in the host [157]. Furthermore, Turnbaugh *et al.* demonstrated that obese *ob/ob* mice have increased capacity for dietary energy harvest compared with lean control mice [158]. Germ-free mice transplanted with *ob/ob* microbiome have greater adiposity than transplantation with microbiome from lean donor, suggesting that the obese phenotype is transmittable through gut microbiota [158].

Short chain fatty acids (SCFAs) are the principle products of the bacterial fermentation of non-digestible carbohydrates (dietary fiber and resistant starch). The most abundant SCFAs are acetate, propionate and butyrate, presenting in the gut with an approximate ratio of 60: 20: 20, which can vary depending on diet and microbiota composition. Acetate and propionate are mostly produced by *Bacteroidetes*, while butyrate is mainly produced by *Clostridium clusters IV and XIVa* belonging to the *Firmicutes* phylum. Butyrate is the major energy source for colonocytes. Three G-protein coupled receptors, GPR41 (free fatty acid receptor 3), GPR43 (free fatty acid 2) and GPR109A (hydroxycarboxylic acid receptor 2, HCA_2) are mediators of the physiological effects of SCFAs. GPR41 and GPR43 can bind to all three SCFAs, while only butyrate activates GPR109A. SCFAs may increase intestinal energy harvesting and promote the development of obesity. Compared with lean conventionally raised mice, obese mice have increased acetate and butyrate levels in caeca and less energy remaining in their feces [158]. In addition, the increase of butyrate is consistent with the increase of *Firmicutes*, butyrate producers, in obese mice. The total amount of SCFAs, particularly propionate, is higher in the fecal samples of obese subjects than lean subjects [159]. Consistent with these findings, the concentrations of butyrate and propionate are significantly higher in obese than normal weight children [160]. However, contradictory results are found in diet-induced obese mice. Acetate, propionate and butyrate concentrations are significantly reduced in the cecal content of HFD-fed mice [155]. A possible explanation is that the decreased SCFAs may be due to lack of fermentable fiber in their HFD. Therefore, matching fiber content in different diets is very critical in microbiota studies. In fact, the deleterious effects of HFD in the pathophysiology of obesity are not just caused by the high-fat content but also by lacking fermentable fiber.

Low-grade inflammation is a key characteristic of obesity, with adipose tissue being believed to be the primary source of inflammatory mediators [161]. However, recent studies have demonstrated that another source of inflammation in obesity may be the gut. LPS, also known as endotoxin, is the major component of the outer membrane of the cell of Gram-negative bacteria. Cani *et al.* demonstrated that as early as four weeks HFD feeding, the proportion of LPS-containing microbiota and plasma LPS concentrations increase in the gut [162]. Infusion of LPS to achieve endotoxemia level similar to that of HFD-fed mice results in body weight gain, insulin resistance and increased markers of inflammation, suggesting that LPS is a causative factor contributing to inflammation and insulin resistance in obesity [162]. Moreover, HFD-induced obesity disrupts mucosal barrier integrity by decreasing gut epithelial tight-junction protein expression [163, 164]. This is important because the gut epithelial layer acts as a defense line to prevent the translocation of gut bacteria into the body, which can be pathogenic to other tissues. After only one week of HFD consumption, the translocation of live commensal intestinal bacteria can be detected in adipose tissue and blood, where they induce inflammation [165]. Changes in gut microbiota composition with antibiotic treatment decreases endotoxemia and LPS in cecal content in both HFD-fed and *ob/ob* mice [166]. These antibiotic-treated mice also have reduced body weight gain, fat mass, glucose tolerance and inflammation [166].

Shortened colon length has been reported in mice with chronic HFD feeding [167]. However, this decrease in colon length is more likely due to the lack of fiber in the diet rather than the high fat content [168]. Chassaing *et al.* elegantly designed a study to differentiate the effect of fat and fiber in colon length by using compositionally defined diets (CCD) with different fat contents and normal chow diet (NCD), which is a low-fat diet with undefined plant and animal products [168]. Mice fed with CDD with either 10% or 60% fat have decreased

colon length and weight compared with NCD, indicating other factors that differentiate CDD and NCD rather than fat content contribute to colon atrophy. Further, they identified that the other factor is soluble fiber (inulin) but not insoluble fiber (cellulose) [168]. Inulin but not cellulose is metabolized by gut microbiota to produce SCFAs, which serve as a major fuel source for colonic epithelia, thus enhancing intestinal barrier function.

There are several strategies that modulate the gut microbiota to improve obesity and metabolic disorders. Probiotic supplementation is a direct way of increasing beneficial bacteria in the gut microbiota. Probiotics containing *Bifidobacterium* or *Lactobacillus* strains have been shown to reduce fat mass and improve serum lipid profiles and insulin sensitivity in animal models of obesity [169-172]. Prebiotics, mainly inulin, fructooligosaccharides and galactooligosaccharides, promote the growth of beneficial bacteria in the gut and exert protective effects in metabolic diseases by increasing the production of SCFAs. The majority of prebiotics target the growth of *Bifidobacterium* and *Lactobacillus* [173, 174]. In humans, prebiotic treatment has been associated with improved glucose tolerance, insulin sensitivity and weight loss [175, 176]. However, long-term clinical trials that evaluate the safety and efficacy of prebiotics in treating metabolic disorders are still needed. Recently, fecal microbiota transplantation (FMT) has emerged as a new therapeutic potential for treating gastrointestinal diseases as well as other diseases. FMT is the transfer of stool from a healthy donor to another patient's intestine. Currently, FMT is mostly studied and effective in treating recurrent *Clostridium difficile* infections [177]. However, extensive and well-designed clinical trials are needed before the use of FMT in treating obesity and associated metabolic diseases.

Niacin

Niacin is a water-soluble B vitamin (B3), also known as nicotinic acid. The recommended adult daily dosage of niacin as a vitamin is 15-20 mg/day (16 mg/day for men and 14 mg/day for women). Niacin can be acquired from a variety of food sources, including poultry (e.g. chicken, turkey), red fish (e.g. tuna, salmon), beef, cereals (especially fortified cereals), legumes (e.g. lima beans, lentils), whole-wheat bread, milk, green leafy vegetables, and coffee. Corn and wheat also contain niacin but with very low bioavailability. Therefore, people in areas that use corn as the main component in their diet have insufficient bioactive niacin supply. Severe niacin deficiency results in a disease called pellagra. The symptoms of pellagra are known as the four "Ds": diarrhea, dermatitis, dementia, and finally death. Daily oral therapy with niacin administration is effective in reversing the clinical manifestations of pellagra.

In 1955, Dr. Rudolf Altschul discovered that pharmacological doses of niacin at 3000 mg/day profoundly reduces serum cholesterol concentrations, which is more prominent in hypercholesterolemic patients than normal individuals [178]. A significant side effect of skin flushing is observed in all subjects taking niacin [178]. Several subsequent clinical studies have established that niacin, at pharmacological doses, alters plasma lipid concentrations by reducing serum cholesterol, triglyceride, VLDL cholesterol, LDL cholesterol, and lipoprotein(a) levels and increasing high-density lipoprotein (HDL) cholesterol levels [179-181].

Several forms of niacin with different pharmacological characters are available, including immediate-release (IR), sustained-release (SR), and extended-release (ER) formulations [182, 183]. The IR formulation is a crystalline powder that easily dissolves after oral administration [182]. However, the IR formulation is highly associated with the intolerable side effects of flushing, limiting its clinical use. The SR formulation has reduced incidence of flushing.

However, other adverse effects have been observed with the use of SR formulation, including gastrointestinal intolerance and hepatotoxicity [184]. The ER formulation, prescribed as Niaspan, exhibits a release rate between IR and SR formulation. It produces equivalent efficacy in treating dyslipidemia and less incidence of side effects compared with IR and SR formulations [182, 185].

Niacin is primarily metabolized in the liver through two metabolic pathways: the conjugative pathway and amidation pathway [183]. In the conjugative pathway, niacin conjugates with glycine, resulting in the formation of nicotinuric acid. This pathway has low affinity but high capacity. On the contrary, the amidation pathway has high affinity but low capacity. Therefore, the conjugative pathway is only utilized when amidation pathway is saturated [182, 186]. The products of the amidation pathway are nicotinamide and pyrimidine metabolites. Nicotinamide is the precursor for nicotinamide adenine dinucleotide and nicotinamide adenine dinucleotide phosphate, which are two major cofactors in redox reactions and metabolism.

In 2003, the discovery of niacin receptor, HCA_2, previously known as GPR109A, broadened the mechanisms of niacin's action in various tissues and disease states [187-190]. HCA_2 is a G_i protein-coupled receptor that is highly expressed in adipocytes [188]. During fasting, elevated plasma concentrations of β-hydroxybutyrate, an endogenous agonist of HCA_2, lead to activation of HCA_2, which induces a G_i-mediated inhibition of adenylyl cyclase activity, resulting in a decrease of cAMP levels and inhibition of protein kinase A (PKA) activity. PKA phosphorylates various proteins, including perilipin and hormone-sensitive lipase, which are essential for triglyceride breakdown [191]. Niacin inhibits lipolysis by the activation of HCA_2 on adipocytes, leading to reduced FFA release from adipose tissue. In addition, activation of

HCA_2 receptor also results in anti-inflammatory effects due to its expression in various immune cells, including macrophages, monocytes, neutrophils and dermal dendritic cells [190]. In adipocytes and macrophages, niacin treatment decreases LPS-induced expression of pro-inflammatory cytokines, including IL-6, TNF-a, and IL-8, through activation of HCA_2 [192]. *In vivo*, niacin reduces HFD-induced adipose tissue inflammation by decreasing M1 macrophage markers, including MCP-1, which is also dependent on HCA_2 [193].

Niacin has been used to treat dyslipidemia for decades. However, the lipid-altering effects of niacin are not mediated by HCA_2 receptor. In mice lacking HCA_2, the anti-lipolytic effect of niacin is completely abrogated, but niacin-induced changes in plasma HDL and LDL cholesterol or triglyceride levels are still observed [194]. Originally, it was believed that the anti-atherosclerotic effect of niacin was due to its ability to decrease LDL cholesterol and increase HDL cholesterol levels [195]. Several recent studies have demonstrated that the atherosclerotic benefits of niacin are independent of its lipid-altering effects [194, 196, 197]. Inflammation induced by recruitment of circulating monocytes to the arterial intima and subsequent formation of foam cells has been identified as an important process in atherosclerosis development [198]. The increased production of chemokines such as MCP-1 and vascular cells adhesion molecule-1 (VCAM-1) are responsible for the recruitment of circulating monocytes [198]. In a mouse model of atherosclerosis, niacin reduces the progression of atherosclerosis by inhibiting recruitment of macrophages into the atherosclerotic plaques, whereas the serum lipid profile does not change with niacin treatment in those mice [196]. Heme oxygenase-1 (HO-1) is a cytoprotective protein that possesses cardioprotective properties and protects against atherosclerosis when upregulated [199]. Niacin supplementation reduces vascular inflammation through induction of HO-1 [199]. Blocking HO-1 activity by an inhibitor or knockdown HO-1

by siRNA attenuates the ability of niacin to inhibit vascular inflammation [199]. Besides HO-1, niacin inhibits vascular inflammation through decreased endothelial expression of VCAM-1, MCP-1 and intracellular adhesion molecule-1 [197]. These effects of niacin are independent of the changes in plasma lipid concentrations [197]. Niacin also inhibits progression of atherosclerosis through regulation of macrophage functions. In RAW264.7 murine macrophages, niacin suppresses LPS-induced expression of TNF-α [200]. The activation of macrophages and MCP-1 induced chemotaxis is also inhibited by niacin, which is not observed in bone marrow macrophages from HCA_2 KO mice [200]. Furthermore, in a mouse model of atherosclerosis, niacin induces expression of the cholesterol transporter, ATP-binding cassette sub-family G member 1 (ABCG1), and promotes cholesterol efflux in immune cells, which is also mediated by HCA_2 [196]. Therefore, the expression of HCA_2 on macrophages partially contributes to the anti-atherosclerotic effects of niacin.

Niacin also acts on adipocytes to increase adiponectin secretion in a receptor-dependent manner [193, 201-203]. Adiponectin protects the vasculature and possesses anti-atherogenic effects [204]. Ouchi *et al*. demonstrated in human monocytes that physiological concentrations of adiponectin reduce lipid content and suppress the expression of class A macrophage scavenger receptor, leading to decreased macrophage-to-foam cell transformation [205]. The same group also demonstrated that adiponectin suppresses the development of atherosclerosis by decreasing lesion formation and expression of VCAM-1 and TNF-α in apolipoprotein E-deficient mice, a mouse model of atherosclerosis [206]. Additional studies suggest that other mechanisms may be also involved in the anti-atherogenic properties of adiponectin, including decreased oxidative stress, inhibition of NF-κB-mediated inflammation and changes in the phenotype of smooth muscle cell within atherosclerotic lesions [207-209]. Therefore, niacin may improve

atherosclerosis indirectly through increasing adiponectin secretion from adipose tissue. However, it is important to note that niacin-induced increases in plasma adiponectin concentrations are negatively correlated with insulin-mediated glucose disposal in obese subjects with NAFLD [203].

The liver is the major site of lipid metabolism and also a primary target of niacin's lipid-modifying action. In human subjects that received a single dose of niacin treatment orally, plasma triglyceride and VLDL-cholesterol levels are significantly reduced [210]. This is most likely due to decreased FFA flux to the liver resulting from decreased lipolysis in adipose tissue induced by niacin. Substrate shortage limits hepatic triglyceride and VLDL cholesterol synthesis [191]. Alterative mechanisms also have been investigated. In human hepatoblastoma cell lines, niacin significantly increases intracellular ApoB degradation by inhibiting triglyceride synthesis, leading to a decrease in ApoB-containing VLDL and LDL particles secretion [211]. Recent studies demonstrated that inhibition of DGAT2 activity, a key enzyme catalyzes the final step in triglyceride synthesis, may also contribute to the decreased triglyceride content in niacin-treated hepatocytes [212, 213].

Currently, the mechanism responsible for niacin-induced increase in plasma HDL cholesterol is less clear. One hypothesis on the cholesterol ester transfer protein (CETP)-mediated exchange of triglyceride and cholesterol between ApoB-containing lipoproteins and HDL particles has been proposed for years. This hypothesis is supported by a study in which niacin treatment results in a decrease in HDL cholesterol levels in mice that do not express CETP [214]. Moreover, in mice expressing human CETP, niacin treatment leads to an increase in HDL cholesterol concentration [214]. A subsequent study also showed a critical role of CETP in niacin's ability in increasing HDL cholesterol concentrations [195]. Niacin dose-dependently

decreases hepatic CETP expression and activity. The increased HDL cholesterol induced by niacin is lost in mice not expressing CETP [195]. Another potential mechanism involves the activation of PPARγ in macrophages. Niacin stimulates prostaglandin D2 (PGD_2) formation, the major metabolite of which is a potent PPARγ agonist. Increased PPARγ expression and transcriptional activation of scavenger receptor CD36 and cholesterol transporter ABCA1 leads to enhanced cholesterol removal from macrophages, resulting in decreased progression of atherosclerosis [215, 216].

Hepatic steatosis is characterized by excess accumulation of fat in the liver. In a rat model of hepatic steatosis, niacin prevents fat deposition in the liver through inhibition of DGAT2 [217]. In the same study, niacin treatment also regresses hepatic fat content in rats with hepatic steatosis, which makes niacin a potential therapeutic agent for treating hepatic steatosis and NAFLD [217]. More evidence reveals that niacin also inhibits fat accumulation in human hepatocytes and reduces liver fat in hypertriglyceridemic patients by suppressing DGAT2 activity [213, 218]. In addition, niacin has been demonstrated to protect the liver against fibrosis and alcoholic fatty liver disease through different mechanisms [219, 220]. In experimental liver fibrosis, niacin administration prevents fibrosis through inhibition of transforming growth factor beta (TGF-β) expression and oxidative processes [219]. Increased hepatic fatty acid oxidation and decreased hepatic DNL contributes to the positive effects of niacin in alcoholic fatty liver in rats fed with ethanol [220]. Recent studies discovered that HCA_2 receptor is expressed in hepatocyte and regulates lipid metabolism in liver [221, 222]. In HFD-fed mice, the expression of HCA_2 in hepatocytes is elevated. Niacin reduces liver triglyceride content by inhibiting lipogenesis through activation of HCA_2 [222]. Moreover, age-induced hepatic steatosis is

observed in mice lacking HCA_2 receptor with increased lipogenesis and decreased lipolysis [221].

Despite the beneficial effects of niacin in regulating lipid metabolism in liver, a number of case reports have reported hepatotoxicity in patients taking niacin, especially in SR preparations [223-228]. The typical liver injury induced by high doses of niacin includes an elevation in aminotransferase levels, liver necrosis and centrilobular cholestasis and steatosis [223, 226, 229, 230]. Acute liver failure with symptoms of nausea and vomiting is rare but has been observed in human patients [224, 227, 228]. In fact, early studies observed an increased liver fat content in rats fed a HFD in combination with 0.1% niacin compared with HFD alone [231, 232]. The mechanism of niacin-induced fatty liver in these HFD-fed rats may involve nicotinamide, a metabolite of niacin produced through the amidation pathway [232, 233]. In the liver, SAM provides methyl groups for methylation processes, including the conversion of nicotinamide to N-methylnicotinamide by nicotinamide N-methyltransferase and PC synthesis from PE catalyzed by PEMT [234]. The excess niacin intake may result in methyl group deficiency and subsequent decrease in PC formation, which plays an important role in the secretion of VLDL cholesterol from liver. Therefore, decreased transport of fat leads to an accumulation of fat in the liver and consequently hepatic steatosis.

In 2009, Thangaraju *et al*. reported that HCA_2 is also expressed in the mouse intestinal tract and human colon [235]. The expression of HCA_2 is silenced in colon cancer. After transfecting with human HCA_2 cDNA, HCA_2 agonists, including niacin, induce colon cancer cell apoptosis [235]. As a tumor suppressor, HCA_2 activated by niacin and butyrate, also inhibits breast cancer cell survival and tumor growth [236]. HCA_2 is present in several cell types in colon, including dendritic cells, macrophages and colonic epithelial cells. Activation of HCA_2

on these cells by niacin induces immunoregulatory IL-10 and cytoprotective IL-18 production, which favors the development of T regulatory cells from naïve T cell and suppresses generation of pro-inflammatory Th17 cell, thereby preventing the development of colitis and colitis-associated colorectal cancer [237]. A more recent study also supports the anti-inflammatory property of niacin in a receptor-dependent manner in a murine model of ulcerative colitis [238]. Gut microbiota have profound effects on host metabolism and health. In humans, delayed-release niacin targets the gut microbiome to increase the abundance of *Bacteroidetes* and improve biomarkers of systemic insulin sensitivity and metabolic inflammation [239]. However, the role of niacin and HCA_2 in the HFD-induced colonic inflammation and dysbiosis is less clear.

Niacin has also been demonstrated to across the blood brain barrier, especially under disease conditions with increased leakage of the blood brain barrier [240]. Through binding to the niacin receptor, HCA_2, expressed in resident microglia as well as monocytes, macrophages and neutrophils, niacin may have neuroprotective potential in neurologic diseases that involve these immune cells. There are clinical cases demonstrating niacin's ability to ameliorates symptoms of Parkinson's disease (PD) and modulates HCA_2 protein levels in white blood cells [241, 242]. In a human study of PD, Wakade *et al*. demonstrated increased HCA_2 expression in blood and brain of PD subjects compared with their age-matched controls [243]. Shortly after this study, they discovered that niacin treatment promotes a shift in macrophage polarization from pro-inflammatory M1 phenotype to anti-inflammatory M2 phenotype and reduces HCA_2 expression in macrophage in the peripheral blood, which may be associated with improved quality of life in these PD patients [244]. The ER formulation of niacin, Niaspan, has been demonstrated to have neuroprotective effects in treating stroke through multiple mechanisms,

including promoting angiogenesis, increasing synaptic plasticity and axon growth and reducing apoptosis and pro-inflammatory cytokine TNF-α expression [245-248]. In 2014, the role of HCA_2 in niacin's neuroprotective effects in ischemic stroke was recognized [249]. Niacin activates HCA_2 on monocytes and macrophages that infiltrate into the ischemic area and increases the production of neuroprotective PGD_2, resulting in decreased infarct volume [249].

Niacin has also been demonstrated to be beneficial in other disease conditions including diabetic retinopathy [250-252], chronic kidney disease [253, 254], sepsis [255, 256] and hemorrhage shock [257, 258]. The expression of HCA_2 in retina and retinal pigment epithelial cells is increased in diabetic mice and humans [250, 251]. Niacin suppresses pro-inflammatory IL-6 and MCP-1 secretion through activation of HCA_2 in ARPE cells, a human retinal pigment epithelial cell line [250]. Since inflammation is a key factor contributing to the pathogenesis of diabetic retinopathy, the anti-inflammatory effects of niacin may have therapeutic potential in treating this disease. Indeed, Niaspan improves clinical and histological outcomes of diabetic retinopathy in diabetic rats [252]. However, the beneficial effects of niacin are mediated by microRNA-126-induced vascular restoration, not a decrease in inflammation [252]. Chronic kidney disease is a condition characterized by a gradual loss of kidney function over time. Cho *et al*. demonstrated that niacin ameliorates chronic kidney failure induced pathology, including oxidative stress, inflammation, proteinuria, hypertension and dysregulated renal lipid metabolism in rats [253, 254]. Sepsis is a condition caused by the body's response to an infection, which could be life-threatening in severe conditions. Niacin alone or in combination with selenium attenuates sepsis-induced lung injury and improves survival in a rodent model of sepsis. This beneficial effect of niacin may be associated with decreased lung inflammation mediated by down-regulation of the NF-κB pathway [255, 256]. Hemorrhage shock occurs in severe blood

loss which leads to insufficient oxygen supply to the tissues. Death follows quickly if the patient is left untreated. Niacin treatment improves the survival rate of hemorrhage shock in part by reducing lung inflammation and damage, which is mediated by HCA_2 [257, 258].

As a vitamin, niacin can be sufficiently acquired from a non-corn-based diet. Severe deficiency of niacin will cause pellagra, which leads to death if left untreated. At pharmacological doses, niacin possesses beneficial effects in various disease conditions, including dyslipidemia, obesity, atherosclerosis, NAFLD, colon inflammation and colorectal cancer, neurological diseases, diabetic retinopathy, chronic kidney disease, sepsis and hemorrhage shock (Table 1). However, the use of niacin may be associated with side effects, including skin flushing, hepatic toxicity, mild hyperglycemia and insulin resistance. The effects of niacin are in part mediated by its receptor, HCA_2, expressed in adipocytes, immune cells, colonic epithelial cells and retina pigment epithelial cells. Future use of niacin should be considered in treating diseases other than dyslipidemia. Since niacin is available over the counter, people that take niacin should be aware of the adverse effects, especially for those who have diabetes and liver disease.

Mouse Strains

A number of mouse models, including inbred strains, have been utilized in studies of obesity and associated metabolic diseases. Mice within an inbred strain have identical genetic backgrounds achieved by ten or more generations of successful brother to sister mating, which allows researchers throughout the world to use the same animals with the same phenotype. Inbred strains are also used to create genetically engineered strains, including transgenic, KO and knockin mice, to test the physiological functions of a specific gene. C57BL/6J (B6) mice are the

Disease	Effects	Mechanism	Ref*
Obesity	↓ Adipose tissue inflammation	↑ **Adiponectin** ↓ CLS number	[193]
Atherosclerosis	↓ Atherosclerotic lesion size ↓ Vascular inflammation	↑ ABCG1 and cholesterol efflux ↓ MCP-1 and VCAM-1 ↑ HO-1 and adiponectin	[196, 199, 206]
NAFLD	↓ Triglyceride	↓ DGAT2	[213, 217, 218]
Colorectal Cancer and Colitis	↓ Intestinal inflammation ↓ Number and size of the colon polyps	↑ **IL-18, IL-10, and Aldh1a**	[238]
Parkinson's Disease	↓ Rigidity ↓ Bradykinesia	Likely ↓ Neuro-inflammation	[241, 242]
Stroke	↓ Infract size ↑ Angiogenesis ↑ Synaptic plasticity	↑ **PGD_2** ↑ TACE ↑ VEGF, Ang1, and eNOS	[245-248]
Diabetic Retinopathy	↓ Inflammation ↓ BRB leakage	↓ IL-6 and MCP-1 ↑ MicroRNA-126 and its target gene	[250, 252]
Chronic Kidney Disease	↓ Hypertension ↓ Proteinuria ↓ Tubulointerstitial injury ↓ Glomerulosclerosis ↓ Renal lipids	↓ MCP-1, PAI-1, TGF-β, p47phox, p22phox, Cox-1, and NF-kB ↓ CD36, ChREBP, LXR, ABCA-1, ABCG-1, and SR-B1 ↑ PPAR-a and L-FABP	[253, 254]
Sepsis	↓ Lung inflammation ↓ Lung damage ↑ Survival	↓ NF-kB ↑ NFE2L2	[255, 256]
Hemorrhage Shock	↓ Lung inflammation ↓ Lung damage ↑ Survival	↓ **NF-kB, TNF-a, IL-6, IL-8**	[257, 258]

Table 1: Summary of the beneficial effects of niacin in various disease states. *Reference; Mechanisms in bold are HCA_2 receptor dependent.

most commonly utilized inbred strain in metabolic studies due to their susceptibility to the development of diet-induced obesity, T2D and NAFLD. The well-known leptin deficient *ob/ob* mice at the Jackson Laboratory were developed from the B6 inbred strain and have been extensively phenotyped. These *ob/ob* mice have mild hyperglycemia and marked hyperinsulinemia, with hypertrophy and hyperplasia of the islets of Langerhans. In contrast, *ob/ob* mice developed with another congenic strain, C57BK/KsJ, have severe diabetes, marked hyperglycemia and temporarily elevated insulin levels associated with atrophy of the islets of Langerhans [259]. Therefore, deletion of the *ob* gene in different mouse strains results in different phenotypes, indicating the importance of genetic background in the phenotype of transgenic mice.

Due to the availability of multiple embryonic stem cell lines, the 129 inbred mice have been widely used in the production of targeted mutations [260]. However, most genetically modified strains produced with 129-derived embryonic stem cells are usually backcrossed to B6 mice for 5 to 10 generations, resulting in a mixed B6;129 background (e.g. adiponectin knockout mice, The Jackson Laboratory, Stock No: 008195). Mice that are backcrossed for 10 generations to an inbred strain (e.g. B6) are considered as congenic mice. Researchers often choose B6 mice as controls for these congenic mice and omit 129 embryonic stem cell-derived genetic background effects, which leads to the problem of passenger genes [261]. The passenger genome typically contains mutations in the regions flanking the target gene, named as passenger mutations, which may influence the phenotype in genetically modified mice [262]. For example, *Panx1* null mice generated with 129-derived embryonic stem cells and backcrossed to B6 for 5 generations are resistant to LPS-induced death and hypothermia. In contrast, *Panx1* deficient mice generated from B6-derived embryonic stem cells are susceptible to LPS-induced death and

hypothermia [262]. These conflicting findings demonstrate that the phenotype in *Panx1* null mice is associated with their genetic background not the deletion of *Panx1* gene. There are approximately 8000 genetically modified mice derived from 129 embryonic stem cells, which comprise 80% of total systemically genetic modified mice [262]. Passenger mutations are found in 99.5% of these mouse lines [262]. Therefore, it is of great importance to choose appropriate controls for the mutant strains with mixed background.

B6129SF2/J (B6129) are F2 hybrid mice generated by intercrossing the F1 hybrid offspring from B6 females and 129S1/SvImJ males. The Jackson Laboratory generated these F2 hybrid mice to serve as approximate controls for mixed B6;129 background strains. They are better appropriate controls than F1 hybrids because F2 hybrid population carries a unique combination of alleles that are segregating between the two parental strains, which makes their genetic background similar to the mixed background of the mutant strains.

B6129 mice have been studied as controls for various genetically modified strains, including 5LOX-deficient [263], IL-1R1 KO [264, 265], TNFR1/2 KO [266, 267], Cav-1 KO [268], 3XTg-AD [269, 270] and Tg2576 mice [271], which have been used in studies of anxiety, sleep deprivation, wound healing and Alzheimer's disease. However, only a limited number of studies have characterized physiological and metabolic changes of B6129 mice in response to diet-induced obesity compared those responses with that of B6 mice. When fed a HFD containing 15% dietary fat, 1% cholesterol and 0.5% cholic acid for 14 weeks, 129 mice have significantly higher percent fat, BMI, plasma triglyceride and HDL concentrations and lower non-HDL levels than B6 mice [272, 273]. B6129 mice (F2 hybrids) display parameters intermediate between and significantly different from those of the parental strains, including percent fat, BMI, plasma triglyceride, HDL and non-HDL levels [272, 273]. In addition, 129

mice do not develop fatty-streak aortic lesions when fed a HFD, but B6 mice do [272]. In this study, B6129 mice (F2 progeny) are separated into two groups with one group having no or small lesions that resemble the 129 parental strain, with the other group having large lesions similar to the B6 parental strain [272]. Similarly, both male and female 129 mice display greater percent fat than that of B6 mice after feeding an atherogenic diet containing 50 Kcal% glucose, 32 Kcal% fat, 1% cholesterol and 0.5% cholic acid for 8 weeks [274]. The percent fat of B6129 mice (F2 progeny) also falls between that of B6 and 129 parental strains [274]. Interestingly, there is a sex difference between 129 and B6 mice when fed a chow diet. The percent fat is significantly higher in male 129 than B6 mice, whereas no difference is observed in female mice. Under chow diet conditions, the percent fat of B6129 mice (F2 hybrids) are more similar to that of B6 mice, especially in males [274].

Long-term HFD induces higher body weight, fat pad weight, fasting glucose and total cholesterol in B6129 mice, which can be used as a model of insulin resistance [275]. Furthermore, B6129 mice are susceptible to the development of diet-induced NAFLD and hepatocellular cancer [276]. After feeding a high-fat western diet and high fructose/glucose sugar water up to 52 weeks, B6129 mice have increased body weight, liver weight, aspartate aminotransferase and alanine aminotransferase levels and plasma total and LDL cholesterol concentrations [276]. During these 52 weeks, B6129 mice sequentially develop a fatty liver, steatohepatitis, advanced fibrosis and finally liver tumors, which can be used as a model of NAFLD and hepatocellular cancer [276]. However, both of the parental strains have milder histological changes within the liver and are less insulin resistant than B6129 mice [276]. B6 mice also do not develop hepatocellular cancer as observed in B6129 mice [276]. As B6129

mice are being more frequently used as controls in various studies, additional studies are needed to address the unique features of B6129 mice, including their metabolic characteristics.

Conclusions and Objectives

Obesity is serious health problem that has great impact on adipose tissue, liver and gut physiology and functions. In obesity, adipose tissue expands to accommodate excess dietary fat, which results in hypoxia, adipocyte dysfunction and altered secretory adipokine profile. Together with increased secretion of pro-inflammatory cytokines from adipocyte, macrophage activation and recruitment leads to an inflammatory environment in adipose tissue. The inflamed adipose tissue is insulin resistant, leading to increased flux of non-esterified fatty acids (NEFA) to the liver. Increased ectopic fat accumulation in liver has been observed in obese individuals, which leads to the development of hepatic steatosis. The major lipid component in liver is triglyceride. There are four mechanisms contributing to changes in hepatic triglyceride content, including FA transporter-mediated FA uptake, enzyme and transcriptional factor controlled DNL, FA breakdown through FA oxidation and phospholipid-associated VLDL secretion. In recent years, the role of the gut microbiota in obesity and metabolic disease has been extensively studied. Obesity is associated with altered gut microbiota composition, abnormal SCFA production, impaired gastrointestinal barrier integrity and endotoxemia induced by increased plasma LPS levels. As a result of these obesity-induced changes in adipose tissue, liver and gut structure and function, Konrad and Wueest proposed a gut-adipose-liver axis in the development of the metabolic syndrome, suggesting an important role of the cross talk among these tissues [277] (Figure 1).

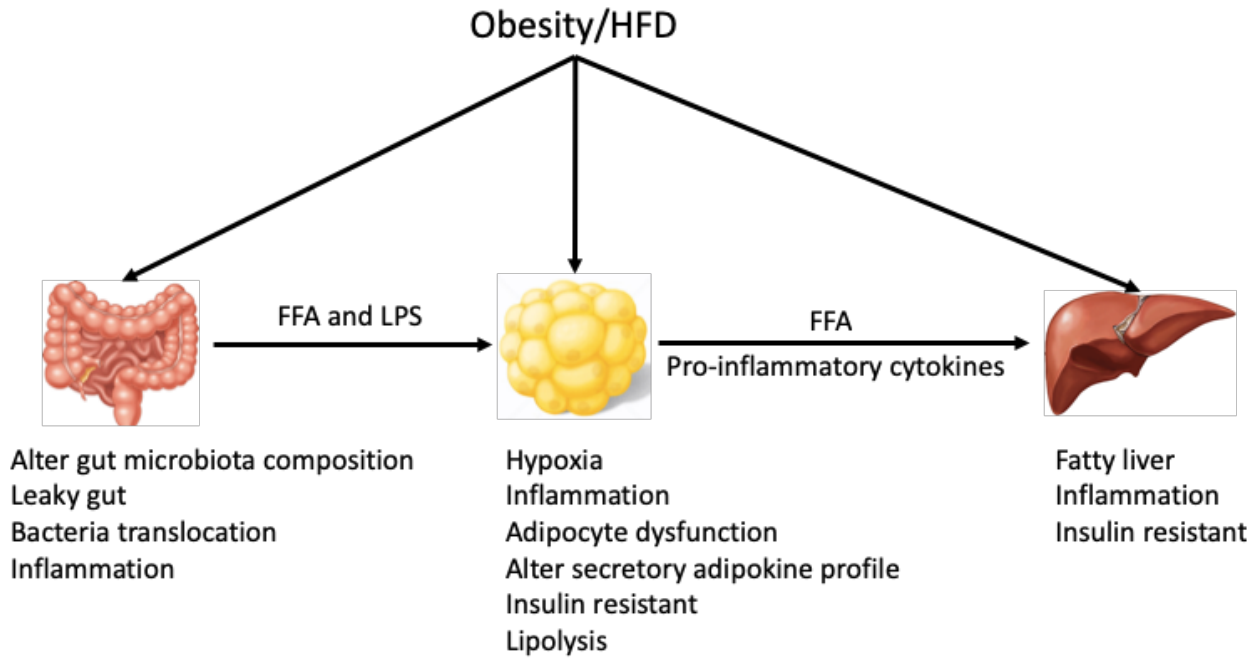

Figure 1: Effects of obesity/HFD on gut, adipose tissue and liver. HFD consumption alters gut microbiota composition, induces intestinal inflammation, impairs intestinal barrier integrity and promotes bacteria translocation. Due to increased Gram-negative bacteria and leaky gut, serum LPS levels are elevated, leading to low-grade systemic inflammation. Adipose tissue stores excess fat from diet, leading to adipose tissue expansion and obesity. Abnormal enlargement of adipose tissue leads to hypoxia, adipocyte dysfunction and altered secretory adipokine profile. Together with increased secretion of pro-inflammatory cytokines by adipocytes, macrophage activation and recruitment lead to an inflammatory environment in adipose tissue. The inflamed adipose tissue is insulin resistant, leading to increased flux of FFA to the liver. The increased ectopic fat accumulation in the liver results in the development of hepatic steatosis, which can progress to steatohepatitis with inflammation and insulin resistance.

Previous studies from our laboratory demonstrate that niacin increases adiponectin and has anti-inflammatory property in adipose tissue of diet-induced obese B6 mice through the activation of HCA_2 receptor [193, 202]. However, whether the anti-inflammatory effect of niacin in adipose tissue is observed in B6129 mice is not known and is a major component of this dissertation. Theoretically, niacin activates HCA_2 receptor on adipocytes and inhibits lipolysis, which leads to decreased FFA flux to the liver and substrate shortage for hepatic triglyceride synthesis, thereby decreasing fat accumulation in the liver. In fact, niacin treatment decreases hepatic triglyceride content in a rat model of NAFLD through inhibition of DGAT2 activity [217]. However, whether niacin is therapeutic in treating HFD-induced NAFLD in mice is not known. In addition, Singh *et al.* demonstrated that activation of HCA_2 receptor via niacin suppresses colonic inflammation and carcinogenesis [237]. However, whether niacin is beneficial for obesity-induced dysbiosis in gut microbiota and colonic inflammation has not been studied. Therefore, the goals of this dissertation were to comparatively assess the impact of HFD and niacin on 1) adipose tissue inflammation, 2) NAFLD development, and 3) gut microbiota composition in B6 and B6129 mice.

Chapter 2

Differential Effects of High-Fat Diet and Niacin on Adipose Tissue Inflammation and Nonalcoholic Fatty Liver Disease in C57BL/6J and B6129SF2/J Mice

Abstract

Background: Mice fed a high-fat diet (HFD) develop obesity, which can progress to nonalcoholic fatty liver disease (NAFLD). Pharmacological doses of niacin improve adipose tissue inflammation and NAFLD in rodents chronically fed a HFD. However, recent mouse studies have demonstrated significant differential responses to HFD in commonly utilized strains of mice. **Objectives:** To comparatively assess the impact of HFD and niacin on adipose tissue inflammation and NAFLD development in C57BL/6J (B6) and B6129SF2/J (B6129) mice. **Methods:** Thirty-two male B6 and thirty-two male B6129 mice were randomized into four groups: Chow/Vehicle (CV), Chow/Niacin (CN), HFD/Vehicle (HV), and HFD/Niacin (HN). They were fed either a chow (10% fat) or HFD (60% fat) for 20 weeks. Niacin (360 mg/kg/day) or vehicle was added to the drinking water from week 5 until the end of the study. **Results:** HFD-fed mice gained more weight than chow-fed mice of both strains. Adipose tissue crown-like structure (CLS) number was increased in HFD-fed mice of both strains, with a greater increase observed in B6 mice. Liver/body weight ratio, liver triglyceride content and NAFLD score were increased in HFD-fed B6 mice. In contrast, only NAFLD score was increased in HFD-fed B6129 mice. Niacin decreased body weight in B6 mice and increased liver weight in

B6129 mice. Niacin decreased CLS number in HFD-fed B6129 mice, but not B6 mice. Niacin had no impact on liver/body weight ratio, triglyceride content, or NAFLD score in B6 mice. However, niacin increased all three parameters in HFD-fed B6129 mice. **Conclusions:** B6 and B6129 mice develop adipose tissue inflammation and NAFLD after HFD feeding, but to a lesser degree in B6129 mice. Niacin has no impact on NAFLD development in B6 mice but potentiated hepatic steatosis in HFD-fed B6129 mice. Researchers should consider the metabolic differences between B6 and B6129 mice when choosing appropriate controls for study design.

Background

Obesity is a global epidemic, with approximately one-third of the world's population obese or overweight [2]. During the course of obesity development, adipose tissue undergoes extensive remodeling to dynamically adjust to excess nutrient consumption [278]. Adipose tissue expansion and remodeling is characterized by both adipocyte hyperplasia and hypertrophy. Rapidly expanding adipose tissue becomes hypoxic, leading to adipocyte cell death [279]. Macrophages surround and engulf dead adipocytes, resulting in crown-like structure (CLS) formation. Hypoxic and inflamed adipose tissue is insulin resistant, leading to decreased adiponectin secretion and increased flux of non-esterified fatty acids (NEFA) to the liver. In the liver, free fatty acids from adipose tissue and diet re-esterify and promote the synthesis of intrahepatic triglycerides, which play a critical role in the development of nonalcoholic fatty liver disease (NAFLD) [280].

Niacin, also known as vitamin B3 and nicotinic acid, has been used to treat dyslipidemia for decades by lowering plasma triglycerides, very low-density lipoprotein-cholesterol (VLDL),

and low-density lipoprotein-cholesterol (LDL) concentrations and increasing high-density lipoprotein-cholesterol (HDL) levels [281, 282]. More recent studies have demonstrated that pharmacological doses of niacin increase plasma adiponectin concentrations and decrease adipose tissue inflammation in a receptor-dependent manner [193, 283]. Ganji *et al*. demonstrated that niacin prevents NAFLD development and promotes NAFLD regression in rats fed a HFD and also inhibits triglyceride accumulation in hepatocytes through inhibition of diglyceride acyltransferase 2 (DGAT2), a key enzyme in triglyceride synthesis [213, 217].

C57BL/6J (B6) mice are commonly used as controls for various knockout mice used in diabetes, obesity, cardiovascular, immunological and neurobiology research. B6129SF2/J (B6129) mice are F2 hybrid mice generated by intercrossing the F1 hybrid offspring from B6 females and 129S1/SvImJ males. They are used as control mice for various genetically engineered strains, including 5LOX-deficient [263], IL-1R1 KO [264, 265], TNFR1/2 KO [266, 267], Cav-1 KO [268], 3XTg-AD [269, 270] and Tg2576 mice [271], which have been used in studies of anxiety, sleep deprivation, wound healing, and Alzheimer's disease. B6129 mice are a more appropriate control for mixed B6;129 background strains than either of the parental strains or the F1 hybrid mice, because the F1 hybrid mice are heterozygous at all loci and not segregating as opposed to those in the mixed genetic background mutant mice. A limited number of studies have demonstrated physiological differences between B6 and B6129 mice fed a HFD. Almind and Kahn demonstrated that when fed a HFD for 18 weeks, B6 and B6129 mice have similar weight gain, plasma leptin and insulin concentrations [284]. However, B6129 mice are distinct from B6 mice in their susceptibility to develop diet-induced NAFLD and hepatocellular cancer [276]. After feeding high fat western diet and high fructose/glucose sugar water up to 52 weeks, B6 mice have milder histological changes within the liver and are less

insulin resistant than B6129 mice [276]. B6 mice also do not develop hepatocellular cancer as observed in B6129 mice [276]. Furthermore, in a series of 14-week HFD studies, B6129 mice have higher plasma triglycerides, percent fat, body mass index, and plasma HDL than B6 mice [272, 273]. Besides these metabolic differences, total and vertebral bone mineral density of B6129 mice is also higher than B6 mice [285]. Even though both B6 and B6129 mice are used as control mice in metabolic studies, the metabolic impact of HFD and drug administration on B6129 mice is still not clear.

Therefore, in the present study we comparatively assess the impact of HFD and niacin in both B6 and B6129 mice by evaluating body and tissue weight, plasma metabolic profile, adipose tissue inflammation and the development of NAFLD.

Materials and Methods

Materials

Niacin (nicotinic acid) was purchased from Sigma-Aldrich (St. Louis, MO).

Animal studies

All animal studies were approved by the Auburn University Institutional Animal Care and Use Committee prior to initiation. Male 3-week-old C57BL/6J (B6; n=32) and B6129SF2/J mice (B6129; n=32) were purchased from The Jackson Laboratory (Bar Harbor, ME). All mice were housed with a 12 h light/dark cycle at 20-22°C and had *ad libitum* access to food and water. After two days of acclimatization, mice were placed on a chow diet (10 kcal % fat; D12450J) or a high-fat diet (HFD; 60 kcal % fat; D12492) from Research Diets (New Brunswick, NJ) for 20 weeks. At week 5, niacin (360 mg/kg/day) or vehicle was added to the drinking water until the

end of the study. Food intake was measured every 8 days. At week 20, mice were fasted for 5 h and euthanized by decapitation. Whole blood was collected and serum was isolated. Epididymal white adipose tissue (eWAT) and liver were collected and weighed. Portion of these tissues were flash frozen in liquid nitrogen and then stored at −80°C, while another portion of the tissues was fixed in 10% neutral buffered formalin.

Serum analysis

Fasting blood glucose was determined using the AccuChek Active Handheld glucometer (Roche, Indianapolis, IN). Serum insulin and total adiponectin concentrations were measured using ELISA kit from Millipore (Temecula, CA). Serum NEFAs were measured using a kit from Wako Chemicals (Richmond, VA).

Real-time PCR

RNA was isolated from eWAT and liver using E.Z.N.A.® Total RNA Kit II and E.Z.N.A.® Total RNA Kit I (Omega Bio-tek, Norcross, GA), respectively with on-column DNA digestion using RNase-free DNase Set I (Omega Bio-tek, Norcross, GA). RNA (1 μg) was reverse transcribed into cDNA using iScript cDNA Synthesis Kit (Bio-Rad, Hercules, CA). PCR primers used in the real-time-PCR analysis were previously published [193]. Analyses were performed on a Bio-Rad CFX96 Touch™ Real-Time PCR Detection System (Bio-Rad, Hercules, CA). Samples were analyzed in 20 μl reactions using SYBR Green FastMix for iQ (Quantabio, Beverly, MA). All expression levels were normalized to the corresponding 36B4 mRNA levels, and analyzed using the $2^{-\Delta\Delta CT}$ method [286]. 36B4 levels were unchanged in response to HFD or niacin treatment.

Histopathological analysis

Formalin fixed eWAT and liver tissues were processed, and paraffin embedded. Five micron thick, hematoxylin and eosin (H&E) stained sections were used for evaluation. eWAT and liver slides were scanned using the Aperio ScanScope scanner (Vista, CA). eWAT slides were evaluated on VisioPharm software (Hoersholm, Denmark) for adipocyte size and number. CLS number was counted for each slide and then normalized by 1000 adipocytes. A board-certified pathologist evaluated liver slides based on a modified NAFLD scoring system for rodent models [287]. Evaluation criteria included macrovesicular steatosis, microvesicular steatosis, hepatocellular hypertrophy and inflammation.

Statistical analysis

All data are presented as the mean ± SEM. Statistical analyses, including One-way ANOVA followed by Tukey's post-hoc test, were performed on Graph Pad Prism 8 Software (La Jolla, CA). Significance was set $P < 0.05$.

Results

HFD and niacin differentially impact metabolic parameters in B6 and B6129 mice

There was no statistical difference in body weight in any of the groups at the beginning of the study (data not shown). No difference in food intake was observed in any of the groups during the course of study (Figure 2). At week 20, body weight was significantly increased in HFD-fed mice of both strains. B6129 mice weighed approximately 3.7 g (↑ 7.1 %) more than B6 mice after 20 week on a HFD (Table 2). Niacin treatment decreased end point body weight in HFD-fed B6 mice, but not B6129 mice.

Compared with mice maintained on a chow diet, eWAT weight was not different in mice of both strains after 20 weeks of HFD feeding (Table 2). However, HFD-fed B6129 mice had a trend towards increased eWAT weight compared with chow-fed mice. Niacin had no effect on eWAT weight in either B6 or B6129 mice. Liver weight was increased in HFD-fed mice of both strains, but to a lesser degree in B6129 mice (Table 2). Unexpectedly, niacin treatment increased liver weight in HFD-fed B6129 mice but had no effect in B6 mice.

Fasting glucose was not significantly affected between chow and HFD-fed B6 mice (Table 2). However, it was increased in HFD-fed B6129 mice due in part to the fact that the chow-fed B6129 mice had a lower plasma glucose concentration than the B6 mice (Table 2). Plasma insulin concentration and HOMA-IR were increased in both strains of mice fed a HFD (Table 2). Plasma adiponectin and NEFA were decreased in HFD-fed B6 mice. In B6129 mice, NEFA level was also significantly decreased in HFD-fed mice, but adiponectin was unchanged. Niacin treatment increased plasma adiponectin in chow-fed mice of both strains, but had no effect in HFD-fed mice. Taken together, these data indicate that both B6 and B6129 mice fed a HFD develop obesity and insulin resistance. However, when compared with B6 mice, B6129 mice have higher body and eWAT weight, but lower liver weight after 20 weeks of HFD feeding. In addition, plasma adiponectin concentrations were decreased in HFD-fed B6 mice, but not B6129 mice.

HFD increases greater adipose tissue inflammation in B6 mice than in B6129 mice

Although no difference was observed in eWAT weight in B6 mice, eWAT/body weight ratio was decreased in HFD-fed mice, due to an increase in body weight (Figure 3). eWAT/body weight ratio was lower in chow-fed B6129 mice than B6 mice, due to a lower eWAT weight in

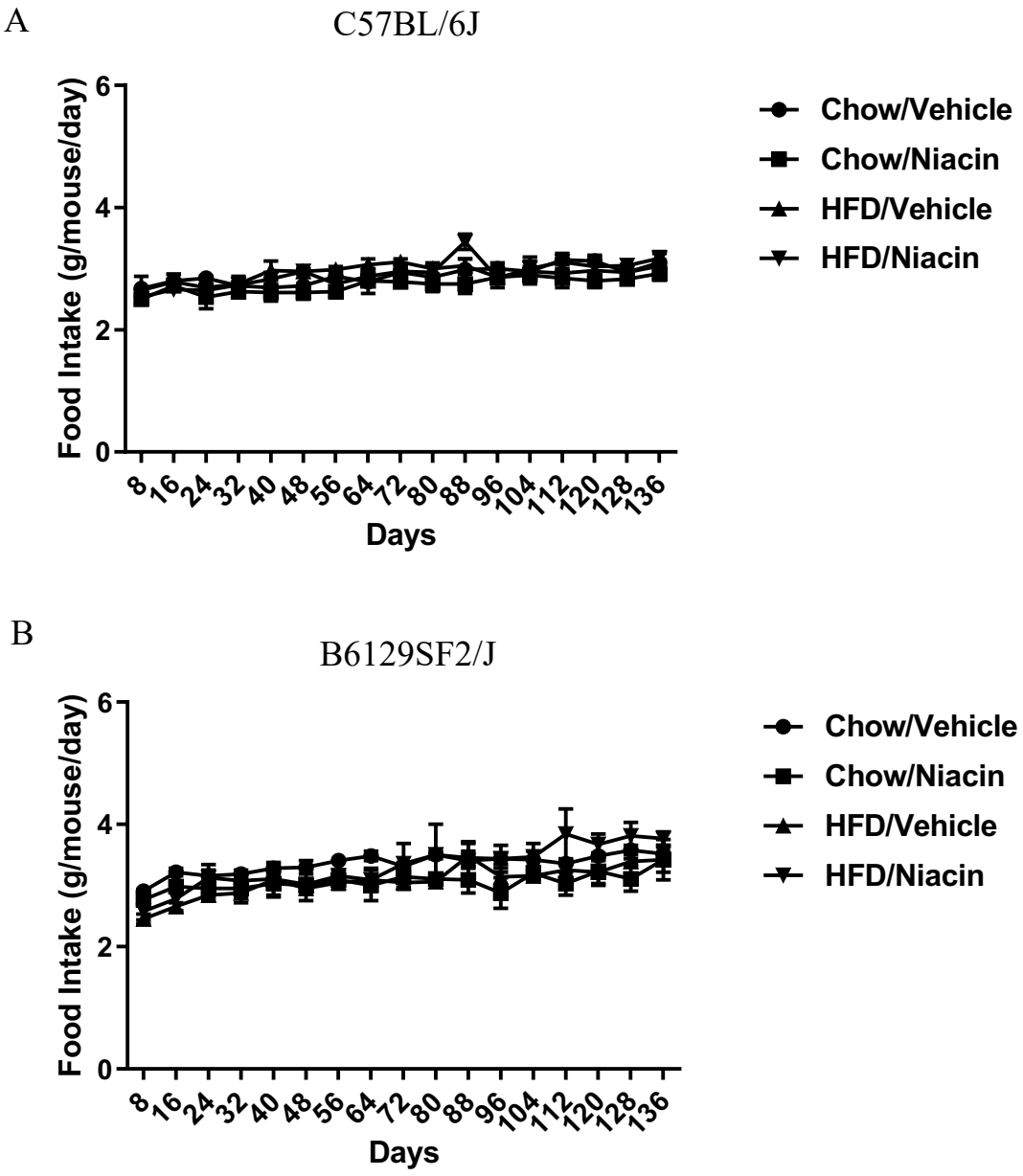

Figure 2. Food intake in (A) B6 and (B) B6129 mice.

	C57BL/6J				B6129SF2/J			
	Chow Diet		High-Fat Diet		Chow Diet		High-Fat Diet	
	Vehicle	Niacin	Vehicle	Niacin	Vehicle	Niacin	Vehicle	Niacin
Body Weight (g)	36.6 ± 0.9	34.6 ± 1.1	51.9 ± 1.0[a]	47.4 ± 1.0[ab]	38.9 ± 1.2	36.3 ± 1.5	55.6 ± 1.1[a]	52.2 ± 1.6[a]
eWAT Weight (g)	1.59 ± 0.12	1.62 ± 0.15	1.66 ± 0.19	1.50 ± 0.19	1.31 ± 0.15	1.12 ± 0.15	1.91 ± 0.19	1.48 ± 0.19
Liver Weight (g)	1.25 ± 0.05	1.32 ± 0.07	2.75 ± 0.19[a]	2.41 ± 0.19[a]	1.41 ± 0.06	1.28 ± 0.08	2.03 ± 0.12[a]	2.70 ± 0.19[ab]
Glucose (mg/dL)	161.8 ± 9.2	165.9 ± 5.9	182.5 ± 10.2	186.6 ± 8.1	123.1 ± 6.3	130.8 ± 9.4	170.4 ± 15.5[a]	144.8 ± 9.1
Insulin (ng/mL)	3.53 ± 0.52	4.92 ± 0.81	14.93 ± 1.97[a]	14.25 ± 1.32[a]	5.73 ± 0.58	4.31 ± 0.96	17.30 ± 3.20[a]	23.75 ± 3.85[a]
HOMA-IR	37.0 ± 6.3	51.4 ± 7.7	174.3 ± 24.4[a]	169.7 ± 15.5[a]	45.2 ± 5.2	37.8 ± 10.0	183.2 ± 32.2[a]	211.5 ± 25.7[a]
Adiponectin (mg/mL)	10.67 ± 0.37	13.01 ± 0.33[b]	8.38 ± 0.52[a]	9.97 ± 0.66[a]	9.66 ± 0.52	12.50 ± 0.67[b]	9.61 ± 0.53	8.50 ± 0.86[a]
NEFA (mMol)	1.00 ± 0.08	0.98 ± 0.08	0.48 ± 0.02[a]	0.52 ± 0.03[a]	0.94 ± 0.10	0.99 ± 0.09	0.50 ± 0.02[a]	0.60 ± 0.05[a]

Table 2. Effects of HFD and niacin on metabolic parameters in B6 and B6129 mice. [a]$P<0.05$ indicates difference between chow diet and HFD; [b]$P<0.05$ indicates difference between vehicle and niacin. Values are mean ± SEM.

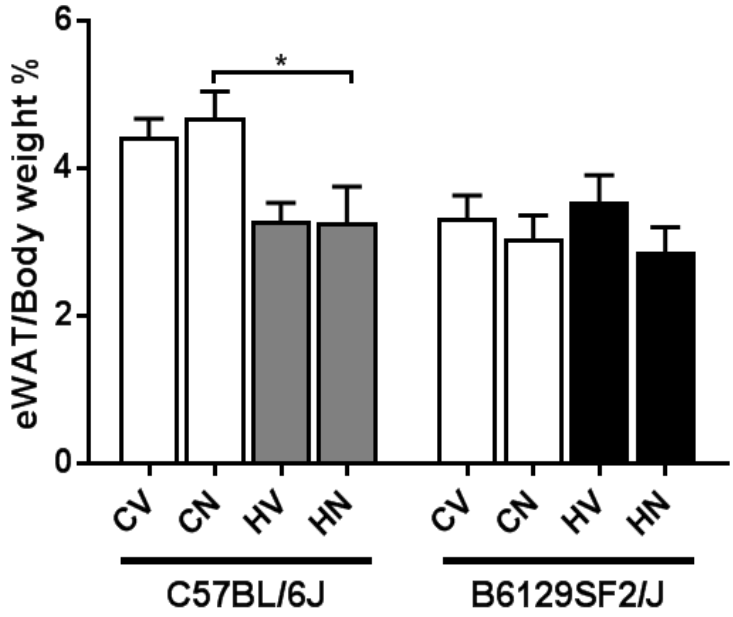

Figure 3. eWAT/body weight ratio in B6 and B6129 mice.

B6129 mice (Figure 3). CLS number, a hallmark feature of adipose tissue inflammation, was increased in HFD-fed mice of both strains, but it was higher in B6 mice (Figure 4A and C). The average adipocyte area did not change in any of the groups in both strains of mice, suggesting adipocyte hypertrophy was limited at week 20 (Figure 4B). Niacin treatment decreased CLS number in HFD-fed B6129 mice but not B6 mice (Figure 4C). In summary, HFD-induced adipose tissue inflammation is greater in B6 mice than B6129 mice. In addition, niacin decreased adipose tissue inflammation in B6129 mice, but had no effect in B6 mice. Additional evaluation of adipose tissue inflammation was assessed by gene expression of pro-inflammatory cytokines. MCP-1 gene expression was significantly increased in both B6 and B6129 mice fed a HFD, which was decreased by niacin treatment (Figure 5A). TNF-α gene expression was increased only in HFD-fed B6 mice, but did not change in B6129 mice (Figure 5B).

Niacin potentiates NAFLD development in B6129 mice

The HFD livers of both mouse strains were enlarged and pale in color, indicating lipid accumulation in these livers (Figure 6A). However, the livers of the HFD-fed B6129 mice weighed less than B6 mice (Table 2; Figure 6A). Consistent with this data, liver/body weight ratio was increased in HFD-fed B6 mice, but unchanged in B6129 mice fed a HFD (Figure 6B). Similarly, liver triglyceride content was increased in HFD-fed B6 mice, but not B6129 mice (Figure 6C). Niacin had no impact on appearance or weight of HFD-fed livers in B6 mice (Table 2; Figure 6A and B). However, when HFD-fed B6129 mice were treated with niacin, the livers became enlarged and paler in color (Table 2; Figure 6A). Niacin treatment also increased liver/body weight ratio and triglyceride content in HFD-fed B6129 mice but had no impact on B6 mice (Figure 6B and C).

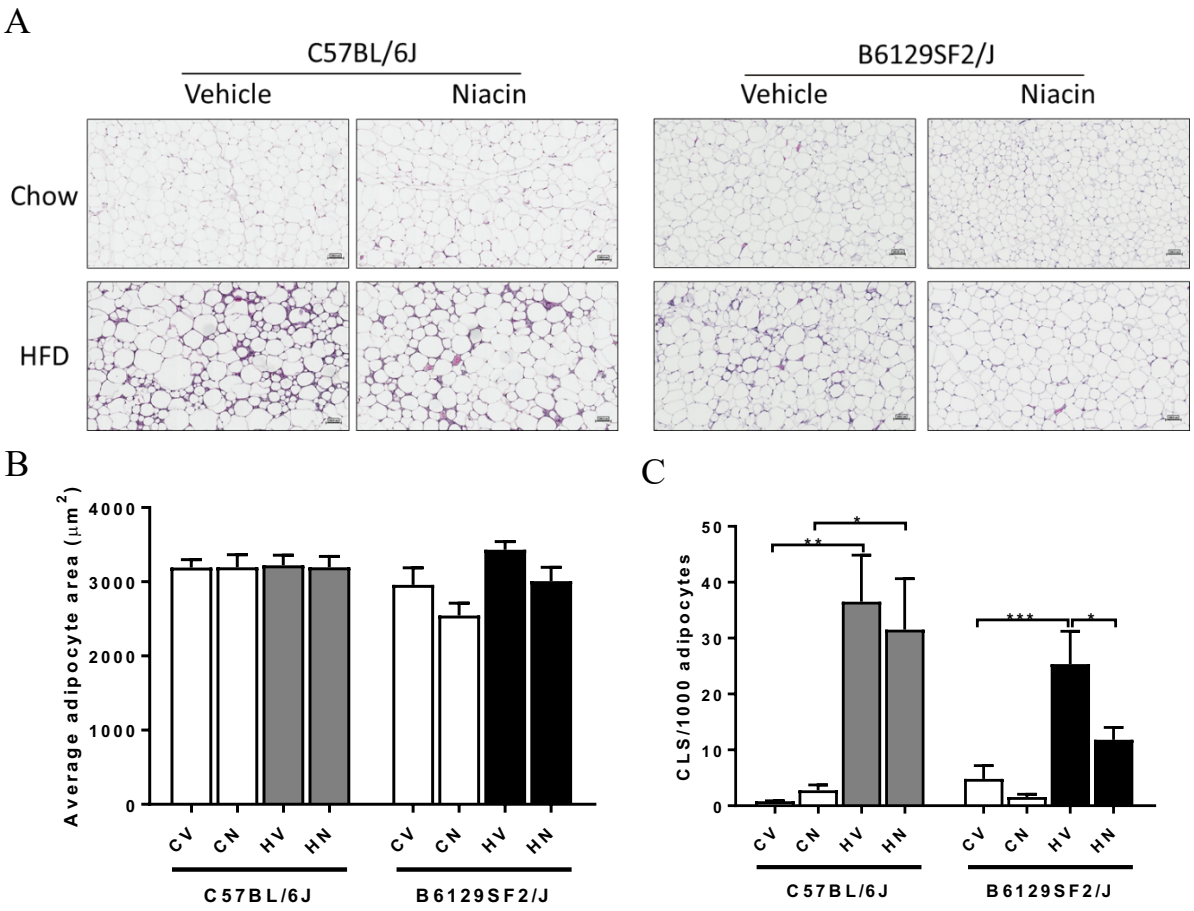

Figure 4. HFD induced adipose tissue inflammation greater in B6 than B6129 mice. (A) Representative images of H&E stained eWAT sections. (B) Average adipocyte area. (C) Crown-like structure number. *P<0.05, **P<0.01, ***P<0.001.

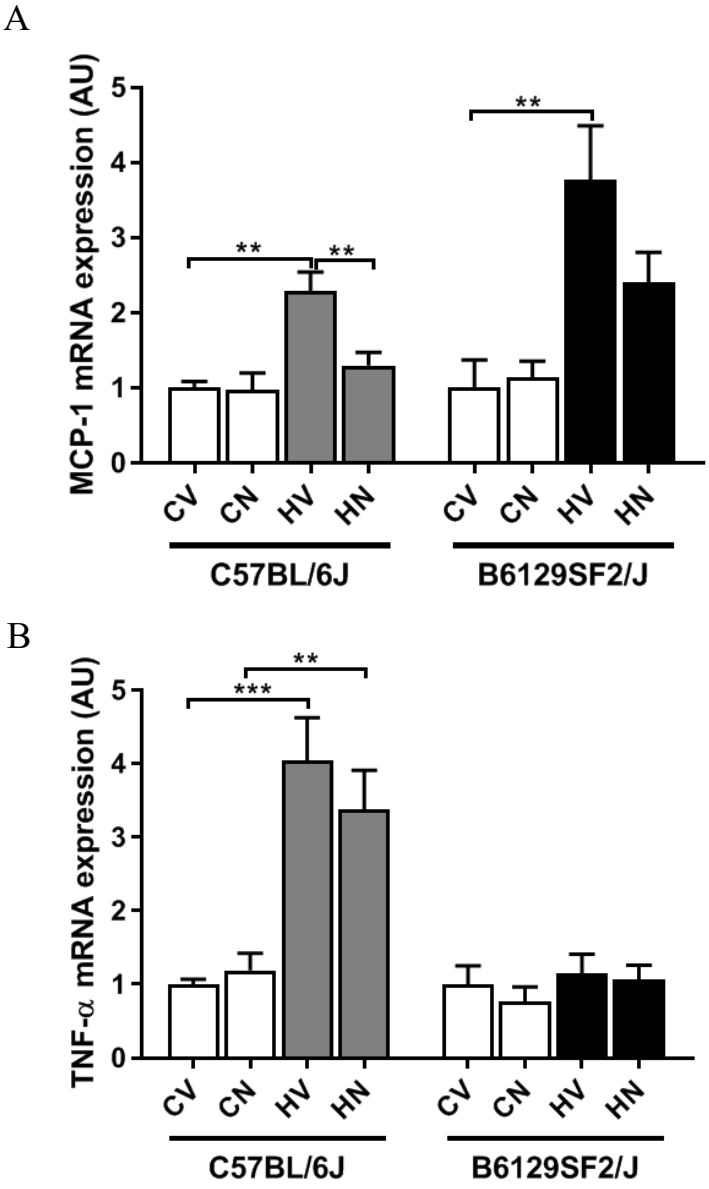

Figure 5. Pro-inflammatory cytokine gene expression in eWAT of B6 and B6129 mice. (A) MCP-1. (B) TNF-α. $^{**}P<0.01$, $^{***}P<0.001$.

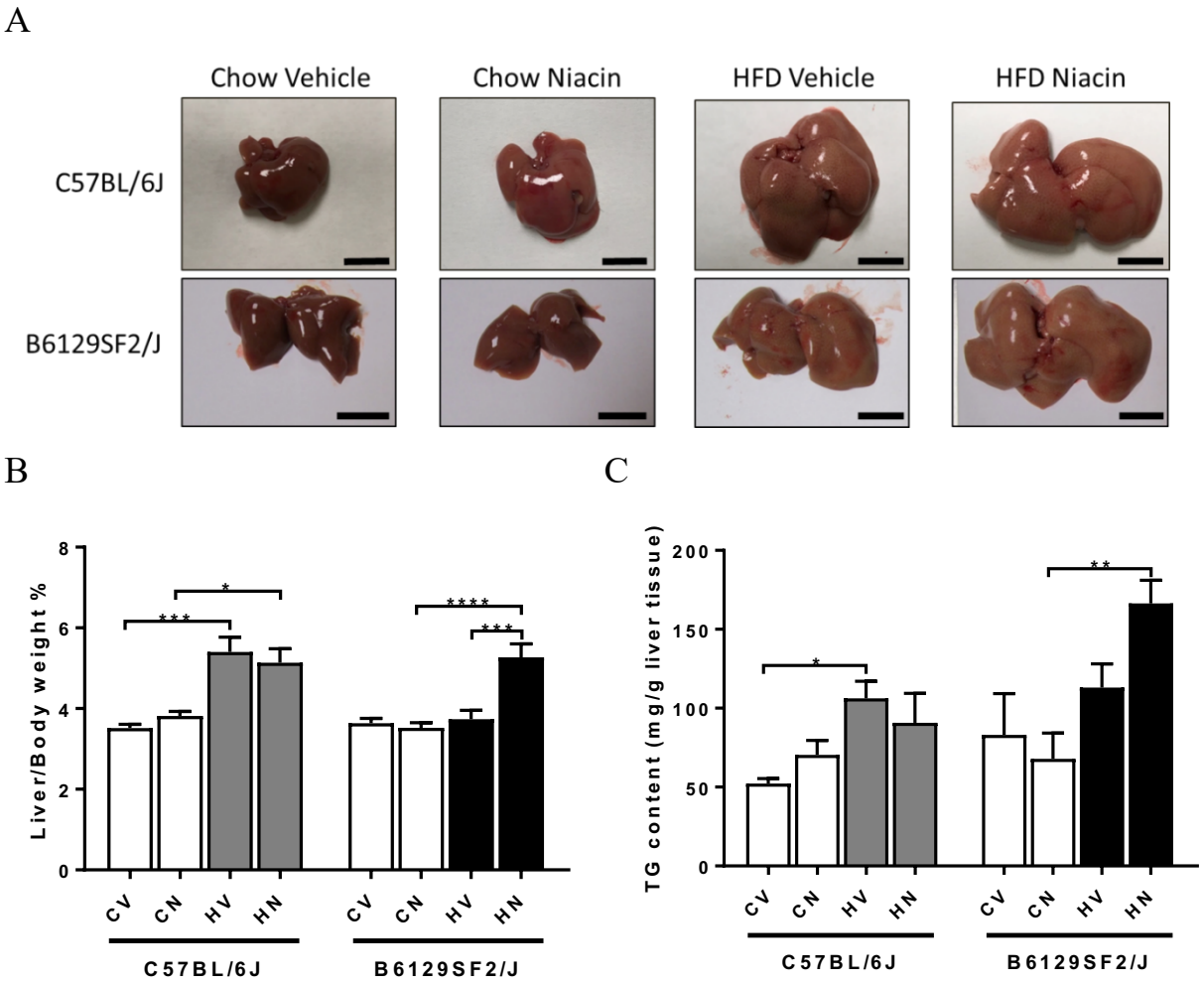

Figure 6. Niacin increases liver steatosis in HFD-fed B6129 mice but not B6 mice. (A) Representative liver pictures. (B) Liver/body weight ratio. (C) Liver triglyceride content. **P*<0.05, ***P*<0.01, ****P*<0.001, *****P*<0.0001.

In order to evaluate the development of NAFLD, the H&E stained liver sections were evaluated for macrovesicular steatosis, microvesicular steatosis, hypertrophy, and inflammation (Figure 7A). Macrovesicular steatosis, characterized by large lipid vacuoles in the hepatocytes that displace the nucleus to the side, did not change in HFD-fed B6 or B6129 mice (Figure 7B). In contrast, microvesicular steatosis, characterized by small lipid droplets present within the hepatocytes, was increased in both strains of mice fed a HFD (Figure 7C). Hypertrophy score was significantly increased in HFD-fed B6129 mice but not B6 mice (Figure 7D). Niacin increased macrovesicular steatosis and microvesicular steatosis score in HFD-fed B6129 mice, which was not observed in B6 mice (Figure 7B-D). The sum of these three scores was utilized to calculate NAFLD score. NAFLD score was significantly increased in both strains of mice fed a HFD (Figure 7E). Interestingly, niacin treatment resulted in an even higher NAFLD score in HFD-fed B6129 mice, which was not observed in B6 mice (Figure 7E). Inflammation was also evaluated in these liver sections by counting the number of inflammatory foci per field, but was very minimal, indicating hepatic steatohepatitis was not developed in either strains of mice at week 20. Inflammation was further evaluated by gene expression of pro-inflammatory cytokines. MCP-1 gene expression was significantly increased in HFD-fed B6 mice and further increased with niacin treatment, but did not change in B6129 mice (Figure 8A). TNF-α gene expression did not change in B6 and B6129 mice with either HFD feeding or niacin treatment (Figure 8B). All together, these data demonstrate that the livers of B6 and B6129 mice fed a HFD for 20 weeks respond similarly with regard to macrovesicular steatosis, microvesicular steatosis, and hypertrophy. Treatment of these HFD-fed mice with niacin has no effects on these NAFLD parameters in B6 mice, while dramatically increasing them in B6129 mice.

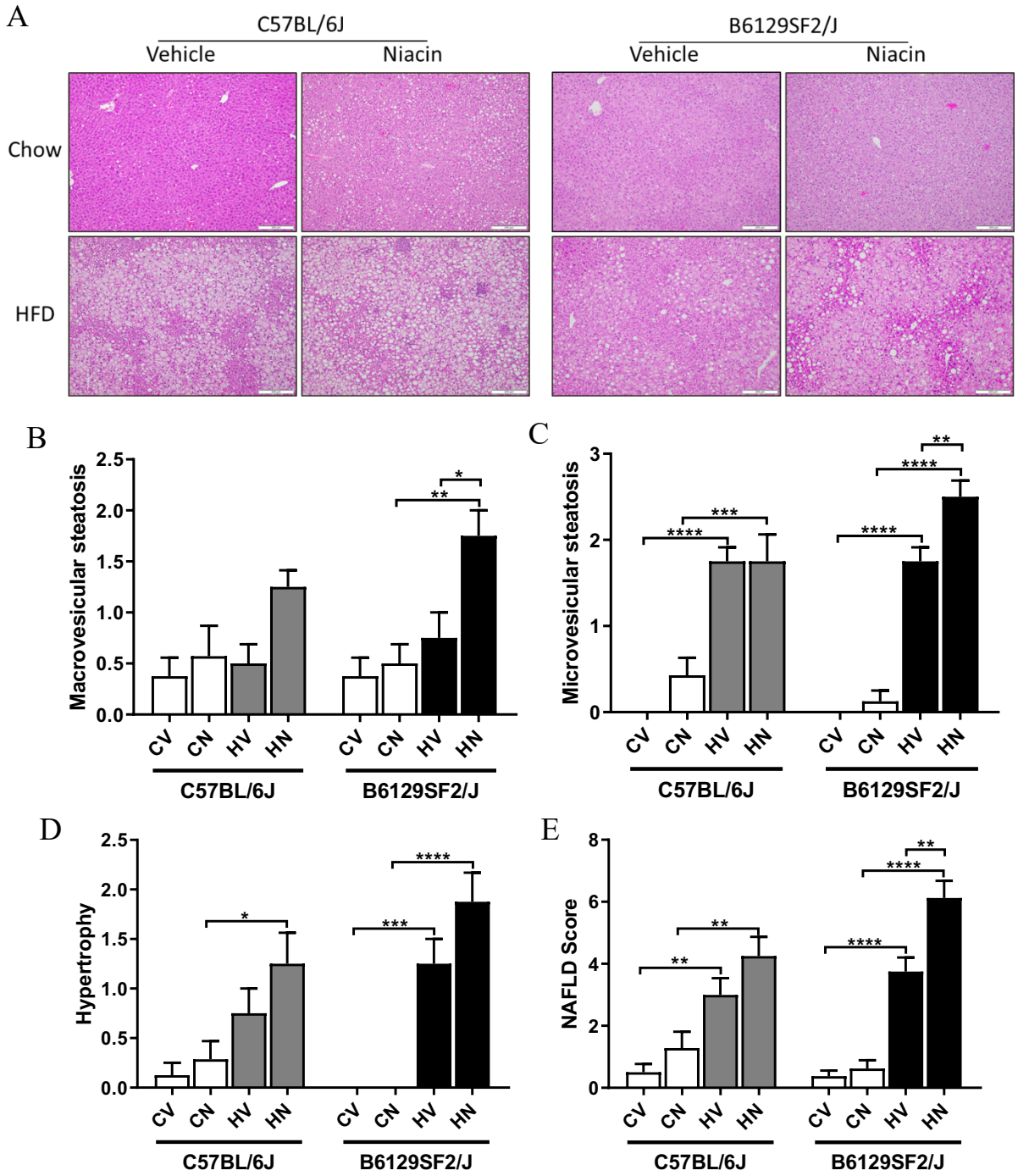

Figure 7. Niacin potentiates NAFLD development in B6129 mice. (A) Representative images of H&E stained liver sections. (B) Macrovesicular steatosis score. (C) Microvesicular steatosis score. (D) Hypertrophy score. (E) NAFLD score. *P<0.05, **P<0.01, ***P<0.001, ****P<0.0001.

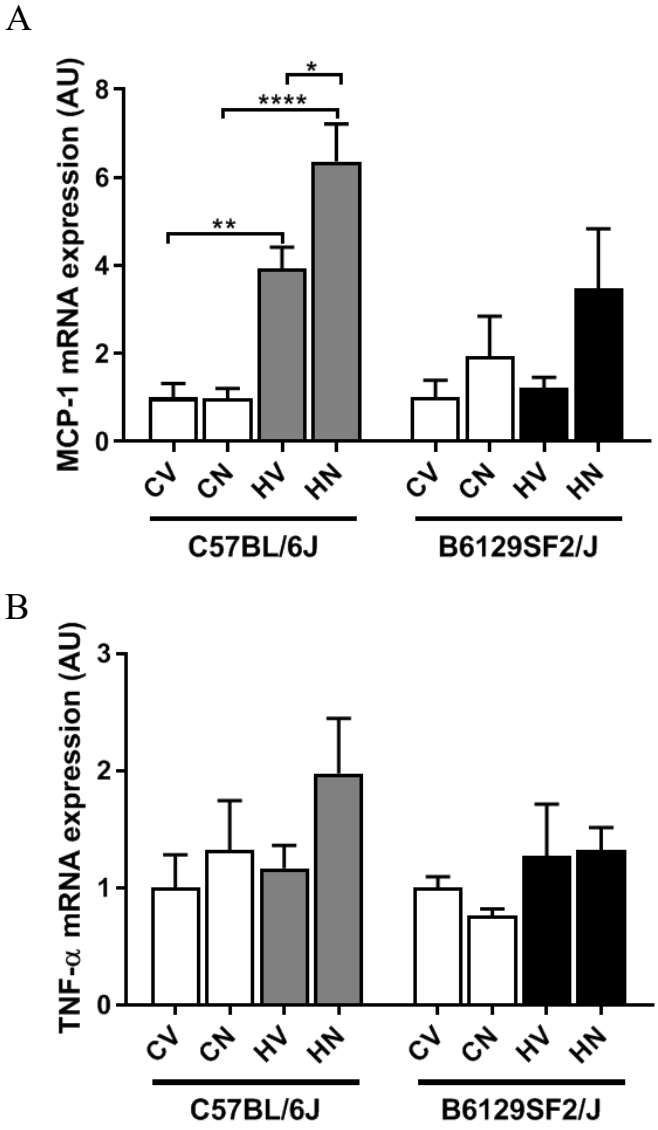

Figure 8. Pro-inflammatory cytokine gene expression in liver of B6 and B6129 mice. (A) MCP-1. (B) TNF-α. *P<0.05, **P<0.01, ****P<0.0001.

Discussion

B6 mice are the most widely used inbred mouse strain in studies of obesity development and other metabolic disorders. In HFD-fed B6 mice, eWAT expands during the early weight gain phase of obesity development and reaches maximum hypertrophy when the mice weigh approximately 40 g [288]. Adipocyte hypertrophy increases local tissue hypoxia, resulting in adipocyte cell death and the infiltration of macrophages [279, 289]. Macrophages invade adipose tissue and surround dead adipocytes to form CLS, with increasing CLS number associated with increased adipocyte death [288]. In line with this, eWAT weight peaks when the mouse body weight is around 40 g and decreases as they continue to gain weight, with ectopic fat distribution occurring in other organs, including the liver [288]. Therefore, there is an inverse association between eWAT weight and liver weight after the peak point [289]. Increases in insulin resistance and decreases in plasma adiponectin and NEFAs are also observed in obese B6 mice [290, 291].

In contrast to B6 mice, limited information is known about the metabolic impact of a HFD on B6129 mice. In our current study, we discovered B6129 mice fed a HFD for 20 weeks have a significantly different metabolic profile compared with B6 mice. Specifically, even though the overall weight gain trend was similar between the B6 and B6129 mice, B6129 mice gained slightly more weight than B6 mice when fed a HFD for 20 weeks. This weight difference is due in part to a greater total fat content in B6129 mice [274], as we observed that eWAT weight was higher in HFD-fed B6129 mice than B6 mice. Despite the increased total body and eWAT weight, CLS number and liver weight were less in HFD-fed B6129 mice compared with HFD-fed B6 mice. These data suggest that eWAT expandability is greater in B6129 mice and the peak point of eWAT expansion is higher than 40 g of body weight. It is also important to

note that adiponectin was decreased in HFD-fed B6 mice, but not B6129 mice. Adiponectin exerts anti-inflammatory properties by modulating macrophage functions in various disease conditions, including obesity [204]. Therefore, the higher level of adiponectin in HFD-fed B6129 mice may contribute to the lower adipose tissue CLS number. Fasting glucose was increased in B6129 mice but not B6 mice. Indeed, previous studies have shown that the B6129 mice develop insulin resistance quicker than B6 mice when fed a HFD [276]. Overall, B6129 mice had less adipose tissue inflammation, smaller liver size, and unchanged plasma adiponectin concentrations compared with B6 mice after HFD feeding. These data demonstrated that the impact of HFD on B6129 mice is not as metabolically dramatic as on B6 mice. Of the two parent strains of B6129 mice, B6 is obesity-prone, while 129 is obesity-resistant. Thus, with the mixed B6;129 genetic background, the B6129 mice may be more resistant to HFD-induced obesity than B6 mice.

Niacin has been used as a lipid lowering drug in different formulations, including immediate, extended, and sustained-release preparations. In our study, niacin was added to the drinking water so that the mice were consuming niacin as they drank water throughout the day. In this way, niacin administration is more like the sustained-release formulation, which produces fewer side-effects (e.g. flushing) but increased risk of hepatotoxicity [229]. In the liver, niacin is metabolized through two major metabolic pathways, resulting in the formation of nicotinuric acid and nicotinamide, respectively [292]. Nicotinamide supplementation has been reported to reduce body weight gain in rats fed a 12% casein diet [233]. We also observed decreased body weight in niacin treated mice, but only noted a significant change in B6 mice. Since the food intake was comparable among the groups, the decrease in body weight caused by niacin is more likely due to increased energy expenditure [293].

At pharmacologic doses, niacin has been demonstrated to have anti-inflammatory properties, mediated by activation of the hydroxycarboxylic acid receptor 2, in adipose tissue, immune cells and colonic epithelium [238, 294]. Specifically, previous studies from our lab have demonstrated that niacin decreases adipose tissue inflammation and increases adiponectin in B6 mice fed a HFD for 11 weeks [193]. In the current study, niacin significantly decreased CLS in HFD-fed B6129 mice, but not B6 mice. A possible explanation for this in B6 mice could be increased adipose tissue inflammation after 20 weeks on HFD compared with 11 weeks. In this case, the greater adipose tissue inflammation in HFD-fed B6 mice at 20 weeks is of sufficient magnitude that niacin is unable to overcome it.

After 20 weeks HFD feeding, B6 mice had significantly increased normalized liver weight and triglyceride content, which was not observed in B6129 mice. These findings suggest that B6129 mice are protected from HFD-induced fatty liver. More recent *in vitro* and *in vivo* studies demonstrate that niacin reduces hepatic fat accumulation through inhibition of DGAT2 [213, 217]. However, under our study conditions, niacin had no effect on triglyceride content and NAFLD score in B6 mice, but significantly increased the triglyceride content and NAFLD score in HFD-fed B6129 mice. Previous studies have demonstrated that, under certain conditions, niacin administration can induce fatty liver in rats and hepatotoxicity in humans [223, 225, 231-233, 295, 296]. The mechanism responsible for increased triglyceride accumulation and hepatic steatosis with niacin administration include choline deficiency [232], methyl depletion [233, 234], and impaired β-oxidation [231]. These mechanisms may be also associated with B6129 mice resisting to HFD-induced hepatic steatosis. Further study is needed to explore the mechanism that underline niacin-induced fatty liver in B6129 mice.

Conclusions

We describe the metabolic changes in B6 and B6129 mice fed a HFD and/or niacin. B6 and B6129 mice respond to HFD and/or niacin differently as far as adipose tissue inflammation and NAFLD development. B6129 mice are more resistant to the effect of HFD than B6 mice, since they have unchanged plasma adiponectin concentrations, less adipose tissue CLS number, and lower liver weight when fed a HFD for 20 weeks. Niacin has no impact on the development of NAFLD in B6 mice, but significantly potentiates hepatic steatosis in B6129 mice. This study provides the metabolic profile of two commonly used controls for various mutant mice. Researchers should consider the metabolic differences between HFD-fed B6 and B6129 mice particularly when determining appropriate controls for study design.

Chapter 3

Metabolomics and Lipidomics Analysis Reveal the Mechanisms of Niacin-Induced Nonalcoholic Fatty Liver Disease in B6129SF2/J Mice

Abstract

Background. Recently, niacin has been demonstrated to reduce fat accumulation in NAFLD through inhibition of DGAT2. However, in the previous chapter, niacin increases the hepatic triglyceride content and histological score in HFD-fed B6129SF2/J (B6129) mice but has no effect in C57BL/6J (B6) mice. **Objectives.** Therefore, the aim of this study was to identify the mechanisms responsible for niacin-induced fatty liver in B6129 mice using liver metabolomics and lipidomics analysis. **Methods.** Livers were collected from B6 and B6129 mice, which were fed either a chow (10% fat) or HFD (60% fat) for 20 weeks with niacin (360 mg/kg/day) or vehicle supplementation from week 5 to week 20. **Results.** Two hundred and twenty-four polar metabolites were identified in these livers. A total of 21 and 26 metabolites were identified as different between chow and HFD group in B6 and B6129 mice, respectively. In B6 mice, only 6 metabolites were identified as different with niacin treatment and no specific pathways appeared to be impacted. In contrast to B6 mice, 16 metabolites and 5 pathways were impacted by niacin in HFD-fed B6129 mice. Of the metabolites that were changed in these pathways, hydroxyphenylpyruvate (also known as 4-Hydroxyphenylpyruvate, 4-HPP) did not change with

HFD feeding but significantly decreased with niacin treatment. 4-HPP is an intermediate in the metabolism of phenylalanine/tyrosine and improves mitochondrial oxidation in rats subjected to hemorrhagic shock. Therefore, decreased 4-HPP by niacin may lead to decreased β-oxidation in the liver and subsequent lipid accumulation and liver damage in B6129 mice. Further lipidomic analysis suggested different hepatic lipid profiles with HFD and niacin treatment in B6129 mice. The abundance of phosphocholine (PC), which is critical for VLDL triglyceride production and secretion, was not altered in B6 mice with either HFD feeding or niacin treatment. In contrast, PC was increased in HFD-fed B6129 mice, and decreased with niacin treatment. **Conclusions.** Metabolomics and lipidomics analysis reveal that the mechanisms of niacin-induced hepatic steatosis in HFD-fed B6129 mice may involve decreased β-oxidation and VLDL triglyceride production and secretion.

Background

Niacin, a water-soluble B vitamin (B3), has been used as a lipid-lowering drug for more than half century [178]. When taken in pharmacological doses (2,000-3,000 mg/day vs. 15-20 mg/day as a vitamin), niacin decreases total serum cholesterol, triglycerides, VLDL and LDL cholesterol and lipoprotein(a) levels and increases HDL cholesterol levels [179-181]. Recent *in vitro* and *in vivo* studies demonstrated that niacin reduces hepatic triglyceride content in nonalcoholic fatty liver disease (NAFLD) through inhibition of diacylglycerol acyltransferase 2 (DGAT2), a key enzyme catalyze the final step in triglyceride synthesis [213, 217, 218]. However, in the previous chapter, we demonstrated that niacin treatment increases normalized liver weight, triglyceride content and liver histological score in high-fat diet (HFD)-fed B6129. Even though these findings are contradictory to the recent studies, two studies from 1960s

demonstrated that excess niacin induces fatty liver in Albino rats fed a HFD [231, 232]. Consistent with my findings, the fatty liver is not observed in rats fed a low-fat diet with a high dose of niacin supplementation [231]. Addition of 1% choline completely reverses niacin-induced fatty liver in HFD-fed rats [232]. In addition, a number of case reports have reported hepatotoxicity in patients taking large doses of niacin [223-228].

Niacin is primarily metabolized in the liver through two metabolic pathways: the conjugated pathway and amidation pathway [183]. In the conjugative pathway, niacin conjugates with glycine, resulting in the formation of nicotinuric acid. This pathway has low affinity but high capacity. In contrast, the amidation pathway has high affinity but low capacity. Therefore, the conjugative pathway is only utilized when amidation pathway is saturated [182, 186]. The products of the amidation pathway are nicotinamide and pyrimidine metabolites. Nicotinamide is the precursor for nicotinamide adenine dinucleotide (NAD) and nicotinamide adenine dinucleotide (NADP), which are two major cofactors in redox reactions and metabolism. Excessive niacin in the liver is converted to nicotinamide, which in turn is methylated to N-methylnicotinamide by nicotinamide N-methyltransferase in an S-adenosylmethionine (SAM)-dependent manner. Since SAM is the methyl donor for all endogenous and exogenous methylation reactions, the depletion of methyl groups by excessive niacin limits other methylation processes, including the conversion of phosphatidylcholine (PE) to phosphatidylethanolamine (PC) by phosphatidylethanolamine N-methyltransferase (PEMT). PE and PC are phospholipids, which are required for the assembly and secretion of VLDL particles. Therefore, it is possible that the depletion of methyl groups by excessive niacin results in decreased PC production and limited VLDL formation and secretion, which could be one of the mechanisms contributing to niacin-induced fatty liver in B6129 mice. The other possible

mechanism involves fatty acid oxidation or β-oxidation. Early studies demonstrated an increased fatty acid oxidase activity in livers of rats fed diets high in fat when compared with control animals fed a low-fat diet, which appears to be a mechanism to fight against high level of dietary fat by increasing the utilization of fat through fatty acid oxidation [231]. However, this increase in fatty acid oxidase activity is impaired by excess niacin, indicating that niacin may interfere with the adaptive response of the rats to HFD [231].

Interestingly, niacin-induced fatty liver is only observed in B6129 mice but not B6 mice, suggesting that the effects of niacin in the liver is influenced by genetic background. B6129 hybrid mice are the products of a cross between B6 females and 129S1/SvImJ (129) males. Recent studies have demonstrated that choline- and folate-deficient diets have varying effects on the severity of NAFLD liver damage among 7 inbred strains, including 129 and B6 mice [297, 298]. Choline is precursor for betaine, which provides methyl groups for the conversion of homocysteine to methionine. Dietary deficiency of methyl groups results in higher liver pathology score of hepatic lesions in 129 than B6 mice [297]. Furthermore, 129 mice have lower methionine and SAM levels than B6 mice after feeding choline- and folate-deficient diets for 12 weeks [298], indicating that 129 mice are more susceptible to methyl deficiency than B6 mice. Therefore, it is very reasonable to speculate that B6129 mice may display increased susceptibility to methyl deficiency compared with their parental strain, B6 mice.

Metabolomics and lipidomics technology has rapidly developed during the past decade. Metabolomics is the scientific study of a broad range of metabolites, including nucleotides, amino acids, carbohydrates and lipids, in various biological samples, such as cells, tissues, organs and body fluids. It provides a metabolic snapshot from specific biological source at a single time point. Mass spectrometry and nuclear magnetic resonance spectroscopy are the two

major technologies used to identify and quantify metabolites. Coupled with liquid chromatography, mass spectrometry technology enables the measurement of hundreds of metabolites within a single sample with excellent precision. The metabolic profiles are often related to pathogenic mechanisms. Therefore, metabolomics is suitable for the discovery of metabolic indicators of diseases and assisting drug development. Lipidomics is a branch of metabolomics, which has emerged as an independent field of research due to the wide diversity of lipid structures. Lipidomics involves the identification and quantification of thousands of lipid molecular species. Common extraction methods used in lipidomics includes modified folch method [299], Bligh and Dyer method [300] and more recent methyl tert-butyl ether (MTBE) method [301]. Since MTBE has very low density, the lipid-containing organic phase forms the upper layer, resolving the difficulties associated with chloroform-based methods. Lipidomics has been applied in a wide range of biomedical research, including metabolic syndrome, neurological disorders and cancer.

The goal of the current study was to identify the mechanisms responsible for niacin-induced fatty liver in B6129 mice using liver metabolomics and lipidomics analysis.

Materials and Methods

Materials

HPLC-grade 100% methanol and PBS were purchased from VWR (Radnor, PA). MTBE was purchased from J.T. Baker (Pittsburgh, PA).

Animal study

Same animal study was conducted as in chapter 2. Livers were collected for metabolomics and lipidomics analysis.

Liver metabolite extraction

Liver metabolites were extracted in 80% methanol. Briefly, ~10-15 mg of liver tissue was ground in 500 μL of 80% methanol (precooled to -80°C) on dry ice. Homogenate was vortexed for 1 min and incubated for 4 h at -80°C. Homogenate was then centrifuged at 14,000 g for 10 min at 4-8°C. Supernatant was transferred to a 1.5 mL centrifuge tube and stored at -80°C. Precipitate was re-extracted with 400 μL of 80% methanol. Supernatants from both extractions were combined and dried with a SpeedVac using no heat. Dried metabolite samples were stored at -80°C until analysis.

Liver lipid extraction

Liver lipids were extracted in MTBE/methanol. Briefly, ~5-10 mg of liver tissue was ground in 500 μL of PBS/methanol (2/15, v/v, precooled to -80°C) on dry ice. Homogenate was transferred to a 12 mL glass vial and 1.2 mL of PBS/methanol was added and vortexed for 1 min. 5 mL of MTBE was then added to the vial and then was rocked for 1 hour at room temperature. 1.2 mL of water was added to the vial and vortexed again for 1 min. Samples were centrifuged for 10 min at 1,000 g and the upper MTBE liquid phase containing the non-polar lipids was transferred to a glass tube. The lower liquid phase was re-extracted with 2 mL of MTBE/methanol/water (10/3/2.5, v/v/v). MTBE phases (~7 mL) from both extractions were combined and dried with a nitrogen stream. When MTBE phase was reduced to ~1-1.5 mL, it

was transferred to a 1.7 mL centrifuge tube and dried in a SpeedVac. Dried lipid samples were stored at -80°C until analysis.

Targeted polar metabolomics and untargeted lipidomics profiling

Mass spectrometry polar metabolite analysis and lipidomics profiling was performed at Beth Israel Deaconess Medical Center Mass Spectrometry Facility. Metabolites were measured using a 5500 QTRAP triple quadrupole mass spectrometer (AB/Sciex, Framingham, MA) coupled to a high-performance liquid chromatography system (LC-MS/MS) (Shimadzu, Kyoto, Japan) [302]. Lipid samples were analyzed using untargeted high-resolution liquid chromatography-tandem mass spectrometry (LC-MS/MS) with a hybrid QExactive Plus Orbitrap mass spectrometer (Thermo Fisher Scientific, Waltham, MA) [303].

Statistics and bioinformatics

Mouse liver metabolomics and lipidomics data was analyzed by MetaboAnalyst 4.0 (http://www.metaboanalyst.ca). Peak intensity data of all samples from each mouse strain was normalized by the liver tissue weight and data analyses were performed, including fold change analysis, one-way ANOVA, pattern searching, partial least squares discriminant analysis and hierarchical clustering analysis. Metabolic pathway analysis was performed using *Mus musculus* (KEGG) pathway library with hypergeometric test and relative-betweeness centrality.

Results

Liver metabolomics analysis reveals decreased β-oxidation contributes to niacin-induced fatty liver in B6129 mice

Two hundred and twenty-four metabolites were identified in livers of B6 and B6129 mice. MetaboAnalyst 4.0 was used to analyze the liver metabolomics data and perform pathway analysis. A comprehensive heatmap was generated to assess changes within strains in the top 50 differentially expressed metabolites that were different between B6 and B6129 mice (Figure 9). Partial least squares discriminant analysis was performed using all metabolites (Figure 10). Based on the overlapping area of the treatment groups, niacin had little impact on the targeted metabolites profile in B6 mice, but a significant impact on the metabolite profile of B6129 mice.

One-way ANOVA analysis identified a total of 29 and 46 metabolites that were significantly affected by diet and/or niacin in B6 and B6129 mice, respectively (Figure 11A and B; Table 3 and 4). In B6 mice, 21 metabolites were further identified as different between chow and HFD group (Figure 12A). Utilizing pathway analysis of these metabolites, the arginine and proline metabolism pathway was significantly affected by HFD in B6 mice (Figure 13A; Table 5). Three metabolites, guanidoacetic acid, urea, and hydroxyproline, were significantly decreased in this pathway. However, there were only 6 metabolites identified as different between the HV and HN group in B6 mice (Figure 12B), of which 3 were also affected by HFD. No pathway was identified as impacted by niacin (Figure 13C; Table 6). This supports our metabolic data demonstrating no impact of niacin on liver weight or NAFLD score in B6 mice.

In B6129 mice, 26 metabolites were identified as different between chow and HFD-fed groups (Figure 12B). Pathway analysis determined that HFD affected five pathways, including purine metabolism, amino sugar and nucleotide sugar metabolism, histidine metabolism, pyrimidine metabolism, and pentose phosphate pathway (Figure 13B; Table 7), in which 16 metabolites were found decreased. By comparing the HV and HN group, 16 metabolites were affected by niacin (Figure 12B). Seven of these metabolites were decreased in HFD-fed mice

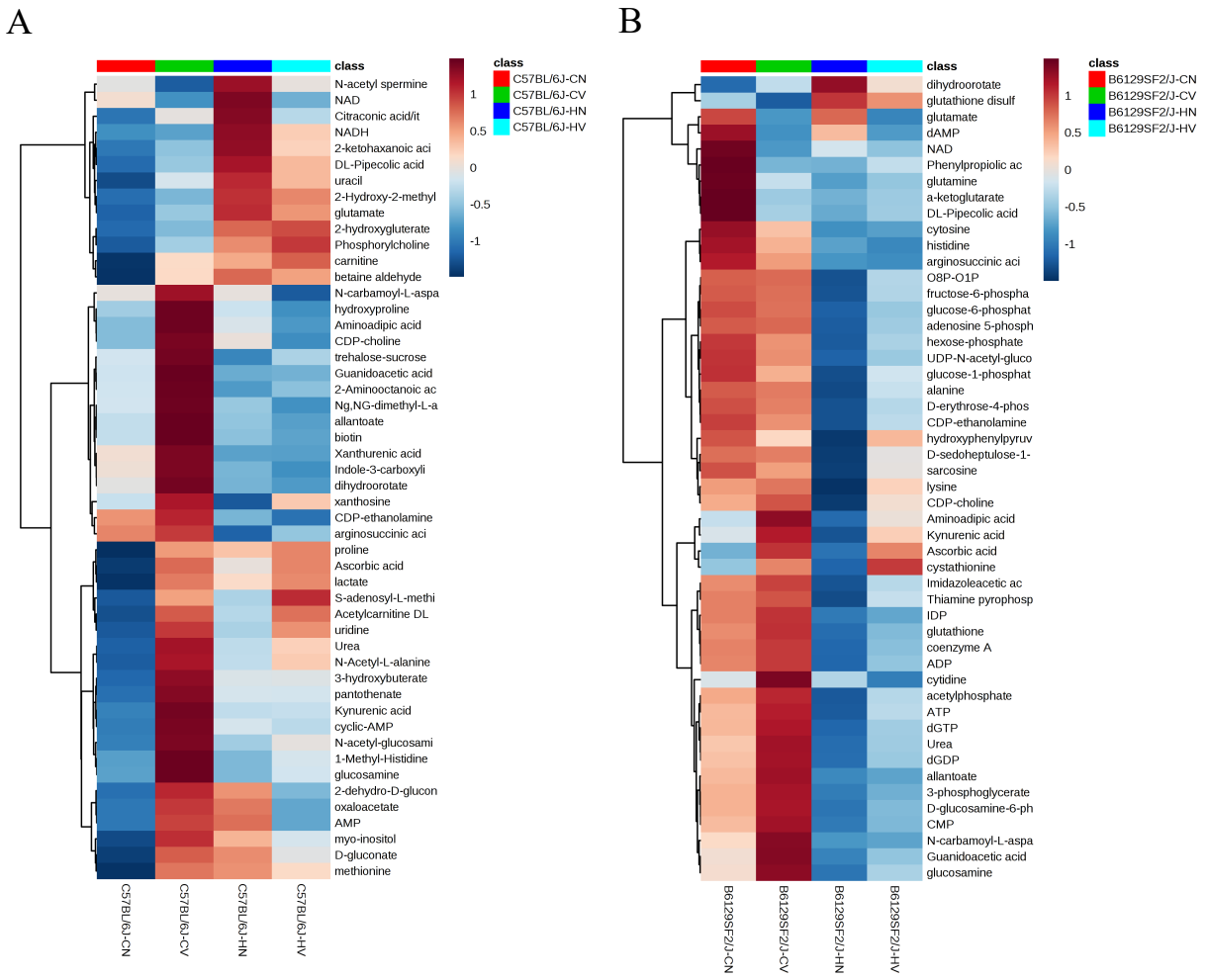

Figure 9. The clustering result of top 50 differential metabolites in (A) B6 and (B) B6129 mice in the form of a heatmap. Metabolite names were limited to an 18-character length in heatmap.

A

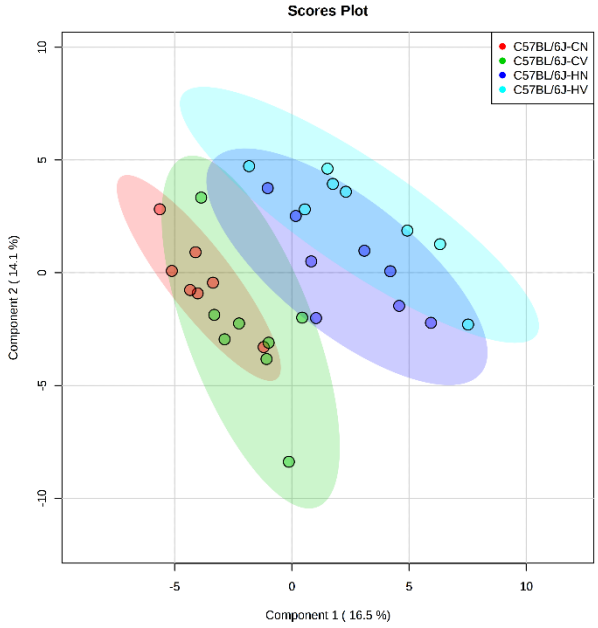

B

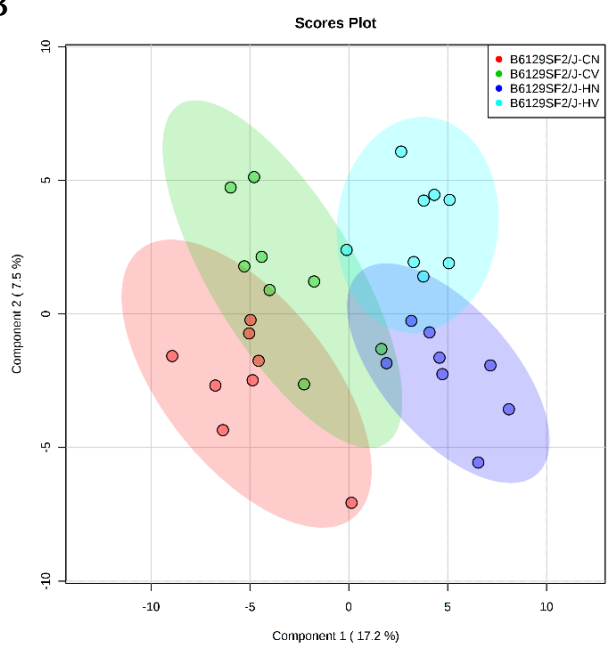

Figure 10. Partial least squares discriminant analysis of metabolites in (A) B6 and (B) B6129 mice.

A

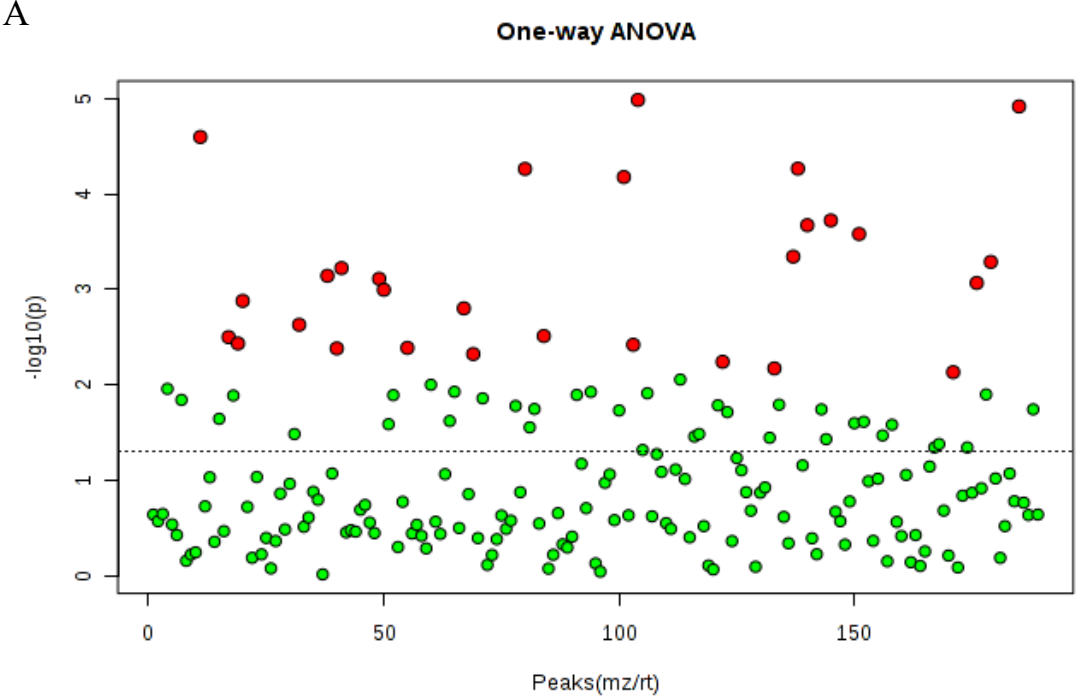

B

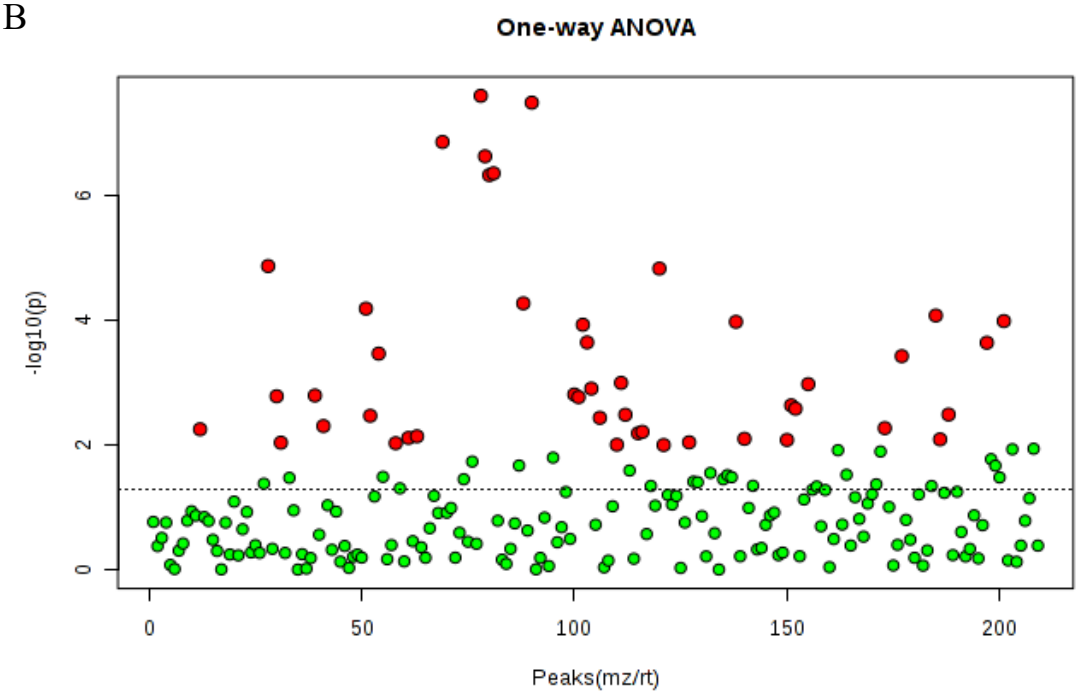

Figure 11. Significant metabolites (red dots) selected by One-way ANOVA plot with *P* value threshold 0.05 in (A) B6 and (B) B6129 mice.

Metabolites	f.value	p.value	-LOG10(p)	FDR	Fisher's LSD
Urea	14.058	1.04E-05	4.9846	0.0011452	CV - CN; HN - CN; HV - CN; CV - HN; CV - HV
N-acetyl spermine	13.786	1.21E-05	4.9166	0.0011452	CN - CV; HN - CN; HN - CV; HV - CV; HN - HV
Guanidoacetic acid	12.547	2.53E-05	4.5962	0.0015964	CV - CN; CV - HN; CV - HV
carnitine	11.335	5.43E-05	4.265	0.0020685	CV - CN; HN - CN; HV - CN
N-acetyl-glucosamine-1-phosphate	11.323	5.47E-05	4.2618	0.0020685	CV - CN; HV - CN; CV - HN; CV - HV
2-hydroxygluterate	11.022	6.66E-05	4.1766	0.0020974	HN - CN; HV - CN; HN - CV; HV - CV
Phosphorylcholine	9.4853	0.00018976	3.7218	0.0050284	HN - CN; HV - CN; HN - CV; HV - CV
1-Methyl-Histidine	9.3238	0.00021284	3.6719	0.0050284	CV - CN; CV - HN; CV - HV
Acetylcarnitine DL	9.0272	0.00026345	3.5793	0.0055325	CV - CN; HV - CN; CV - HN; HV - HN
2-Aminooctanoic acid	8.289	0.00045456	3.3424	0.0085912	CV - CN; CV - HN; CV - HV
NADH	8.1199	0.00051666	3.2868	0.0088772	HN - CN; HV - CN; HN - CV; HV - CV
Indole-3-carboxylic acid	7.9251	0.0005996	3.2221	0.0094436	CV - CN; CV - HN; CV - HV
dihydroorotate	7.6852	0.00072191	3.1415	0.010476	CV - CN; CV - HN; CV - HV
allantoate	7.5926	0.00077601	3.1101	0.010476	CV - CN; CV - HN; CV - HV
S-adenosyl-L-methionine	7.4645	0.00085815	3.0664	0.010813	CV - CN; HV - CN; HV - HN
Ascorbic acid	7.2566	0.0010119	2.9948	0.011953	CV - CN; HN - CN; HV - CN
oxaloacetate	6.9238	0.0013229	2.8785	0.014707	CV - CN; HN - CN; CV - HV; HN - HV
Xanthurenic acid	6.7035	0.0015841	2.8002	0.016633	CV - CN; CV - HN; CV - HV
2-Hydroxy-2-methylbutanedioic acid	6.229	0.0023537	2.6282	0.023413	HN - CN; HV - CN; HN - CV; HV - CV
trehalose-sucrose	5.9112	0.0030874	2.5104	0.02857	CV - CN; CV - HN; CV - HV
Citraconic acid/itaconic acid	5.879	0.0031745	2.4983	0.02857	HN - CN; HN - CV; HN - HV
N-Acetyl-L-alanine	5.7035	0.0036969	2.4322	0.031338	CV - CN; HV - CN; CV - HN
3-hydroxybuterate	5.668	0.0038136	2.4187	0.031338	CV - CN; HV - CN; CV - HN; CV - HV
myo-inositol	5.581	0.0041157	2.3856	0.031497	CV - CN; HN - CN; HV - CN
Aminoadipic acid	5.5672	0.0041662	2.3803	0.031497	CV - CN; CV - HN; CV - HV
pantothenate	5.4135	0.0047723	2.3213	0.034691	CV - CN; CV - HN; CV - HV
hydroxyproline	5.2044	0.0057532	2.2401	0.040272	CV - CN; CV - HN; CV - HV
glutamate	5.0282	0.0067468	2.1709	0.045541	HN - CN; HV - CN; HN - CV
AMP	4.9282	0.0073909	2.1313	0.048169	CV - CN; HN - CN; CV - HV; HN - HV

Table 3. Differential metabolites identified by One-way ANOVA followed by post-hoc analysis in B6 mice.

Metabolites	f.value	p.value	-LOG10(p)	FDR	Fisher's LSD
hexose-phosphate	26.4	2.59E-08	7.5863	3.48E-06	CN - HN; CN - HV; CV - HN; CV - HV; HV - HN
O8P-O1P	25.755	3.33E-08	7.4769	3.48E-06	CN - HN; CN - HV; CV - HN; CV - HV; HV - HN
D-erythrose-4-phosphate	22.262	1.42E-07	6.8475	9.90E-06	CN - HN; CN - HV; CV - HN; CV - HV; HV - HN
glucose-1-phosphate	21.077	2.41E-07	6.6182	1.26E-05	CN - HN; CN - HV; CV - HN; HV - HN
fructose-6-phosphate	19.725	4.51E-07	6.3459	1.68E-05	CN - HN; CN - HV; CV - HN; CV - HV; HV - HN
glucose-6-phosphate	19.583	4.82E-07	6.3166	1.68E-05	CN - HN; CN - HV; CV - HN; CV - HV; HV - HN
acetylphosphate	13.324	1.38E-05	4.861	0.00039445	CN - HN; CV - HN; CV - HV; HV - HN
Urea	13.172	1.51E-05	4.8211	0.00039445	CV - CN; CN - HN; CV - HN; CV - HV
D-sedoheptulose-1-7-phosphate	11.157	5.44E-05	4.2646	0.0012627	CN - HN; CV - HN; HV - HN
allantoate	10.867	6.60E-05	4.1803	0.0013798	CV - CN; CN - HN; CN - HV; CV - HN; CV - HV
glutathione	10.492	8.52E-05	4.0696	0.0016185	CN - HN; CN - HV; CV - HN; CV - HV
coenzyme A	10.197	0.0001045	3.9809	0.0017283	CN - HN; CN - HV; CV - HN; CV - HV
Imidazoleacetic acid	10.156	0.0001075	3.9686	0.0017283	CN - HN; CN - HV; CV - HN; CV - HV; HV - HN
ADP	10.004	0.0001196	3.9223	0.0017855	CN - HN; CN - HV; CV - HN; CV - HV
dGDP	9.0978	0.00022937	3.6395	0.0030316	CN - HN; CV - HN; CV - HV
NAD	9.0818	0.00023209	3.6344	0.0030316	CN - CV; CN - HN; CN - HV
N-carbamoyl-L-aspartate	8.5432	0.00034686	3.4598	0.0042644	CV - CN; CV - HN; CV - HV
D-glucosamine-6-phosphate	8.4197	0.00038094	3.4191	0.0044231	CN - HN; CV - HN; CV - HV
ATP	7.1707	0.0010184	2.9921	0.011163	CN - HN; CV - HN; CV - HV
histidine	7.1121	0.0010682	2.9714	0.011163	CN - HN; CN - HV; CV - HN; CV - HV
IDP	6.9119	0.0012591	2.8999	0.012531	CN - HN; CN - HV; CV - HN; CV - HV
Thiamine pyrophosphate	6.6518	0.0015634	2.8059	0.014423	CN - HN; CV - HN
dihydroorotate	6.6074	0.0016227	2.7898	0.014423	HN - CN; HV - CN; HN - CV; HN - HV
a-ketoglutarate	6.5751	0.0016675	2.7779	0.014423	CN - CV; CN - HN; CN - HV
adenosine 5-phosphosulfate	6.5347	0.0017252	2.7632	0.014423	CN - HN; CN - HV; CV - HN; CV - HV
glutamine	6.1815	0.0023312	2.6324	0.018739	CN - CV; CN - HN; CN - HV
glutamate	6.0391	0.0026364	2.579	0.020407	CN - CV; CN - HV; HN - CV; HN - HV
dAMP	5.7915	0.0032737	2.485	0.023774	CN - CV; CN - HV
dGTP	5.7828	0.0032988	2.4816	0.023774	CN - HN; CV - HN; CV - HV
Ascorbic acid	5.7396	0.0034268	2.4651	0.023873	CV - CN; HV - CN; CV - HN; HV - HN
CDP-ethanolamine	5.6534	0.0036985	2.432	0.024935	CN - HN; CN - HV; CV - HN
Aminoadipic acid	5.3168	0.0050012	2.3009	0.032664	CV - CN; CV - HN; CV - HV
cytidine	5.2319	0.0054015	2.2675	0.03421	CV - CN; CV - HN; CV - HV
Guanidoacetic acid	5.1854	0.0056353	2.2491	0.03464	CV - CN; CV - HN; CV - HV
glutathione disulfide	5.0825	0.0061916	2.2082	0.036973	HN - CN; HN - CV; HV - CV
UDP-N-acetyl-glucosamine	5.0247	0.0065299	2.1851	0.03791	CN - HN; CN - HV; CV - HN
Kynurenic acid	4.904	0.0073	2.1367	0.041235	CV - HN; HV - HN
3-phosphoglycerate	4.8392	0.0077531	2.1105	0.042583	CN - HN; CV - HN; CV - HV
DL-Pipecolic acid	4.8059	0.007998	2.097	0.042583	CN - CV; CN - HN; CN - HV
CMP	4.7827	0.0081725	2.0876	0.042583	CN - HN; CV - HN; CV - HV
lysine	4.7593	0.0083537	2.0781	0.042583	CN - HN; CV - HN; HV - HN
cytosine	4.6662	0.0091158	2.0402	0.044685	CN - HN; CN - HV
Phenylpropiolic acid	4.6536	0.0092244	2.0351	0.044685	CN - CV; CN - HN; CN - HV
hydroxyphenylpyruvate	4.6328	0.0094074	2.0265	0.044685	CN - HN; CV - HN; HV - HN
CDP-choline	4.5717	0.0099655	2.0015	0.045763	CN - HN; CV - HN; HV - HN
alanine	4.5605	0.010072	1.9969	0.045763	CN - HN; CV - HN

Table 4. Differential metabolites identified by One-way ANOVA followed by post-hoc analysis in B6129 mice.

A

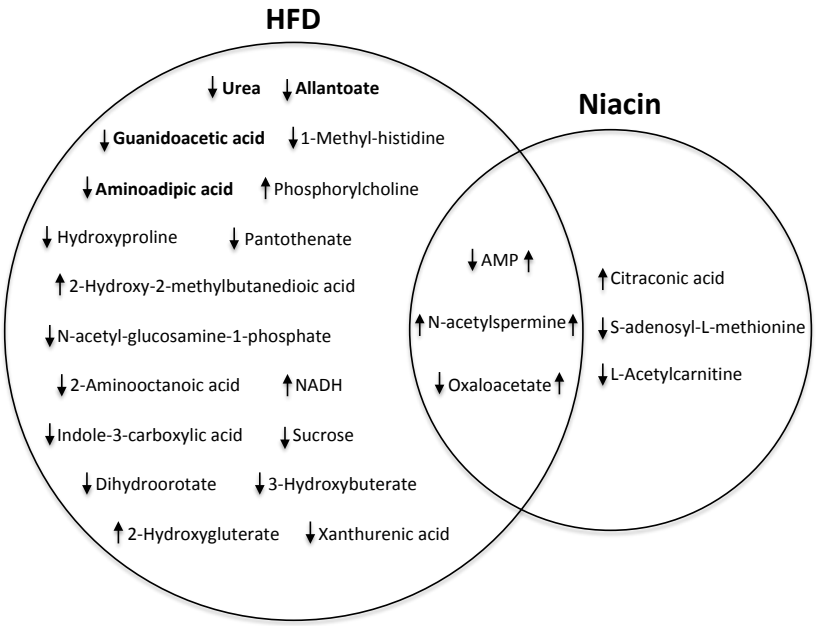

B

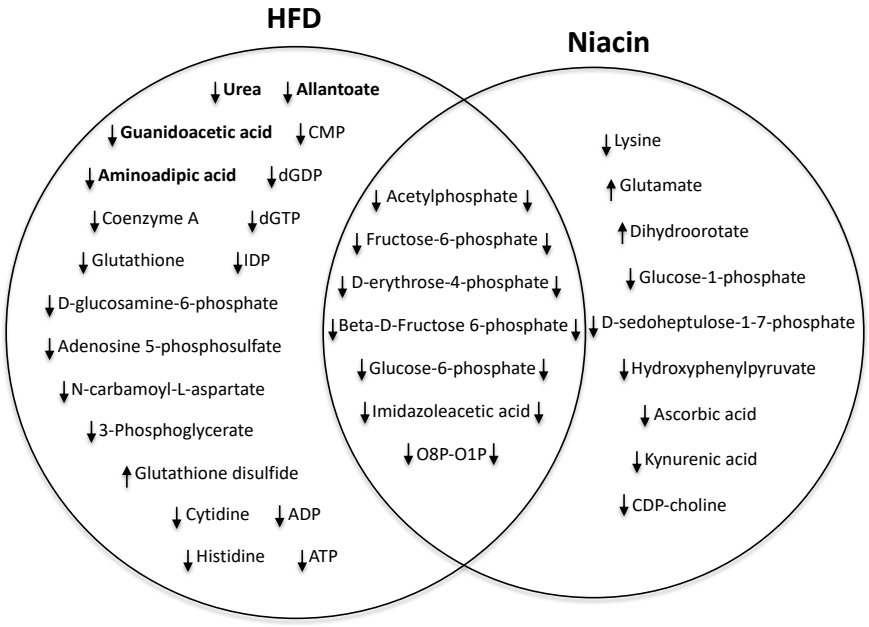

Figure 12. Venn diagram of the metabolites affected by HFD and/or niacin in (A) B6 and (B) B6129 mice. The bold metabolites were affected similarly in the two strains.

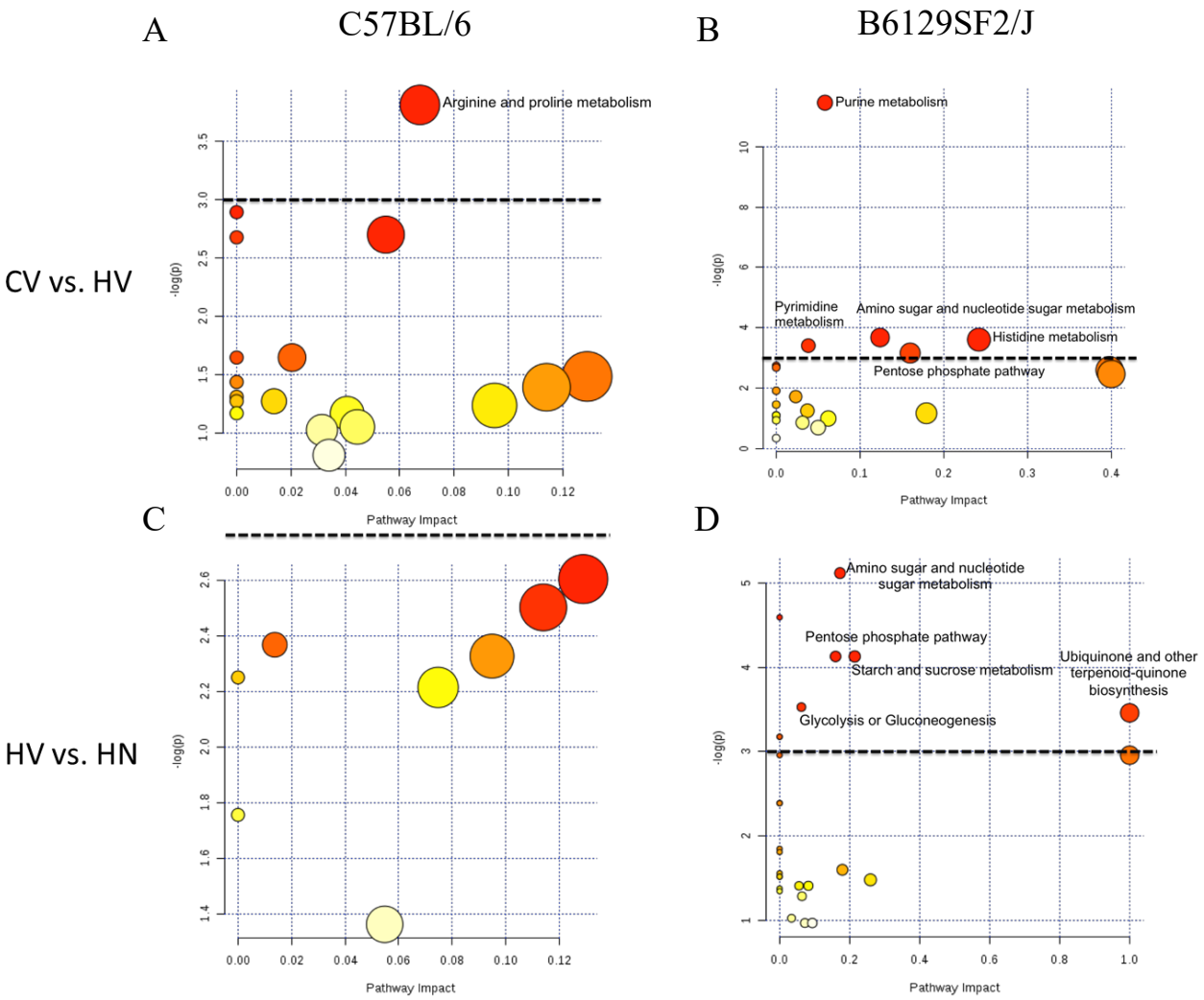

Figure 13. Pathway mapping based on the differential metabolites. (A) Comparison between CV and HV groups in B6 mice. (B) Comparison between CV and HV groups in B6129 mice. (C) Comparison between HV and HN groups in B6 mice. (D) Comparison between HV and HN groups in B6129 mice. The dashed line represents *P* value threshold 0.05 (-log (0.05) ≈ 3.0). Any pathway above this line has an impact factor greater than 0 is considered as significantly impacted. O8P-O1P was excluded from pathway analysis because there was no match found in the database.

Pathway	Total	Expected	Hits	Raw p	-LOG(p)	Holm adjust	FDR	Impact
Arginine and proline metabolism	44	0.62103	3	0.022021	3.8158	1	1	0.06747
Lysine biosynthesis	4	0.056457	1	0.055331	2.8944	1	1	0
Purine metabolism	68	0.95977	3	0.067129	2.7011	1	1	0.05495
Synthesis and degradation of ketone bodies	5	0.070572	1	0.068702	2.678	1	1	0
Histidine metabolism	15	0.21171	1	0.19289	1.6457	1	1	0
Pantothenate and CoA biosynthesis	15	0.21171	1	0.19289	1.6457	1	1	0.02041
Glyoxylate and dicarboxylate metabolism	18	0.25406	1	0.22696	1.483	1	1	0.12903
Starch and sucrose metabolism	19	0.26817	1	0.23801	1.4354	1	1	0
Citrate cycle (TCA cycle)	20	0.28229	1	0.24891	1.3906	1	1	0.11411
Butanoate metabolism	22	0.31052	1	0.27027	1.3083	1	1	0
Lysine degradation	23	0.32463	1	0.28074	1.2703	1	1	0
Pyruvate metabolism	23	0.32463	1	0.28074	1.2703	1	1	0.01375
Alanine, aspartate and glutamate metabolism	24	0.33874	1	0.29105	1.2342	1	1	0.09494
Glycolysis or Gluconeogenesis	26	0.36697	1	0.31127	1.1671	1	1	0
Galactose metabolism	26	0.36697	1	0.31127	1.1671	1	1	0.04068
Glycerophospholipid metabolism	30	0.42343	1	0.35008	1.0496	1	1	0.04444
Glycine, serine and threonine metabolism	31	0.43754	1	0.35945	1.0232	1	1	0.03141
Pyrimidine metabolism	41	0.57869	1	0.44637	0.80661	1	1	0.03401

Table 5. Results from pathway analysis for B6 mice (CV vs. HV).

Pathway	Total	Expected	Hits	Raw p	-LOG(p)	Holm adjust	FDR	Impact
Glyoxylate and dicarboxylate metabolism	18	0.076217	1	0.073964	2.6042	1	1	0.12903
Citrate cycle (TCA cycle)	20	0.084686	1	0.081893	2.5023	1	1	0.11411
Pyruvate metabolism	23	0.097389	1	0.09368	2.3679	1	1	0.01375
Alanine, aspartate and glutamate metabolism	24	0.10162	1	0.097581	2.3271	1	1	0.09494
Glycolysis or Gluconeogenesis	26	0.11009	1	0.10534	2.2506	1	1	0
Cysteine and methionine metabolism	27	0.11433	1	0.1092	2.2146	1	1	0.07479
Arginine and proline metabolism	44	0.18631	1	0.17271	1.7561	1	1	0
Purine metabolism	68	0.28793	1	0.25592	1.3629	1	1	0.05482

Table 6. Results from pathway analysis for B6 mice (HV vs. HN).

Pathway	Total	Expected	Hits	Raw p	-LOG(p)	Holm adjust	FDR	Impact
Purine metabolism	68	1.1997	8	1.05E-05	11.465	0.00086024	0.00086024	0.05824
Amino sugar and nucleotide sugar metabolism	37	0.65279	3	0.025383	3.6737	1	0.68149	0.12396
Histidine metabolism	15	0.26464	2	0.027272	3.6019	1	0.68149	0.24194
Pyrimidine metabolism	41	0.72336	3	0.033243	3.4039	1	0.68149	0.03837
Pentose phosphate pathway	19	0.33522	2	0.042544	3.1572	1	0.69772	0.15991
Alanine, aspartate and glutamate metabolism	24	0.42343	2	0.065087	2.732	1	0.769	0
Lysine biosynthesis	4	0.070572	1	0.068797	2.6766	1	0.769	0
Glutathione metabolism	26	0.45872	2	0.075024	2.5899	1	0.769	0.3979
Sulfur metabolism	5	0.088215	1	0.085272	2.4619	1	0.77693	0.4
Nitrogen metabolism	9	0.15879	1	0.14842	1.9077	1	1	0
Arginine and proline metabolism	44	0.77629	2	0.18057	1.7116	1	1	0.02333
Pantothenate and CoA biosynthesis	15	0.26464	1	0.23536	1.4467	1	1	0
Starch and sucrose metabolism	19	0.33522	1	0.28851	1.243	1	1	0.03725
Fructose and mannose metabolism	21	0.3705	1	0.31374	1.1592	1	1	0.1793
Lysine degradation	23	0.40579	1	0.33811	1.0844	1	1	0
Pyruvate metabolism	23	0.40579	1	0.33811	1.0844	1	1	0
Glycolysis or Gluconeogenesis	26	0.45872	1	0.37311	0.98589	1	1	0.06221
Inositol phosphate metabolism	28	0.494	1	0.39545	0.92774	1	1	0
Glycine, serine and threonine metabolism	31	0.54693	1	0.42753	0.84973	1	1	0.03141
Fatty acid metabolism	39	0.68807	1	0.50529	0.68262	1	1	0.05008
Aminoacyl-tRNA biosynthesis	69	1.2174	1	0.71605	0.334	1	1	0

Table 7. Results from pathway analysis for B6129 mice (CV vs. HV).

and further decreased with niacin treatment. Five pathways were impacted by niacin, including amino sugar and nucleotide sugar metabolism, pentose phosphate pathway, starch and sucrose metabolism, glycolysis or gluconeogenesis, and ubiquinone and other terpenoid-quinone biosynthesis (Figure 13D; Table 8). Of the metabolites that were changed in these pathways, glucose-1-phosphate, fructose-6-phosphate, hexose-phosphate, and D-erythrose-4-phosphate were reduced in HV group and further decreased by niacin treatment (Figure 14). However, hydroxyphenylpyruvate did not change with HFD feeding but significantly decreased with niacin treatment (Figure 14). Hydroxyphenylpyruvate, also known as 4-hydroxyphenylpyruvic acid, is an intermediate in the metabolism of phenylalanine/tyrosine. It has been demonstrated to improve mitochondrial oxidation in rats subjected to hemorrhagic shock [304]. Therefore, the decreased hydoxyphenylpyruvate by niacin may lead to decreased β-oxidation in the liver and subsequent lipid accumulation and liver damage in B6129 mice.

Liver lipidomics analysis suggests decreased VLDL production and secretion contribute to niacin-induced fatty liver in B6129 mice

Lipidomics analysis indentified 2,632 lipid ions in the livers of B6 and B6129 mice, which belonged to 45 classes of lipids (Table 9). The lipid classes that had the greatest number of lipid ions in mouse livers were triglyceride (TG), phosphatidylcholine (PC), diglyceride (DG), phosphatidylethanolamine (PE) and sphingomyelin (SM) (Figure 15). Unsupervised hierarchical clustering was performed, and the top 50 most differential lipid ions and 38 classes of lipids were showed in the form of a heatmap (Figure 16 and 17). To further confirm the alterations in lipid abundance by HFD and niacin in each strain of mice, fold change analysis was performed. In B6 mice, 321 lipid species were upregulated and 174 were downregulated by HFD feeding (Figure

Pathway	Total	Expected	Hits	Raw p	-LOG(p)	Holm adjust	FDR	Impact
Amino sugar and nucleotide sugar metabolism	37	0.39167	3	0.0060105	5.1142	0.49286	0.33057	0.17252
Histidine metabolism	15	0.15879	2	0.010147	4.5906	0.82191	0.33057	0
Pentose phosphate pathway	19	0.20113	2	0.016126	4.1273	1	0.33057	0.15991
Starch and sucrose metabolism	19	0.20113	2	0.016126	4.1273	1	0.33057	0.21459
Glycolysis or Gluconeogenesis	26	0.27523	2	0.029365	3.528	1	0.42551	0.06221
Ubiquinone and other terpenoid-quinone biosynthesis	3	0.031757	1	0.031444	3.4595	1	0.42551	1
Lysine biosynthesis	4	0.042343	1	0.041719	3.1768	1	0.42551	0
Phenylalanine, tyrosine and tryptophan biosynthesis	4	0.042343	1	0.041719	3.1768	1	0.42551	0
Biotin metabolism	5	0.052929	1	0.051892	2.9586	1	0.42551	0
D-Glutamine and D-glutamate metabolism	5	0.052929	1	0.051892	2.9586	1	0.42551	1
Ascorbate and aldarate metabolism	9	0.095272	1	0.091584	2.3905	1	0.62582	0
Nitrogen metabolism	9	0.095272	1	0.091584	2.3905	1	0.62582	0
Pentose and glucuronate interconversions	16	0.16937	1	0.15734	1.8494	1	0.92634	0
Aminoacyl-tRNA biosynthesis	69	0.73042	2	0.16334	1.8119	1	0.92634	0
Fructose and mannose metabolism	21	0.2223	1	0.20155	1.6017	1	0.92634	0.1793
Butanoate metabolism	22	0.23289	1	0.21013	1.56	1	0.92634	0
Lysine degradation	23	0.24347	1	0.21863	1.5204	1	0.92634	0
Pyruvate metabolism	23	0.24347	1	0.21863	1.5204	1	0.92634	0
Alanine, aspartate and glutamate metabolism	24	0.25406	1	0.22703	1.4827	1	0.92634	0.25949
Glutathione metabolism	26	0.27523	1	0.2436	1.4122	1	0.92634	0.05534
Galactose metabolism	26	0.27523	1	0.2436	1.4122	1	0.92634	0.0822
Porphyrin and chlorophyll metabolism	27	0.28582	1	0.25175	1.3793	1	0.92634	0
Inositol phosphate metabolism	28	0.2964	1	0.25983	1.3477	1	0.92634	0
Glycerophospholipid metabolism	30	0.31757	1	0.27573	1.2883	1	0.94209	0.06389
Pyrimidine metabolism	41	0.43402	1	0.35766	1.0282	1	1	0.03401
Tyrosine metabolism	44	0.46577	1	0.37846	0.97166	1	1	0.07225
Arginine and proline metabolism	44	0.46577	1	0.37846	0.97166	1	1	0.09347

Table 8. Results from pathway analysis for B6129 mice (HV vs. HN).

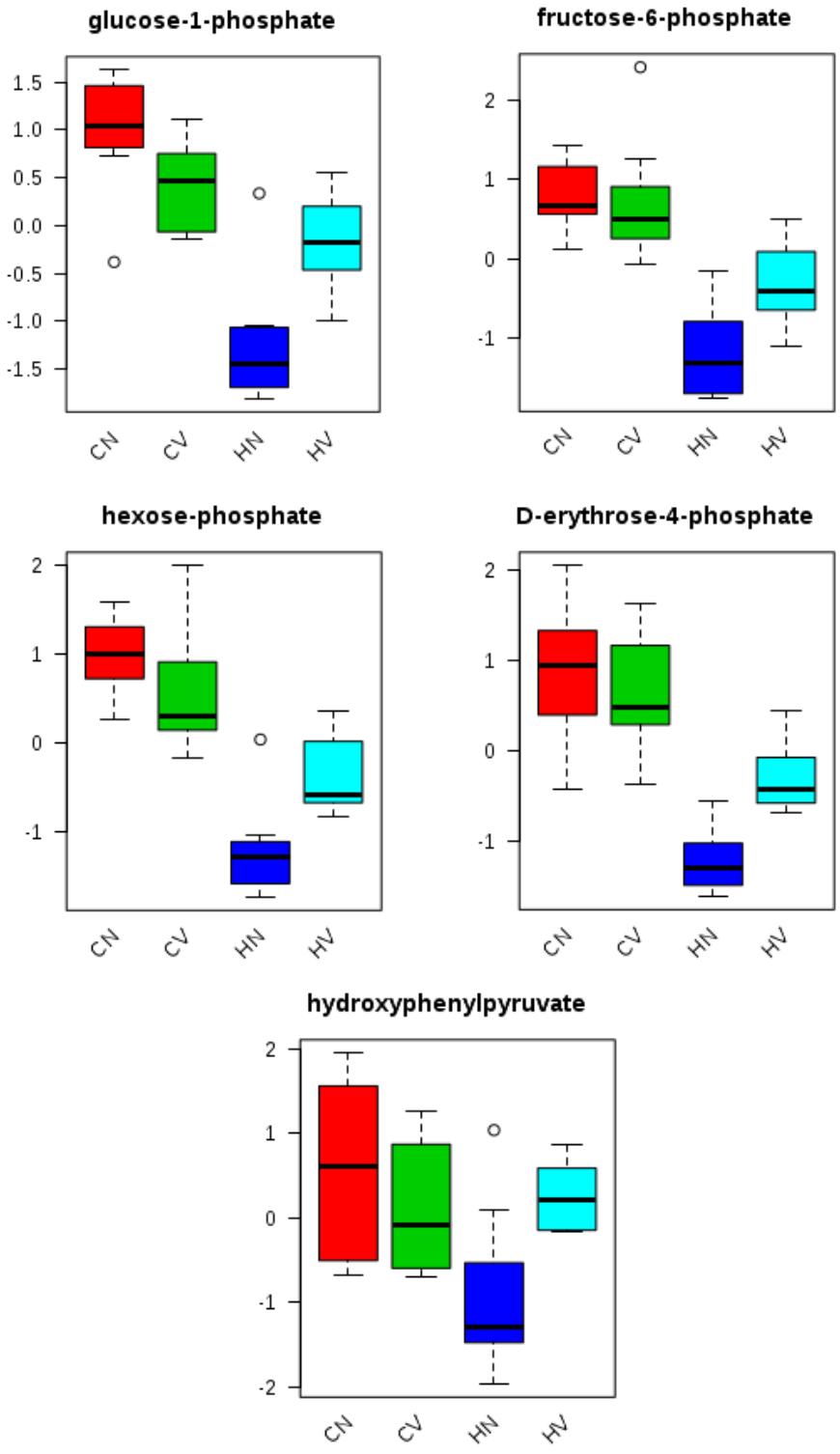

Figure 14. Metabolites which impact pathways in B6129 mice (HV vs. HN).

Lipid class	Subclass	Full name of subclass	# lipid ion
-Choline	LPC	lysophosphatidylcholine	65
	PC	phosphatidylcholine	387
P-Ethanol Amine	LPE	lysophosphatidylethanolamine	20
	LdMePE	lysodimethylphosphatidylethanolamine	4
	PE	phosphatidylethanolamine	190
	dMePE	dimethylphosphatidylethanolamine	55
P-Serine	LPS	lysophosphatidylserine	6
	PS	phosphatidylserine	127
P-Glycerol	LPG	lysophosphatidylglycerol	9
	PG	phosphatidylglycerol	124
P-Inositol	LPI	lysophosphatidylinositol	7
	PI	phosphatidylinositol	104
	PIP	phosphatidylinositol	17
	PIP2	phosphatidylinositol	1
P-Ethanol	PEt	phosphatidylethanol	18
P-Acid	LPA	lysophosphatidic acid	2
	PA	phosphatidic acid	55
P-Methanol	PMe	phosphatidylmethanol	9
Sphingolipids	SM	sphingomyelin	179
	phSM	sphingomyelin(phytosphingosine)	5
Neutral glycerolipid	MG	monoglyceride	7
	DG	diglyceride	223
	TG	triglyceride	537
Fatty Acid	FA	fatty acid	1
	OAHFA	(O-acyl)-1-hydroxy fatty acid	8
Cardiolipin	CL	Cardiolipin	32
Sphingoid base	So	Sphingoshine	6
Glycosphingolipids	Cer	Ceramides	159
	CerP	Ceramides phosphate	2
Neutral Glycosphingolipids	CerG1	Simple Glc series	53
	CerG2	Simple Glc series	16
	CerG3	Simple Glc series	4
	CerG2GNAc1	Simple Glc series	6
	CerG3GNAc1	Simple Glc series	1
Steroid	ChE	Cholesteryl Ester	6
	ZyE	zymosteryl	1
Coenzyme	Co	Coenzyme	2
Glycoglycerolipid	MGDG	Monogalactosyldiacylglycerol	14
	DGDG	Digalactosyldiacylglycerol	5
	SQDG	Sulfoquinovosyldiacylglycerol	4
Fatty acyl and other lipids	AcCa	Acyl Carnitine	30
Derivatized lipids (biotinylation, diazomethane)	BisMePE	Bis-methyl phosphatidylethanolamine	3
Derivatized lipids (biotinylation, diazomethane)	MePC	Methyl phosphatidylcholine	76
Sphingolipids	ST	Sulfatide	1
Fatty acyl and other lipids	WE	Wax esters	51

Table 9. Lipid classes and subclasses identified in lipidomics analysis.

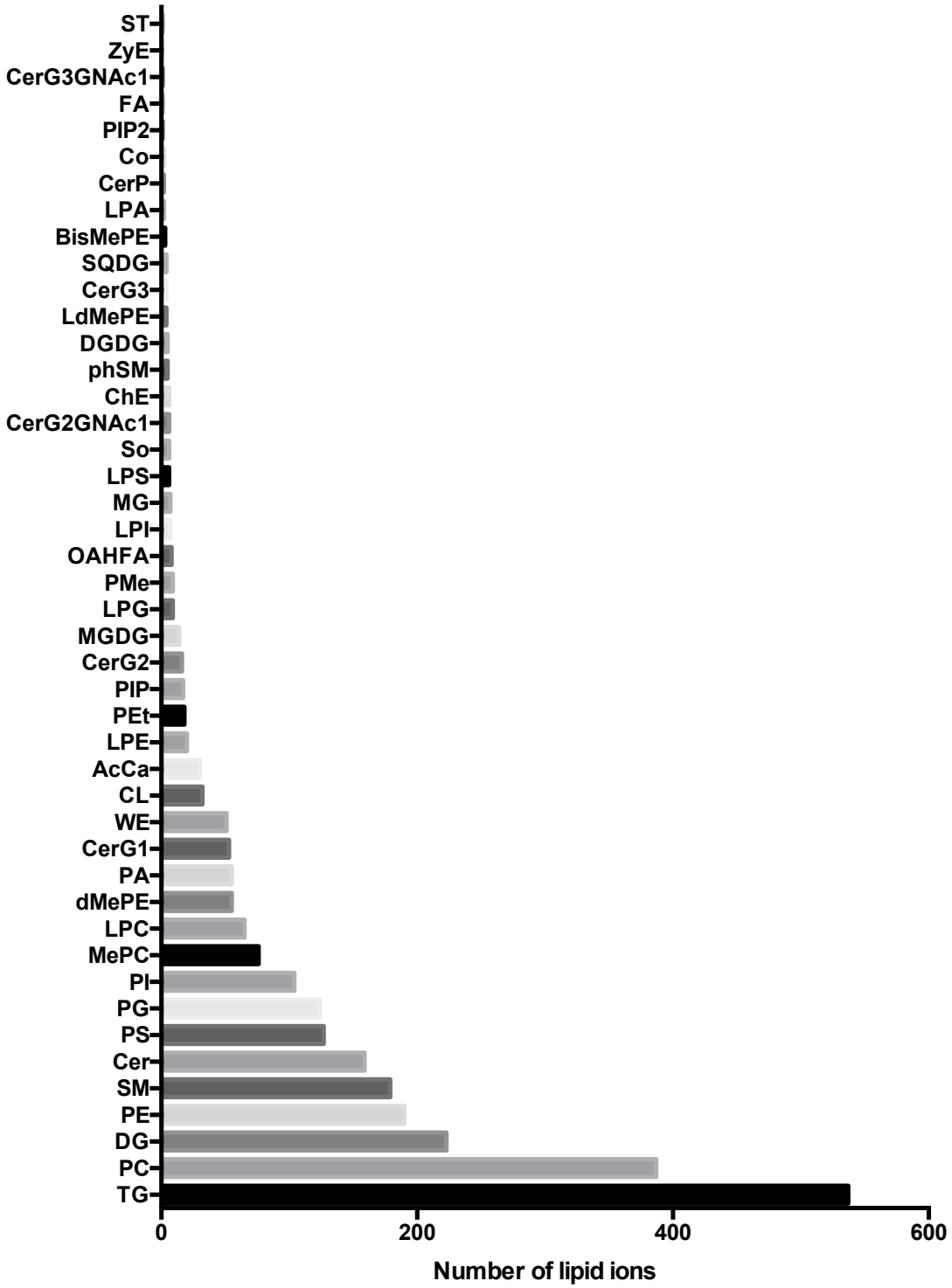

Figure 15. Number of lipid ions in each lipid class from mouse livers.

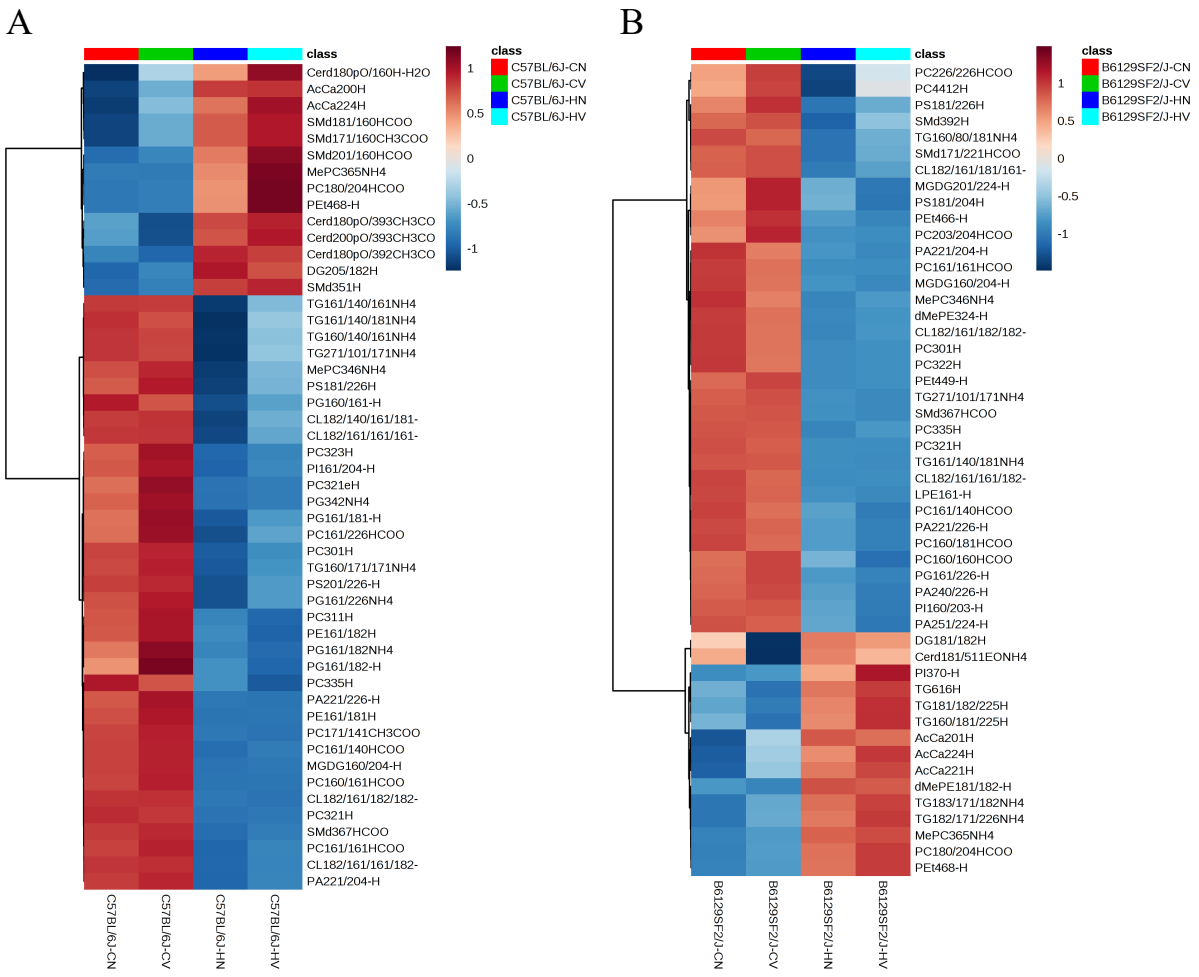

Figure 16. The clustering result of top 50 differential lipid species of (A) B6 and (B) B6129 mice in the form of a heatmap.

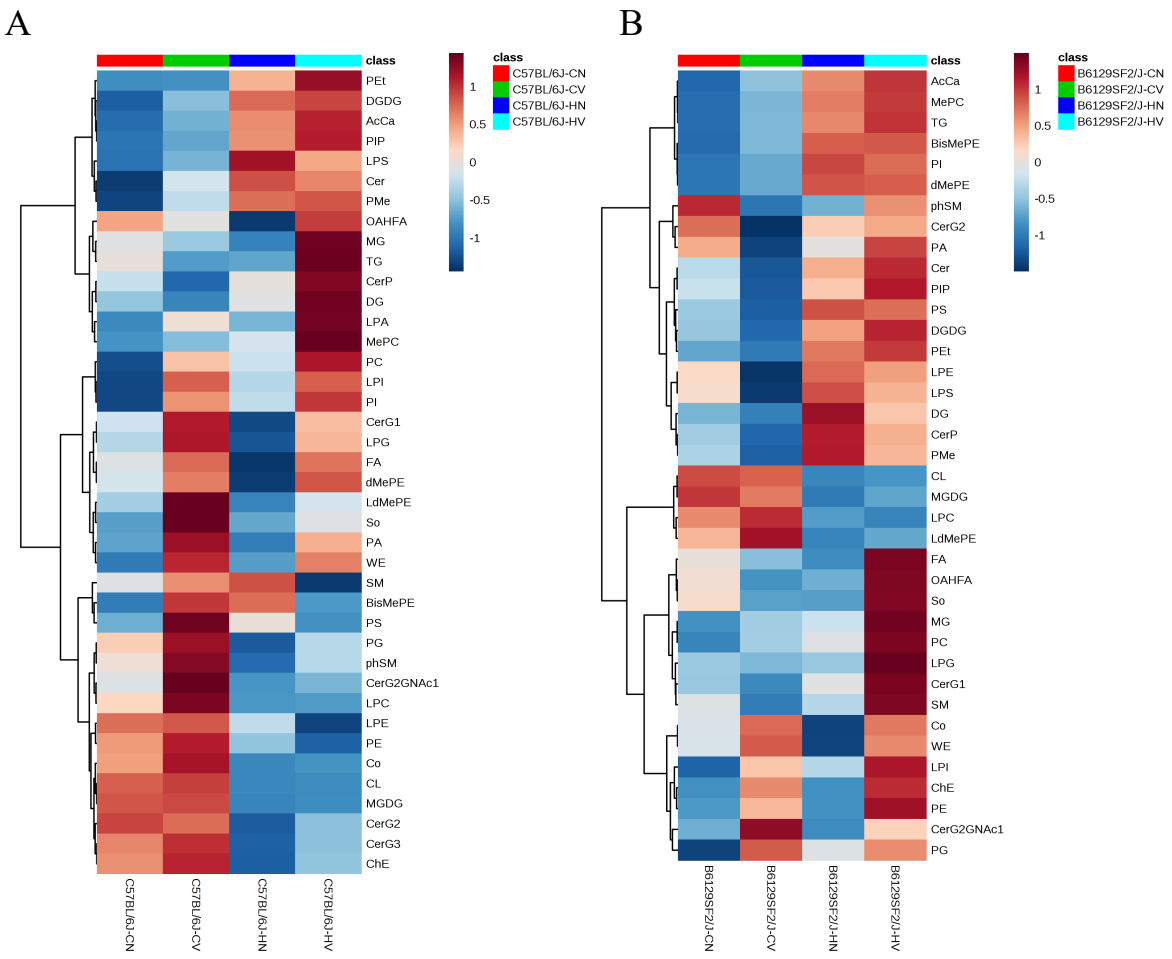

Figure 17. The clustering result of lipid classes of (A) B6 and (B) B6129 mice in the form of a heatmap.

18A). Niacin treatment increased 32 and decreased 80 lipid species in HFD-fed B6 mice (Figure 18C). The total number of lipid species altered in B6129 mice was similar to B6 mice. HFD feeding led to an increase in 178 and decrease in 259 lipid species in B6129 mice (Figure 18B). Fifty-nine and 66 lipid species were upregulated and downregulated by niacin in HFD-fed B6129 mice, respectively (Figure 18D). These data demonstrated a differential effect of HFD and niacin on the alteration of lipid abundance between these two mouse strains. Next, partial least squares discriminant analysis on all lipid species was performed. The overlapping area of the HV and HN groups is larger in B6 than that of B6129 mice, indicating that niacin had greater impact on lipid profile in HFD-fed B6129 than B6 mice (Figure 19).

Next, quantitative changes in lipid classes were examined through correlation analysis. In B6 mice, the abundance of DG was positively correlated with HFD, while negatively correlated with niacin (Figure 20A and C). In B6129 mice, DG was positively correlated with both HFD and niacin (Figure 20B and D). In addition, in B6129 mice, PC was positively correlated with HFD, but negatively correlated with niacin. This was further confirmed by relative abundance of DG and PC. The abundance of DG was increased in HV group and decreased in HN group in B6 mice (Figure 21A). Similar increase in DG was observed in HV B6129 mice (Figure 21B). However, DG was further increased in HN group in B6129 mice. In contrast to unaltered PC abundance in B6 mice, PC was increased in HV group compared with CV group in B6129 mice (Figure 21C and D). Niacin treatment decreased PC abundance in HFD-fed B6129 mice (Figure 21D). PC plays a critical role in the production and secretion of VLDL triglyceride. Therefore, decreased PC abundance in niacin treated HFD-fed B6129 mice may associated with increased fat content.

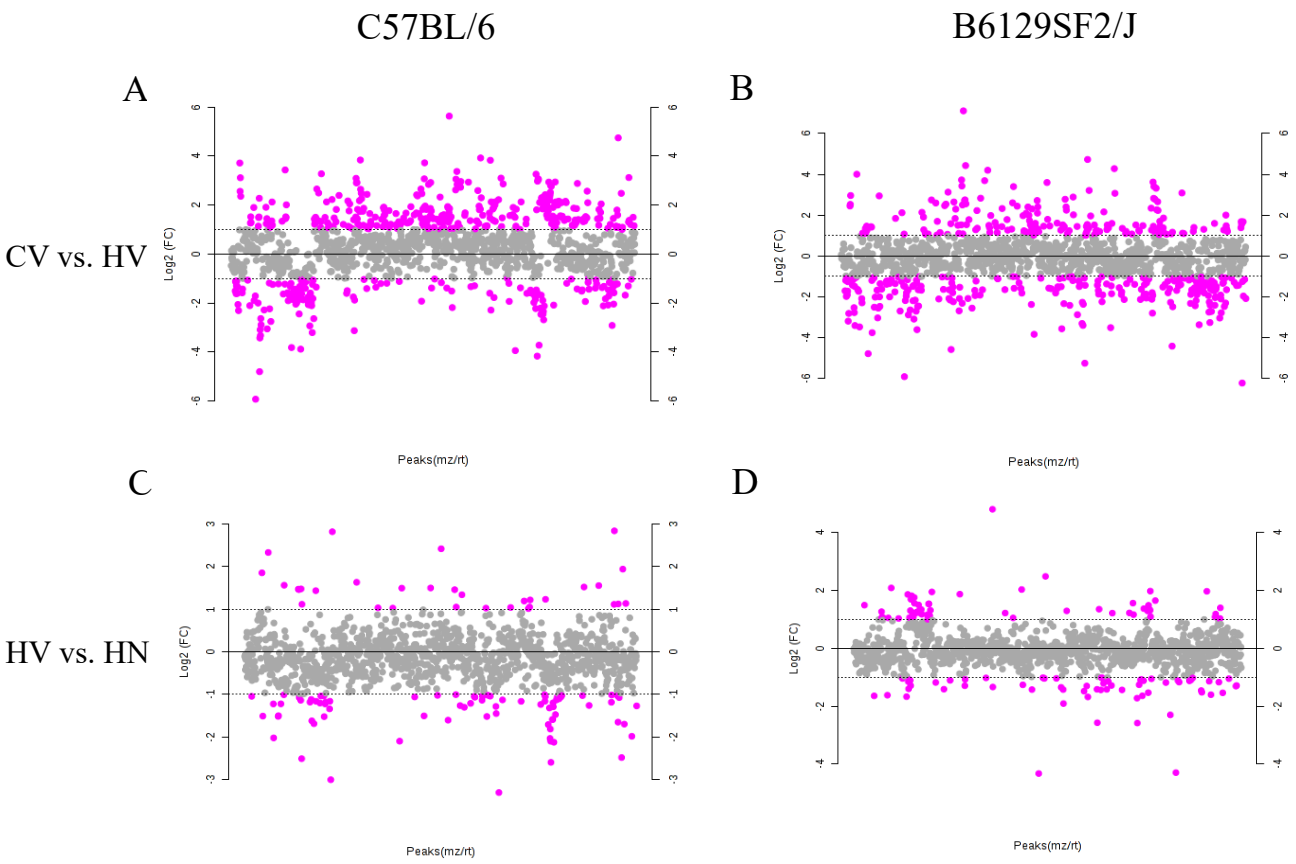

Figure 18. Fold change of each lipid ion between different groups in B6 and B6129 mice. Pink dot represents lipid ions that have at least a two fold change. (A) Comparison between CV and HV groups in B6 mice. (B) Comparison between CV and HV groups in B6129 mice. (C) Comparison between HV and HN groups in B6 mice. (D) Comparison between HV and HN groups in B6129 mice.

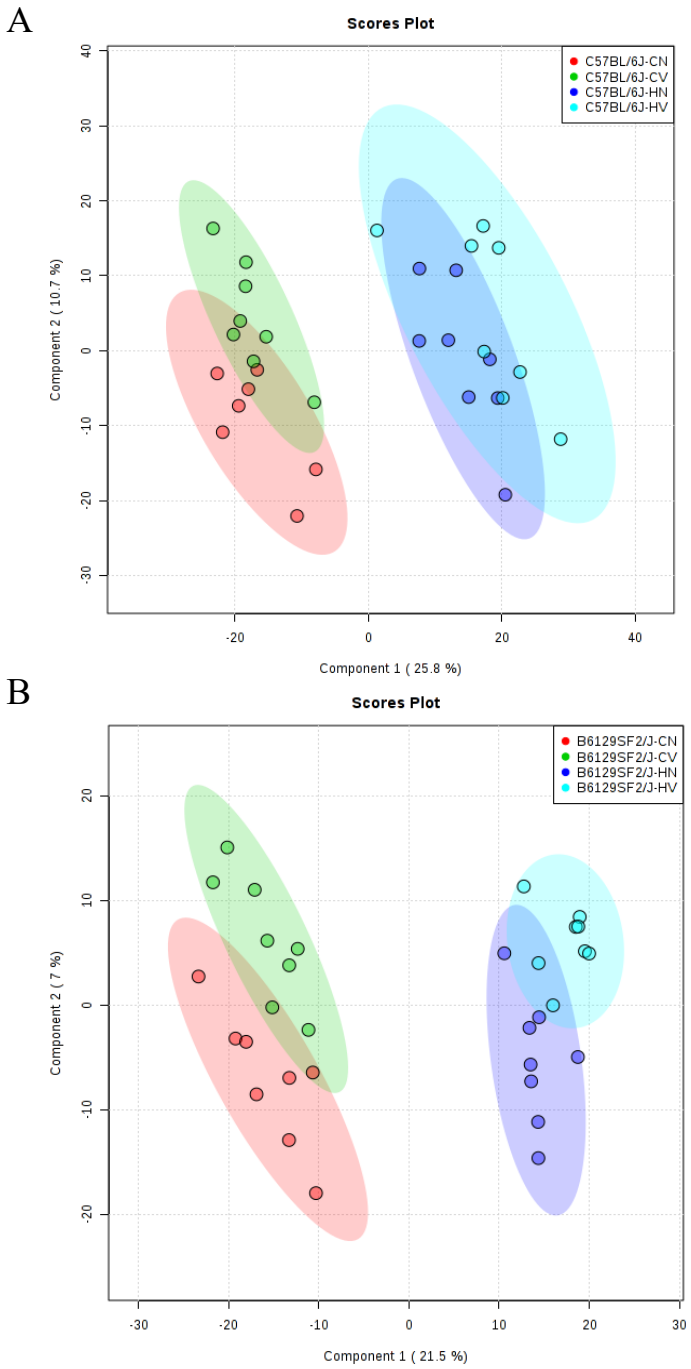

Figure 19. Partial least squares discriminant analysis of lipid species in (A) B6 and (B) B6129 mice.

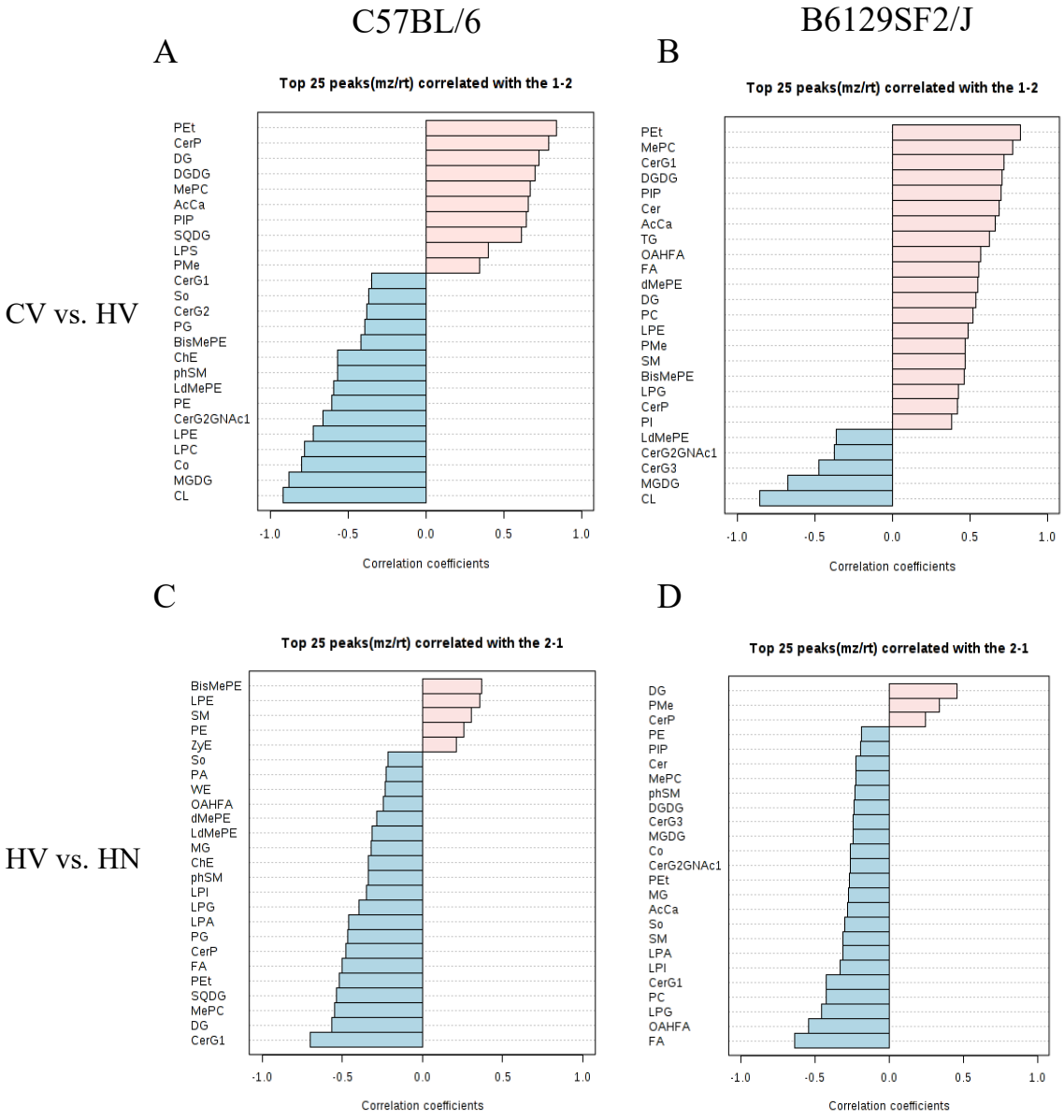

Figure 20. Correlation analysis of lipid class abundance with HFD and niacin. Pink means positive correlation, blue means negative correlation. (A) Correlation of HFD with lipid class in B6 mice. (B) Correlation of HFD with lipid class in B6129 mice. (C) Correlation of niacin with lipid class in B6 mice. (D) Correlation of niacin with lipid class in B6129 mice.

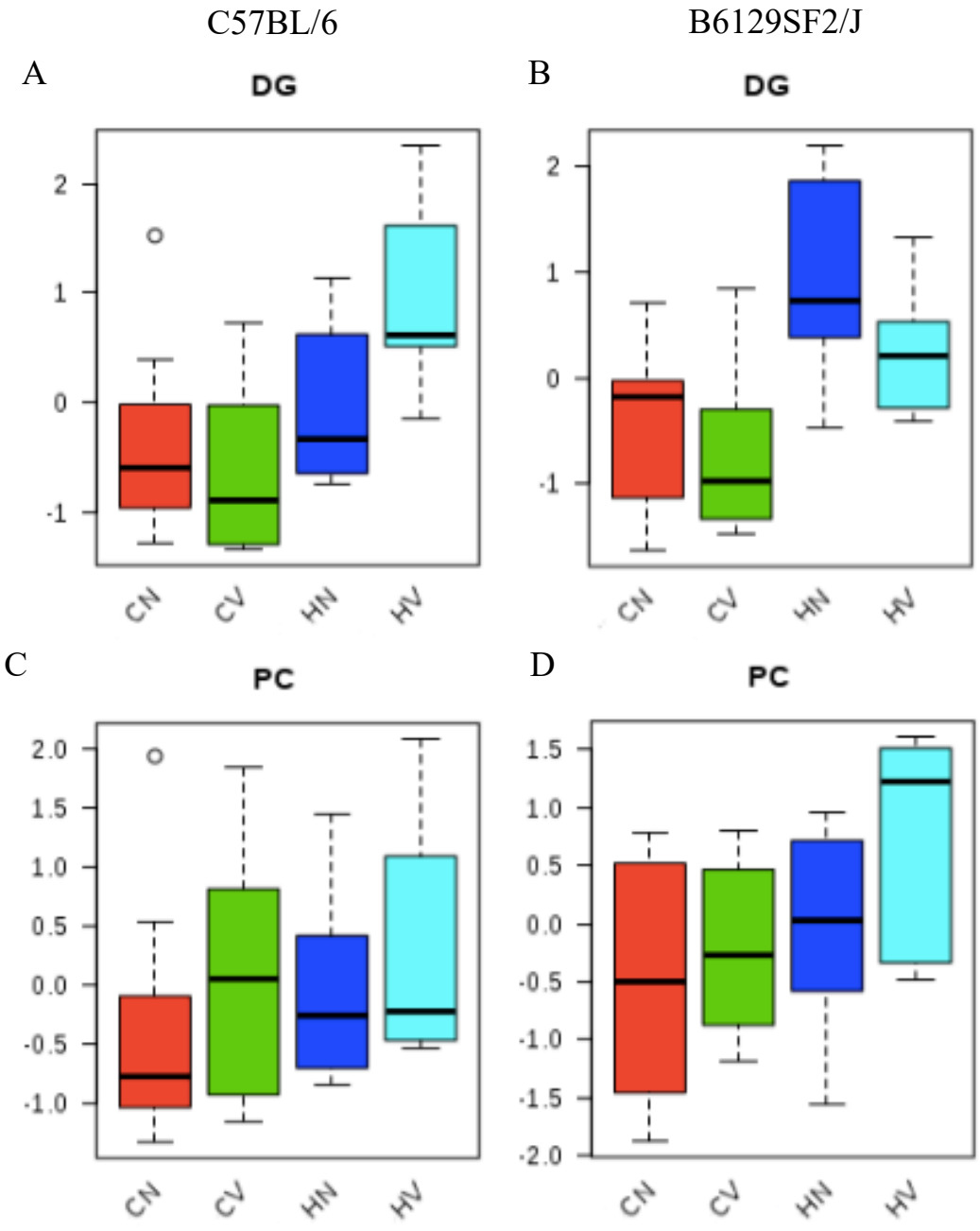

Figure 21. Relative abundance of (A) DG in B6 mice, (B) DG in B6129 mice, (C) PC in B6 mice and (D) PC in B6129 mice.

Discussion

The current study provides a strong metabolic and lipidomic profile of the B6 and B6129 mice under HFD and niacin conditions. In metabolomics analysis, ANOVA analysis revealed that 72% (21 of 29) of the differential metabolites were influenced by HFD alone in B6 mice. Utilizing pathway analysis, it was determined that arginine and proline metabolism was significantly impacted by HFD with three specific metabolites, guanidoacetic acid, urea, and hydroxylproline, decreased in this pathway. The rest of metabolites were spread out into 17 other pathways. Arginine and proline metabolism is one of the pathways responsible for the biosynthesis of arginine and proline from citrulline and glutamate. Dietary arginine supplementation has been demonstrated to ameliorate diet-induced obesity in rats [305, 306]. Therefore, decreases in arginine and proline metabolism may contribute to the fatty liver in HFD-fed B6 mice. In contrast to B6 mice, 57% (26 of 46) of the differential metabolites were affected by HFD alone in B6129 mice, of which only 4 were also affected by HFD in B6 mice. More than half of the metabolites (16 of 26) were changed in 5 pathways significantly affected by HFD, including purine metabolism, amino sugar and nucleotide sugar metabolism, histidine metabolism, pyrimidine metabolism, and pentose phosphate pathway. Interestingly, arginine and proline metabolism was not impacted by HFD in B6129 mice. Together, these findings suggest that HFD feeding differentially affects the metabolites and metabolic pathways in B6 and B6129 mice.

In B6 mice, 21% (6 of 29) of the differential metabolites were impacted by niacin administration, of which AMP, N-acetylspermine, and oxaloacetate were also affected by HFD. However, niacin and HFD had opposite impacts on AMP and oxaloacetate. The larger number of metabolites influenced by HFD than niacin (21 and 6) suggest that the HFD has greater impact

on the liver of B6 mice than niacin. Among the metabolites affected by niacin only, SAM, a methyl group donor, was decreased in both chow and HFD-fed B6 mice treated with niacin. Indeed, previous studies have demonstrated SAM depletion in rodent and humans treated with niacin [233, 234]. However, the decrease in SAM in our study did not have a significant impact on the liver, with triglyceride content only slightly increased in chow-fed B6 mice and unchanged in HFD-fed B6 mice treated with niacin. Therefore, it appears that the methyl depleting effect of niacin does not significantly affect the liver fat content and histology in B6 mice. Compared with B6 mice, a larger portion (35% vs. 21%) of metabolites were influenced by niacin in B6129 mice and are completely different from the 6 metabolites affected by niacin in B6 mice. Pathway analysis revealed that niacin significantly impacted 5 metabolic pathways in B6129 mice, but none in B6 mice. Of the 5 metabolites changed in these 5 pathways, glucose-1-phosphate, fructose-6-phosphate, hexose-phosphate, D-erythrose-4-phosphate are involved in glucose metabolism. They were decreased with HFD feeding and further decreased with niacin treatment. The decreases in glycolysis and pentose phosphate pathway leads to a decrease in the production of L-phenylalanine and L-tyrosine [307], which can be metabolized to the intermediate, hydroxyphenylpyruvate. Hydroxyphenylpyruvate was decreased with niacin treatment, but not HFD feeding. It is involved in ubiquinone and other terpenoid-quinone biosynthesis. The impact factor of niacin on this metabolic pathway was greater than the other 4 pathways. Ubiquinone, also known as coenzyme Q10, plays a critical role in mitochondrial respiratory chain transport and reactive oxidation species production [308]. Decreases in the biosynthesis of ubiquinone may result in decreased β-oxidation and oxidative stress in the liver. Therefore, the excess fat consumption plus decreased β-oxidation is likely responsible for the hepatic fat accumulation and NAFLD in B6129 mice. In contrast to B6 mice, niacin-induced

methyl deficiency was not observed in B6129 mice. Additionally, niacin had no effect on the livers of chow-fed B6 or B6129 mice, suggesting nutritional insult played a significant role in HFD-induced NAFLD development in B6 and B6129 mice.

Lipidomics analysis provides further critical insight on the status of lipid metabolism in mouse livers with different treatments. Partial least squares discriminant analysis showed an obvious separation between chow and HFD-fed group in both strains of mice, indicating a significant different lipid profile after HFD feeding. However, even though HFD had differential effects on lipid profile between B6 and B6129 mice, they shared some common changes in lipid classes with HFD feeding, including increase in PEt, CerP, DG, DGDG, MePC, AcCa, PIP, CerG1, and decrease in LdMePE, CerG2GNAc1, MGDG, CL. The increase of DG is also observed in humans with NAFLD [309], which is associated with hepatic insulin resistance through activation of protein kinase Cε [310].

Niacin treatment affected the lipid profile in chow and HFD-fed mice of both strains, suggesting that niacin has a strong impact on lipid metabolism even under normal conditions. Indeed, niacin is a powerful lipid-altering drug that increases plasma HDL cholesterol concentrations, decreases plasma total, VLDL and LDL cholesterol, and reduces hepatic triglyceride content under certain conditions [311]. Unexpectedly, niacin increased liver weight and triglyceride content in HFD-fed B6129, which seems contradictory to its beneficial lipid-lowing effects. However, as early as 50 years ago, niacin-induced fatty liver in HFD-fed rats had been reported, in which choline deficiency was demonstrated to be the mechanism [231, 232]. In the liver, betaine and SAM, metabolites of choline and methionine, respectively, are two principal methyl donors. Niacin as a methyl consumer, when taken in high doses, depletes the methyl pool in hepatocytes, preventing other methylation reactions, such as the form of PC from

PE. Indeed, decreased PC abundance was observed in HFD-fed B6129 mice treated with niacin. Besides PE, PC can also be synthesized from choline via CDP-choline pathway. Therefore, addition of choline is able to supply sufficient methyl donors and maintain PC levels, which contributes to reverse the fatty liver in niacin-treated rats. In addition, the increased PC in HV B6129 mice may represent a protective mechanism against HFD to export the excess fat from the liver via increased VLDL production. Excess niacin disrupts this protective mechanism by decreasing PC formation and thus leads to hepatic steatosis. The susceptibility of B6129 mice to methyl deficiency closely resembles their parental strain, 129 mice. When fed with ethanol, which is also a methyl consumer, 129 mice have higher NASH histological score than that of B6 mice [312]. Consistent with my findings, PC is increased more than two folds in 129 mice fed a HFD for 7 weeks and decreased with HFD and ethanol feeding [312].

Conclusions

In conclusion, metabolomics and lipidomics analysis in the livers of B6 and B6129 mice suggested that impaired β-oxidation and decreased VLDL-TG production and secretion contributes to niacin-induced fatty liver in B6129 mice (Figure 22). However, further validation studies, such as measuring markers of β-oxidation and plasma VLDL concentrations, are needed to confirm these mechanisms.

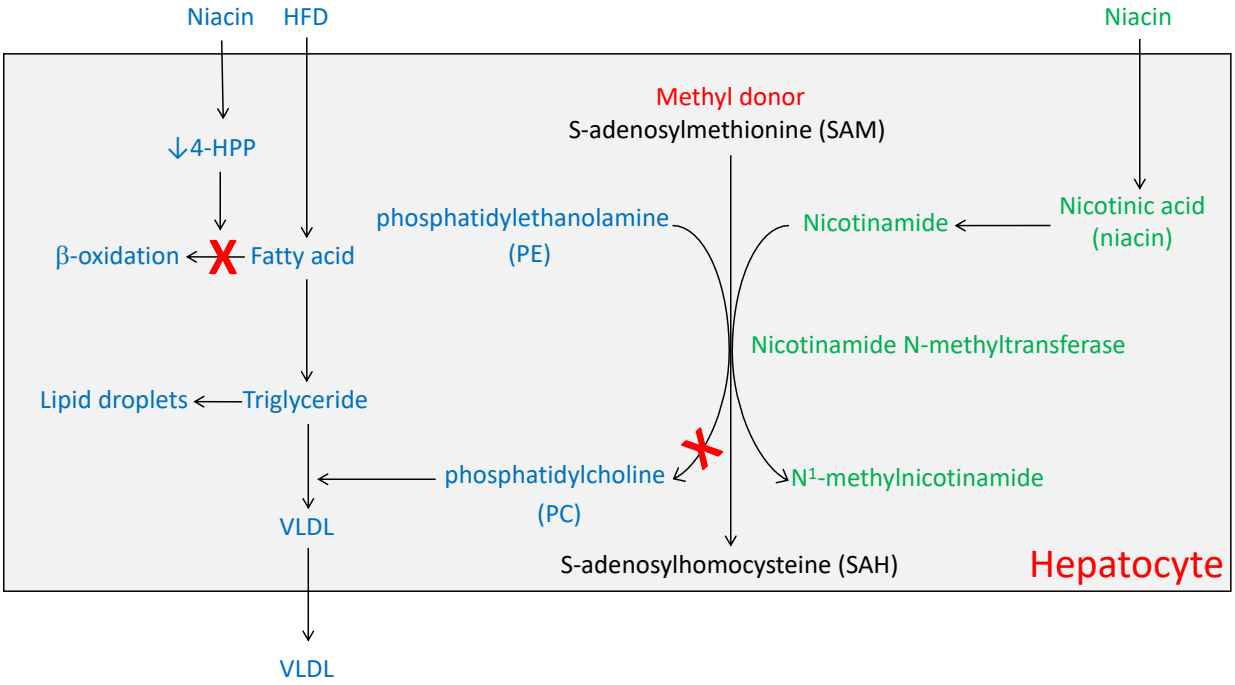

Figure 22. Mechanisms of niacin-induced fatty liver in HFD-fed B6129 mice. HFD consumption leads to increased fatty acid flux to the liver. Decreased 4-HPP induced by niacin is associated with impaired β-oxidation in the liver. In addition, pharmacological does of niacin in the liver are converted to nicotinamide, which is, in turn, rapidly methylated to N-methylnicotinamide. Chronic pharmacological doses of niacin strain the system and deplete the hepatocyte pool of SAM. This prevents the synthesis of phosphatidylcholine, which is essential for VLDL production and secretion.

Chapter 4

Effects of High-Fat Diet and Niacin on Gut Microbiota Composition in C57BL/6J and B6129SF2/J Mice

Abstract

Background. The normal gut microbiota plays an important role in host nutrient metabolism, maintenance of gut barrier integrity, immunomodulation and protection against pathogens. Numerous studies have demonstrated that high-fat diet (HFD) leads to altered gut microbiota composition, disrupted gut barrier integrity, translocation of pathogenic bacteria and intestinal inflammation. Niacin, a water-soluble vitamin, suppresses intestinal inflammation and colon cancer, which could be associated with alterations in gut microbiota composition. **Objectives.** Therefore, the aim of the current study was to investigate the effects of HFD and niacin on the gut microbiota composition in two inbred strains, C57BL/6J (B6) and B6129SF2/J (B6129) mice. **Methods**. Fecal samples and small intestines were collected from B6 and B6129 mice, which were fed either a chow (10% fat) or HFD (60% fat) for 20 weeks with niacin (360 mg/kg/day) or vehicle supplementation from week 5 to week 20. Culture-based method was used to analyze the gut microbiota. **Results.** Anaerobes/aerobes ratio dramatically decreased in HV B6129 mice, while slightly decreased in HV B6 mice. *Firmicutes/Bacteroidetes* ratio remained relatively consistent in B6 mice, whereas increased in HFD-fed B6129 mice, which was brought down by niacin treatment. HFD remarkably increased the proportion of hemolytic bacteria and decreased proportion of *Bifidobacterium* and *Bacteroides* in B6129 mice, which was

greatly reversed by niacin treatment. In B6 mice, HFD and niacin had a minor impact on the composition of gut microbiota. In addition, colon length did not change in B6 mice but increased in HN B6129 mice. Goblet and Paneth cell number did not change in B6 mice. In contrast, goblet cell number was increased in HFD-fed B6129 mice. Paneth cell number was increased in HN B6129 mice. **Conclusions.** B6 mice are more resistant to HFD and niacin-induced alterations in gut microbiota composition and histological changes in small intestine than B6129 mice. Niacin improves gut microbiota composition and small intestine histology in HFD-fed B6129 mice.

Background

Gut microbiota is defined as the community of microbes, mainly bacteria as well as fungi, phages, archaea, protozoa and viruses, that lives in the human gastrointestinal tract. The ratio of bacterial and human cells is very close to 1:1 [144]. The relationship between gut microbiota and human host is considered as symbiotic. Each person has a unique gut microbiota with three major enterotypes, *Bacteroides*, *Prevotella*, and *Ruminococcus*, which are not nation or continent specific [145]. In mouse and humans, the two dominant microbial phyla are *Bacteroidetes* and *Firmicutes*, which together represent over 90% of the bacterial composition of gut microbiota. *Proteobacteria*, *Actinobacteria* and *Verrucomicrobia* are also present in the gut microbiota, but at a relatively small proportion compared to *Bacteroidetes* and *Firmicutes*. The gut microbiota performs many important functions, including metabolism of nutrients (e.g. indigestive fiber), modulation of host immunity, removal of harmful compounds, maintenance of gut barrier integrity and protection against pathogens [146]. Disruption of gut microbiota leads

to an array of disease conditions, including inflammatory bowel disease, allergies, asthma, metabolic disease and even cancer [147].

Many factors affect the composition of gut microbiota, such as diet, disease state, medications and host genetics. Diet is the major contributor, accounting for 57% of the variations in microbiota [151]. Dietary fat is known to have strong influence on microbiota composition in both humans and rodents. A detectable change in microbiome composition is observed within 24 hours of initiating a HFD in humans, whereas enterotype identity remains stable during 10 days of HFD feeding [313]. The gut microbial enterotype depends on long-term dietary patterns, in which high-fat and protein increase the prevalence of *Bacteroides* and *Ruminococcus* and carbohydrate-rich diets promote the growth of *Prevotella* [313]. In C57BL/6J mice, HFD feeding induces a reduced gut microbiota abundance and diversity, which is completely recovered after switching the mice to normal chow diet for 10 weeks [152]. More specifically, the abundance of *Bacteroidetes* is decreased with a proportional increase in *Firmicutes* during HFD feeding [152]. The abundance of *Lactobacillus* and *Bifidobacterium*, two Gram-positive bacteria, is reduced in B6 mice fed a HFD for 4 weeks [166]. Lower number of *Bacteroides*, a genus of Gram-negative bacteria, was observed in HFD-fed rat [314]. In addition, increased *Clostridium subcluster XIVa* has also been observed in mice receiving HFD [155].

Niacin, a B vitamin (B3), has been demonstrated to possess beneficial effects in the colon. Singh *et al.* demonstrated that niacin prevents the development of colitis and colitis-associated colorectal cancer by inducing immunoregulatory IL-10 and cytoprotective IL-18 production [237]. In a murine model of ulcerative colitis, niacin ameliorates pathologic angiogenesis and inflammatory changes through normalizing the colonic levels of TNF-a, VEGF, angiostatin,

endostatin and IL-10 [238]. In addition, severe deficiency of niacin leads to pellagra with symptoms including diarrhea, inflamed skins, dementia and sores in the mouth. Diarrhea always precedes dermatitis, suggesting that pellagra begins in the stomach [315]. Since niacin can be produced by gut microbiota [316], it is reasonable to speculate that niacin may affect the composition of gut microbiota. Indeed, delayed-release niacin preferentially targets the gut microbiome to increase the abundance of *Bacteroidetes* and improves biomarkers of systemic insulin sensitivity and metabolic inflammation in humans [239]. However, the specific effects of niacin on HFD-induced changes in gut microbiota are not clear.

In the current study, we described the gut microbiota composition in two strains of mice after long-term HFD feeding with or without niacin treatment using cultured-based method. The histological changes of small intestine, including goblet and Paneth cell number, were also investigated.

Materials and Methods

Materials

Bouin's solution, Mayer's hematoxylin and Eosin Y (H&E), Eukitt Mounting Medium, Alcian Blue, 0.5% periodic acid, Schiff's Reagent, phloxine B-calcium carbonate and tartrazine saturated cellosolve was purchased from Electron Microscopy Sciences (Hatfield, PA). Hemo-De was purchased from Fisher Scientific (Pittsburgh, PA). Anaerobic Basal Agar was purchased from Alfa Aesar (Tewksbury, MA). Brain Heart Infusion Agar, Blood agar and Violet Red Bile Agar was purchased from Hardy Diagnostic (Santa Maria, CA). *Bifidobacterium* agar and Brucella agar with hemin and vitamin K1 was purchased from HiMedia Laboratories (West

Chester, PA). Difco *Lactobacilli* MRS agar and BBL Mannitol Salt agar was purchased from Becton Dickinson (Sparks, MD).

Animal study

Same animal study was conducted as in chapter 2. During necropsy, small intestine, cecum and large intestine was removed and colon length was measured. Small segment of small intestine and colon were collected in the Bouin's solution for histology. Fecal samples were collected for gut microbiota analysis.

Analysis of the gut microbiota

Determination of the gut microbiota was performed according to methods described previously [317, 318]. Fecal matter was removed from the colon of each mouse using sterile technique, placed in sterile pre-weighed tubes with anaerobic broth, weighed, and vortexed until homogenous. Serial tenfold dilutions from 10^{-1} to 10^{-7} were prepared and from the appropriate dilution, a 0.1 mL aliquot was then spread on four plates with different media: Anaerobic Basal Agar for total anaerobic bacteria; Brain Heart Infusion Agar for total aerobes; Blood agar for hemolytic bacteria; *Bifidobacterium* agar for *Bifidobacterium*; Difco *Lactobacilli* MRS agar for *Lactobacillus*; BBL Mannitol Salt agar for *Staphylococcus*; Brucella agar with hemin and vitamin K1 for *Bacteroides*. For isolation of anaerobic bacteria plates were placed in an anaerobic chamber in a microaerophilic environment generated by a GasPak EZ Anaerobe Container System (Becton Dickinson and Co, Sparks, MD). All plates were incubated at 37°C and colonies were counted after incubation for 24 hours for aerobes and 48 hours for anaerobes. The number of colony-forming units (CFU) per gram of fecal matter was calculated. Bacterial

cultures were identified by morphology of colonies, microscopical analysis of cells' morphology, Gram staining, formation of spores, aerobic and anaerobic growth, as it was recommended elsewhere [318, 319].

Sample preparation for histological analysis

Samples of small intestine (0.5-2 cm in length) were immediately fixed in Bouin's solution for 10-15 min. Tissue samples were cut to proper size (5-7 mm in length) and transferred to fixative to make sure all tissues were completely immersed in fixative. The volume of fixative was 20-30 times the tissue volume. After 48 hours of fixation at room temperature, the excess fixative was washed out in 70% ethanol until most of the yellow color was removed. Washed samples were put into tissue embedding cassettes (VWR, Radnor, PA) and kept in 70% ethanol until processing in an automated tissue processor (Tissue-Tek VIP, Miles/Sakura, Torrance, CA). After processing, samples were embedded in paraffin blocks using embedding center (Tissue-Tek TEC, Sakura, Torrance, CA). Embedded tissue was sectioned at 6 micrometers using the microtome (Reichert-Jung 2040, Autocut, Leica Biosystems Nussloch GmbH. Heidelberger Straße 17-19 69226 Nussloch, Germany).

Goblet cell counting

Four sections from each mouse were stained as previously described [320]. Briefly, sections were subjected to a series of deparaffinizations, stained with Alcian Blue for 30 min, washed with tap and distilled water, treated with 0.5% periodic acid, washed with distilled water for 2 min, stained with Schiff's Reagent for 20 min, washed with tap water for 5 min, stained with hematoxylin (1 min), washed with tap water for 2 min, dehydrated, cleared in Hemo-De and

mounted in Eukitt Mounting Medium. Eight images from each section were taken with a digital camera (Pro series 3CCD camera) coupled to an optical microscope (Olympus BX50) with a 20x objective. The number of goblet cells presented in 1 mm^2 in the mucosa of each animal were quantified using ImagePro Plus software (Media Cybernetics, Rockville, MD).

Paneth cell counting

Phloxine-tartrazine technique were used to analyze Paneth cells, as previously reported [321]. Briefly, sections were treated with alum hematoxylin (5 minutes), washed with tap water (5 min), stained in phloxine B-calcium carbonate for 20 minutes, rinsed in tap water, blot dried, stained in a saturated solution of tartrazine saturated cellosolve for 10 min, rinsed in 95% ethanol, dehydrated in absolute ethanol, cleared in Hemo-De and mounted in Eukitt Mounting Medium. The number of Paneth cells was counted for each sample using a high-resolution microscope system [322]. Four sections from each mouse were analyzed.

Statistics

All data are presented as means ± SEM. Statistical analyses, including One-way ANOVA followed by Tukey's post-hoc test, were performed on Graph Pad Prism 8 software (La Jolla, CA). Differences were considered significant for $P < 0.05$.

Results

HFD and niacin differentially impact gut microbiota in B6 and B6129 mice

In normal gut microbiota, anaerobic bacteria make up a large portion of the total bacteria. The abundance of anaerobes and aerobes was significantly increased in B6 mice fed a HFD

(Figure 23A and B). Niacin treatment decreased anaerobes but not aerobes in HFD-fed B6 mice. In B6129 mice, aerobes but not anaerobes increased with HFD feeding. The anaerobes/aerobes ratio was slightly decreased in HFD-fed B6 mice, whereas it was dramatically decreased in HFD-fed B6129 mice (Figure 23 C). The abundance of *Firmicutes* was increased in B6 and B6129 mice fed a HFD (Figure 24A). *Firmicutes* number was decreased in HFD-fed B6 mice and increased in chow-fed B6129 mice with niacin treatment. HFD feeding increased the abundance of *Bacteroidetes* in B6 mice, which was not observed in B6129 mice (Figure 24B). *Bacteroidetes* number was increased in chow-fed B6 mice and HFD-fed B6129 mice with niacin treatment. *Firmicutes/Bacteroidetes* ratio was not altered in B6 mice, whereas it was increased in B6129 mice with HFD feeding (Figure 24C). Niacin treatment resulted a decrease in *Firmicutes/Bacteroidetes* ratio in HFD-fed B6129 mice.

To further analyze the gut microbiota composition, culture-based bacteria number at genus levels was determined. The abundance of *Bifidobacterium* was increased in HFD-fed B6 mice compared with that of chow-diet fed mice (Figure 25A). However, this increase was not observed in B6129 mice. The number of *Bifidobacterium* was increased in chow-fed B6 mice and decreased in HFD-fed B6 mice with niacin treatment. In B6129 mice, niacin treatment significantly increased the abundance of *Bifidobacterium* in HFD-fed mice. The abundance of *Lactobacillus* was increased in both B6 and B6129 mice after HFD feeding (Figure 25B). In B6129 mice, niacin treatment increased the number of *Lactobacillus* in chow-fed mice but decreased it in HFD-fed mice. The abundance of hemolytic bacteria was increased in both B6 and B6129 mice fed a HFD (Figure 25C). Niacin treatment significantly lowered the number of hemolytic bacteria in HFD-fed B6129 mice, but had no impact on B6 mice. The absolute number of *Bacteroides* was increased in HFD-fed B6 mice, and this was not observed in B6129

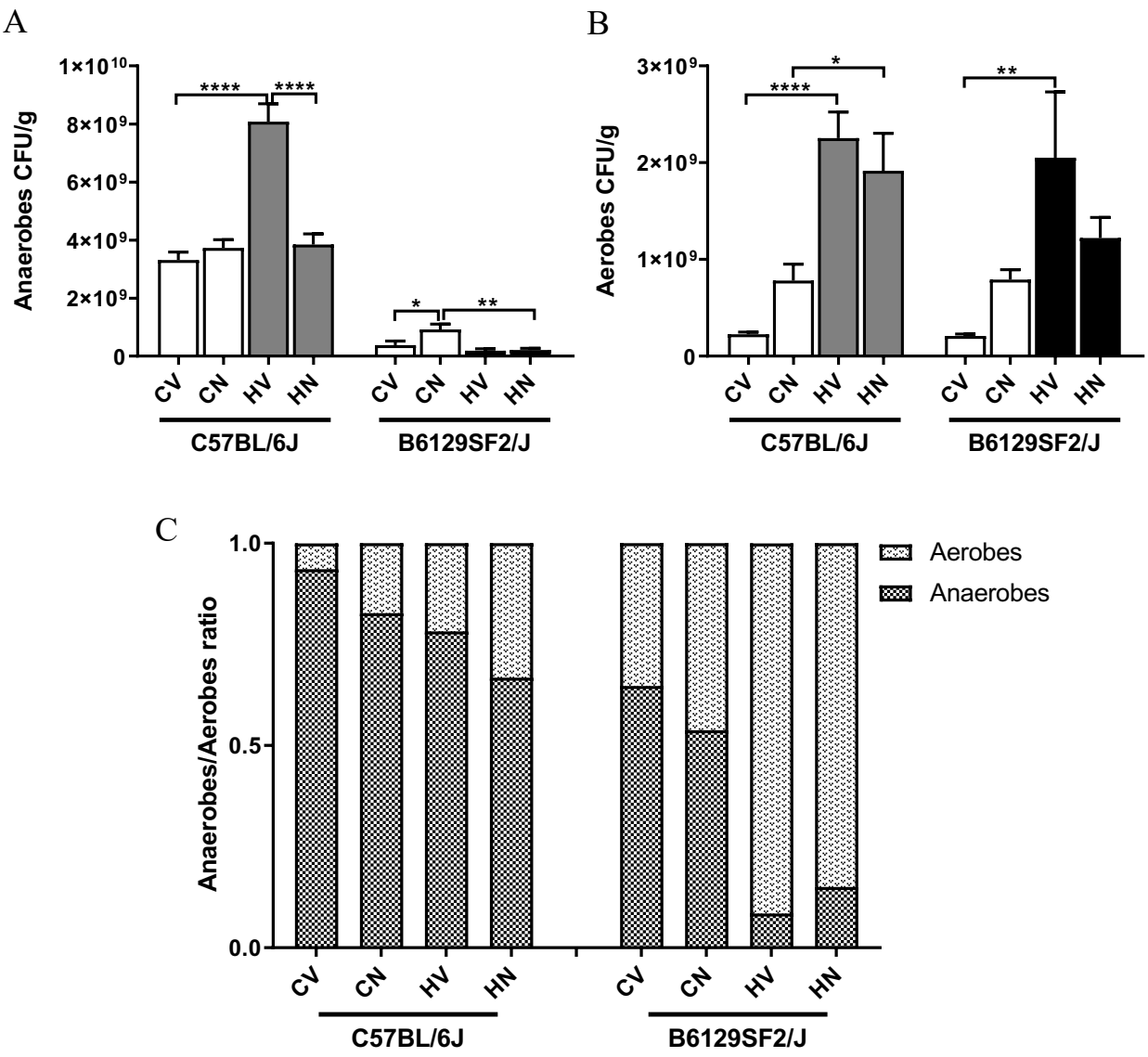

Figure 23. Abundance of (A) anaerobes and (B) aerobes and (C) anaerobes/aerobes ratio in B6 and B6129 mice. **P*<0.05, ***P*<0.01, *****P*<0.0001.

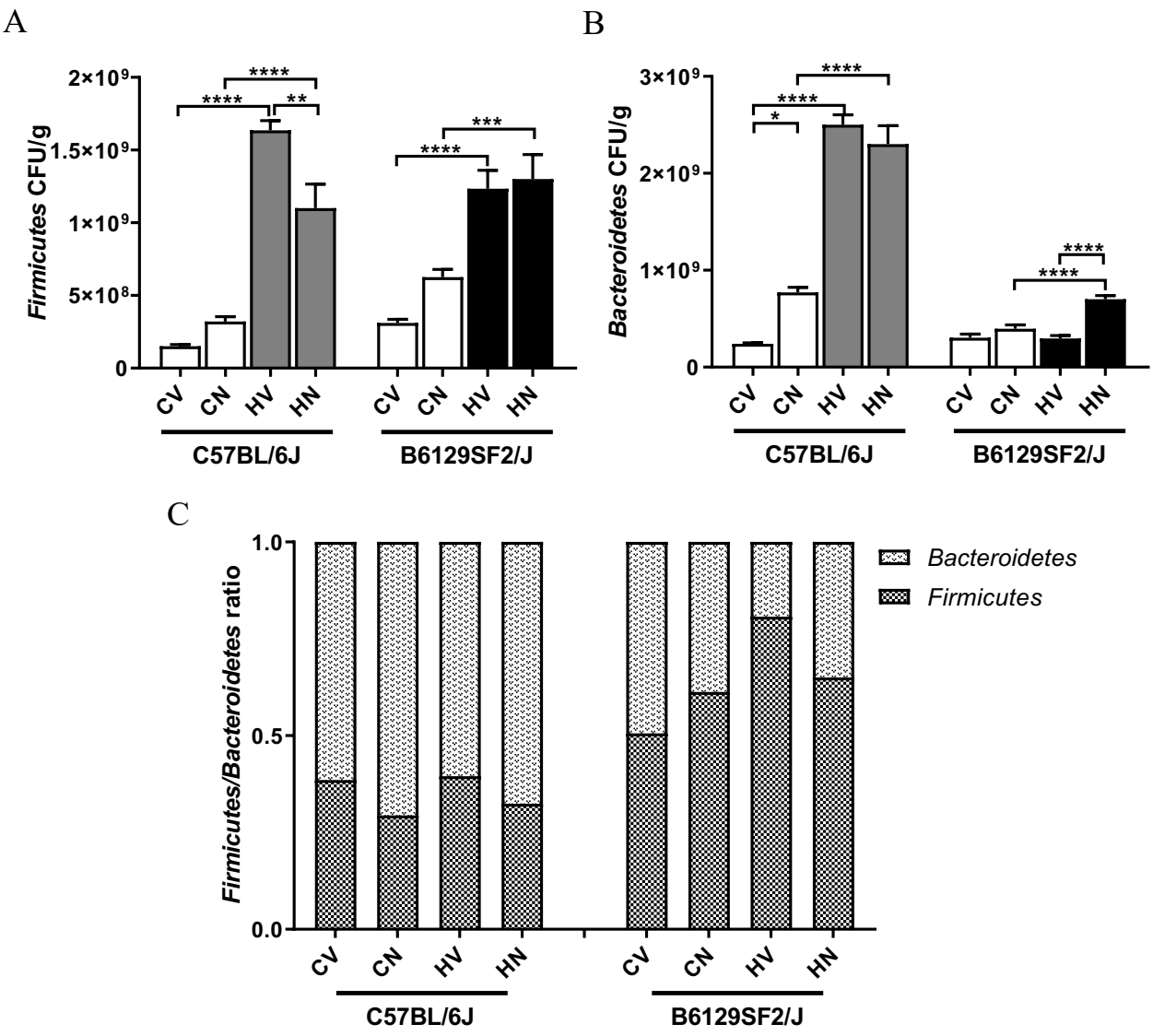

Figure 24. Abundance of (A) *Firmicutes* and (B) *Bacteroidetes* and (C) *Firmicutes/Bacteroidetes* ratio in B6 and B6129 mice. **P*<0.05, ***P*<0.01, ****P*<0.001, *****P*<0.0001.

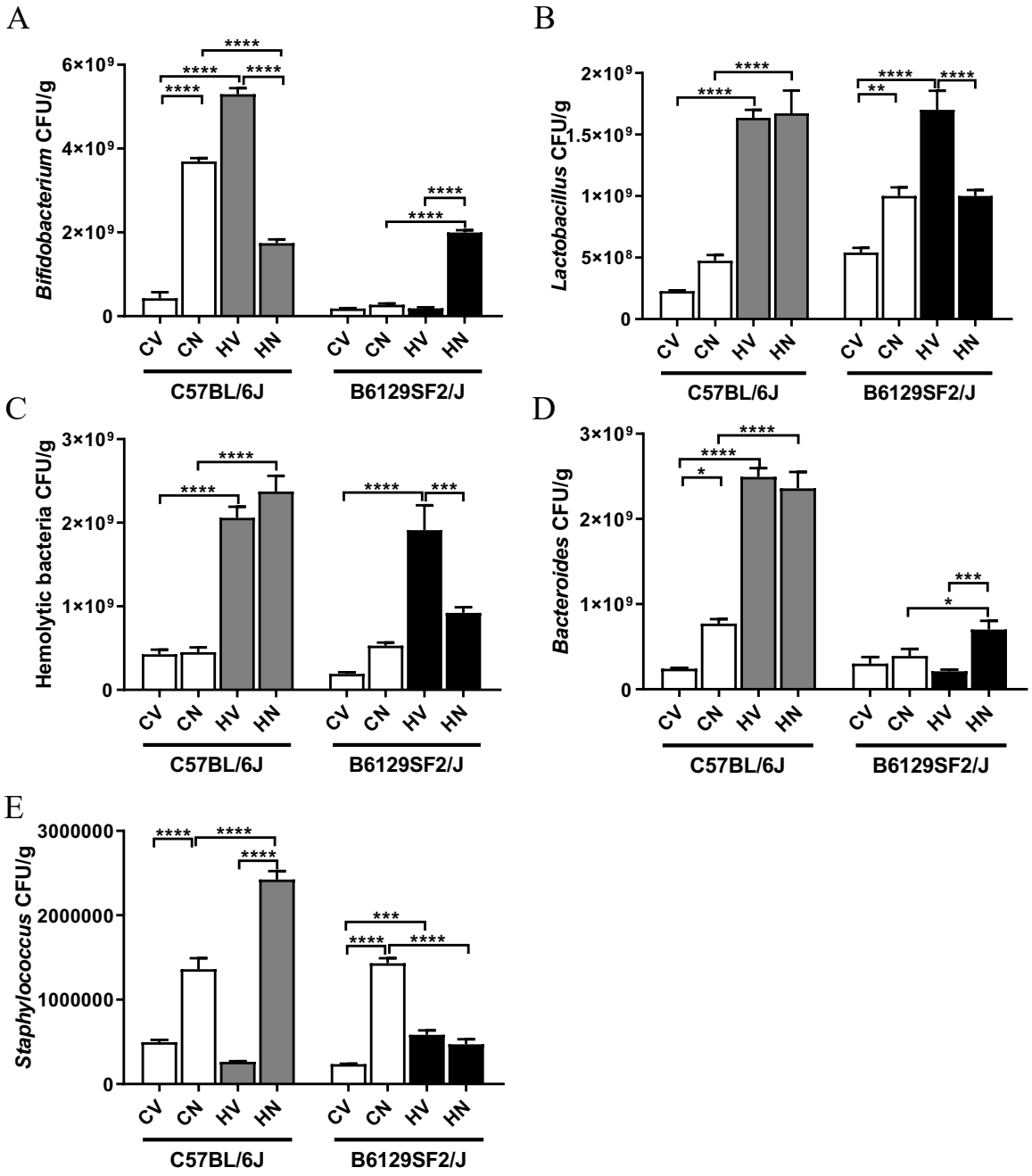

Figure 25. Abundance of bacteria at genus level in gut microbiota of B6 and B6129 mice. (A) *Bifidobacterium*. (B) *Lactobacillus*. (C) Hemolytic bacteria. (D) *Bacteroides*. (E) *Staphylococcus*. **P*<0.05, ***P*<0.01, ****P*<0.001, *****P*<0.0001.

mice (Figure 25D). Niacin increased *Bacteroides* abundance on chow-fed B6 mice and HFD-fed B6129 mice. The abundance of *Staphylococcus* was much lower than the other four bacteria. Niacin treatment increased *Staphylococcus* number in both chow- and HFD-fed B6 mice (Figure 25E). This increase was observed in chow-fed B6129 mice but not HFD-fed B6129 mice.

Staphylococcus was not included in the analysis of gut microbiota composition, since it was less than 1% of total bacteria. In B6 mice, HFD feeding increased the relative proportion of *Bifidobacterium* and decreased hemolytic bacteria (Figure 26). Niacin treatment increased *Bacteroides* and decreased *Bifidobacterium* proportion in both chow- and HFD-fed B6 mice. In contrast, in HFD-fed B6129 mice, the relative proportion of hemolytic bacteria was dramatically increased, while *Bacteroides* and *Bifidobacterium* proportionally decreased. Niacin did not significantly alter the gut microbiota composition in chow-fed B6129 mice. However, in HFD-fed B6129 mice, niacin decreased proportion of hemolytic bacteria and *Lactobacillus* and increased *Bifidobacterium* from 4.7% to 43.2%.

HFD and niacin differentially affect intestinal histology

HFD feeding did not change the colon length in both B6 and B6129 mice compared with chow diet (Figure 27). Niacin treatment significantly increased colon length in HFD-fed B6129 mice but had no impact on B6 mice (Figure 27). Since gut microbiota are important regulators of gastrointestinal function, the number of goblet and Paneth cell in the small intestine was determined. Goblet cells are responsible for the production and maintenance of mucus, which protects small and large intestine. Paneth cells produce antimicrobial peptide and play an important role in gut innate mucosal defense activity. The number of goblet cell and Paneth cell did not change in B6 mice with either HFD feeding or niacin treatment (Figure 28 and 29).

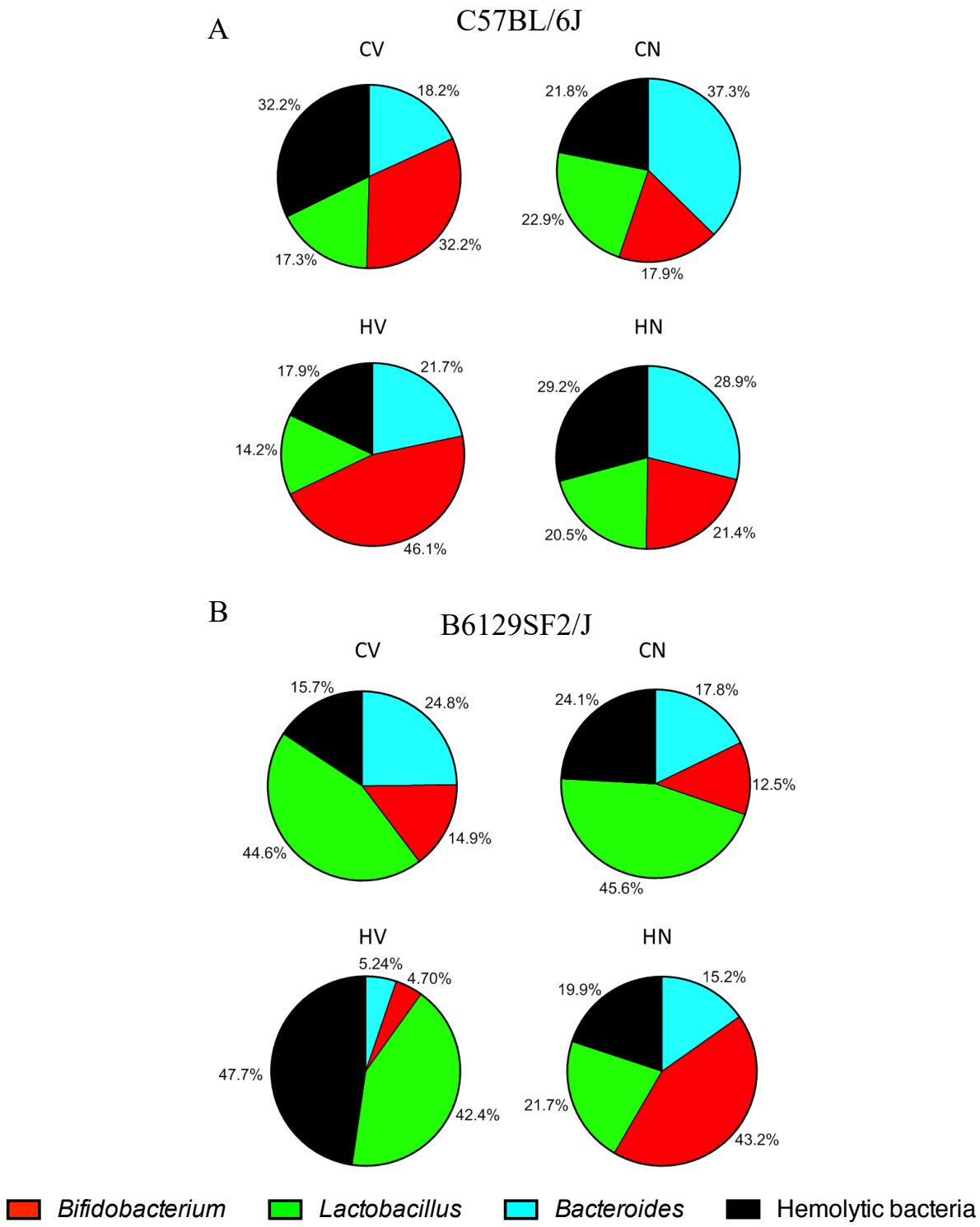

Figure 26. Gut microbiota composition in (A) B6 and (B) B6129 mice.

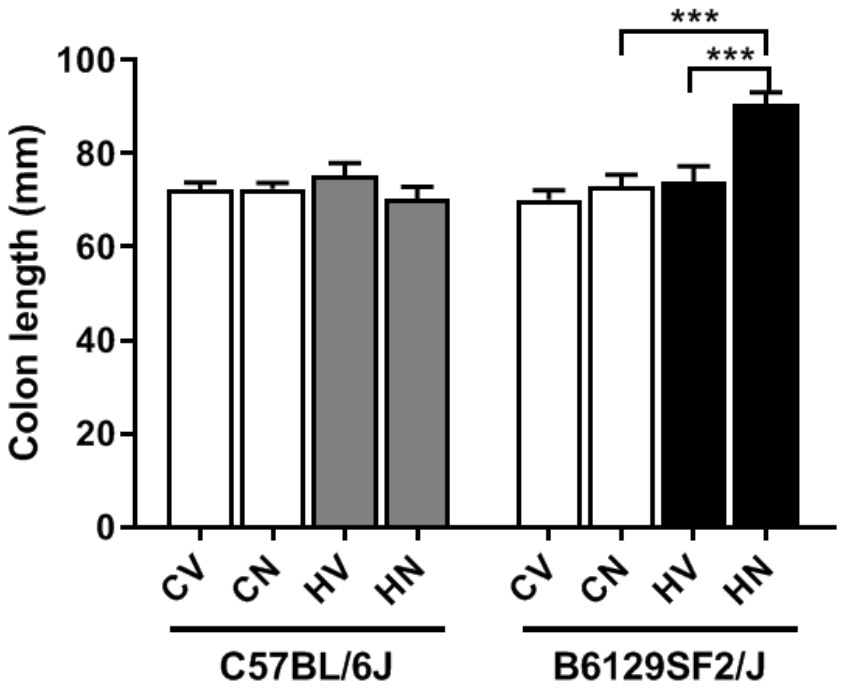

Figure 27. Colon length of B6 and B6129 mice. ***P<0.001.

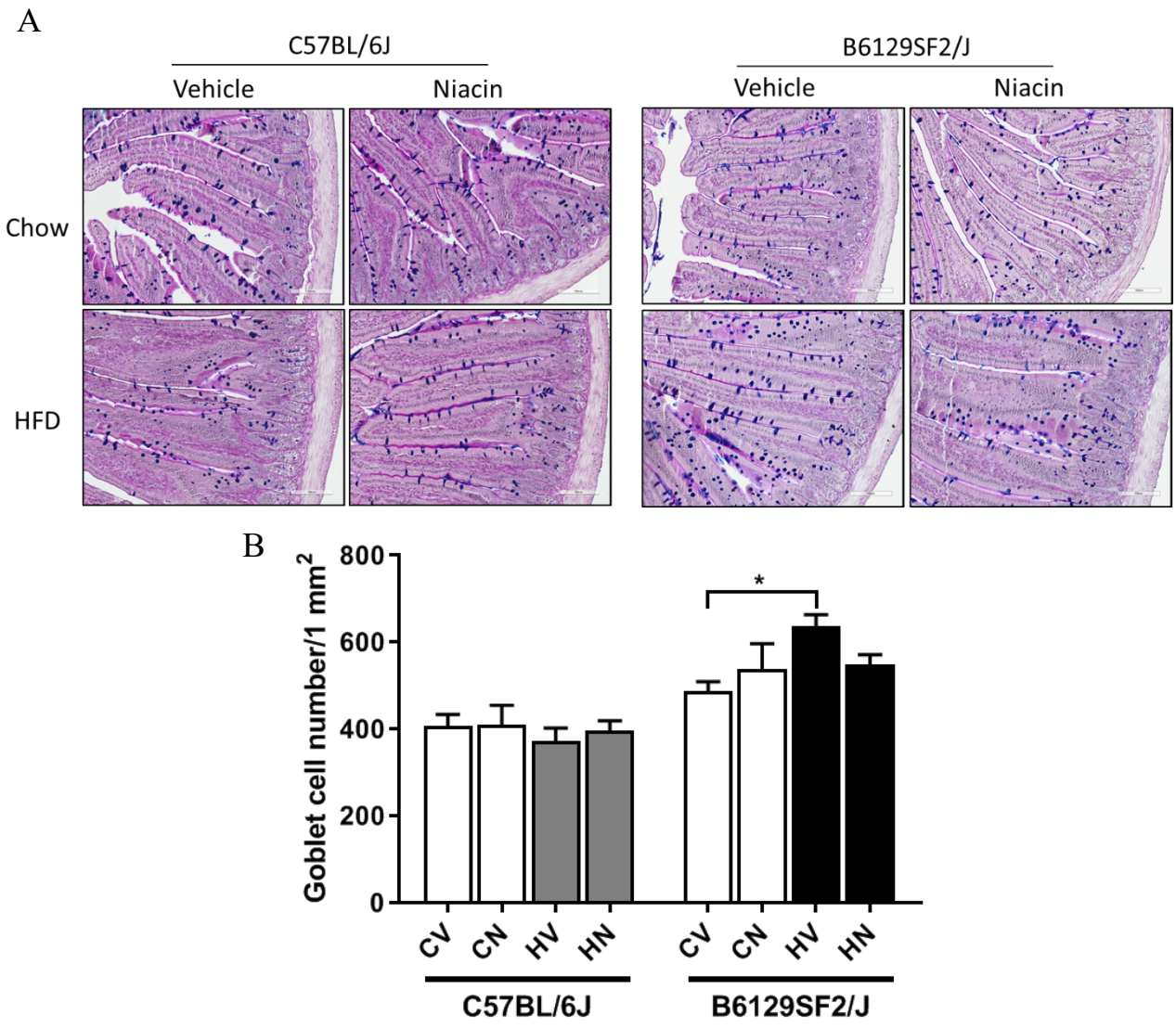

Figure 28. Goblet cell number in B6 and B6129 mice. (A) Representative images of Alcian Blue stained small intestine sections. (B) Quantitative goblet cell number in 1 mm^2 area. *P<0.05.

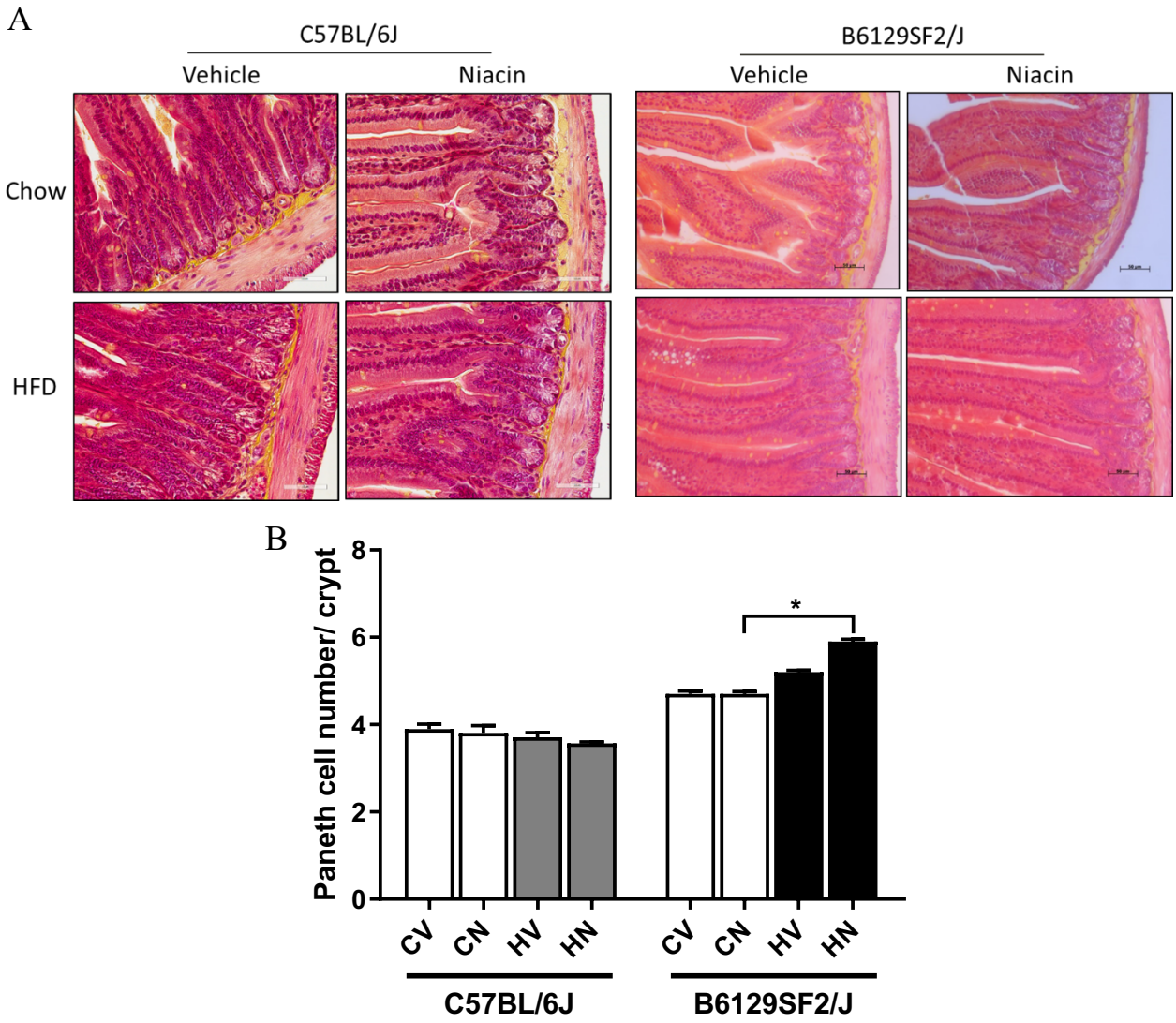

Figure 29. Paneth cell number in B6 and B6129 mice. (A) Representative images of phloxine-tartrazine stained small intestine sections. (B) Quantitative Paneth cell number per crypt. *P<0.05.

However, in B6129 mice, goblet cell number was increased after HFD feeding (Figure 28). HN B6129 mice had greatest number of Paneth cell number among all groups (Figure 29).

Discussion

Normal gut microbiota is important for maintaining homeostasis of the organism. Anaerobes comprise the majority of normal microbiota in the gut. The abundance of anaerobes was greater in B6 than B6129 mice, whereas the abundance of aerobes was comparable between the two strains of mice. Compared with chow-fed B6129 mice, the anaerobes/aerobes ratio was much higher in the B6 mice, indicating a different microbiota composition between B6 and B6129 mice under normal conditions. Since these two strains of mice were housed in the same environment and provided with the same food, other factors, especially genetics, may contribute to this difference. Anaerobes/aerobes ratio was decreased in both B6 and B6129 mice fed a HFD, but it was more dramatic in B6129 mice, suggesting that the gut microbiota in B6129 mice is vulnerable to external disturbance, such as diet. In support of this, after colonization with seven human-derived and inflammatory bowel disease-related intestinal bacterial species, the changes in relative bacterial composition overtime are more dramatic in 129 than B6 mice [323].

Increased *Firmicutes/Bacteroidetes* ratio has been reported in HFD-induced obese mice, genetically obese *ob/ob* mice and obese humans [152-154]. Similar increases were observed in HFD-fed B6129 but not B6 mice, which was decreased by niacin treatment. This decrease was due to increased *Bacteroidetes* abundance induced by niacin, indicating that niacin may favor the growth of *Bacteroidetes* in B6129 mice. In line with this, the abundance of *Bacteroides*, which belongs to the *Bacteroidetes* phylum, was increased in HFD-fed B6129 mice with niacin treatment. Hemolytic bacteria can break down red blood cells and cause hemolysis. Under

normal conditions, the proportion of hemolytic bacteria is very low. However, the proportion of hemolytic bacteria in chow-fed B6 and B6129 mice is 32.3% and 15.7%, respectively. This is very likely due to the lack of fermentable fiber in the chow diet. HFD feeding significantly increased hemolytic bacteria in both B6 and B6129 mice, indicating the adverse effects of HFD on microbiota in these mice. Niacin treatment decreased the abundance and proportion of hemolytic bacteria in HFD-fed B6129 mice, but had no effect in B6 mice. Most of the beneficial bacteria belong to *Bifidobacterium* and *Lactobacillus* genera. The proportion of *Bifidobacterium* was increased from 32.2% to 46.1% and decreased from 14.9% to 4.7% in HFD-fed B6 and B6129 mice, respectively. The absolute number of *Lactobacillus* was increased in HFD-fed mice of both strains. Similar increase is also observed in obese patients [324]. However, the proportion of *Lactobacillus* was remained relatively constant after HFD feeding. Together, these data suggest that gut microbiota of B6 mice was more resistant to HFD-induced disruption than that of B6129 mice. Niacin positively affects the gut microbiota composition in HFD-fed B6129 mice by favoring the growth of *Bifidobacterium* and *Bacteroides* and inhibiting the growth of hemolytic bacteria.

The changes in gut microbiota composition induced by HFD are not entirely consistent with previous studies [152, 166], in which the chow diet is not matched to their HFD. Besides fat content, other differences also exist, including sucrose, fiber and protein, all of which impact the gut microbiota as well. The diets used in the current study are compositionally defined diets and are matched in most of the ingradients, including fiber, protein and sucrose. Therefore, the changes of gut microbiota in this study truly reflect the impact of high fat and low carbohydrate. Although genetic identification of bacteria is prevalent in studying microbiome, the culture-based method used in this study more accurately reflect the real conditions of microorganisms in

the gut. Dead and non-functional microorganisms may be still detected by genetic method, while they cannot grow in culture medium. However, culture-based method is very labor-intensive and limited by the number of microorganisms that can be grown in culture.

The colonic epithelial cells are under constant renewing through cell proliferation and differentiation every 4-5 days. Diets that contain high fat usually lack fiber, leading to decreased production of short-chain fatty acids, which serves as an energy source for colonocytes. Therefore, HFD feeding may result in energy shortage for colonic epithelial cell proliferation and differentiation, resulting in decreased colon length. Indeed, shortened colon length has been reported in mice with chronic HFD feeding [167]. However, in the current study, HFD did not alter the colon length in either B6 or B6129 mice. This is likely due to the fact that colon length is associated with the fiber content in the diet rather than fat [168]. The fiber content in the chow and HFD in this study was matched. Therefore, it is not surprising that no change in colon length after HFD feeding. Interestingly, niacin treatment increased colon length in HFD-fed B6129 mice but not B6 mice, which may be associated with gut microbiota composition change in those mice.

In addition to colon length, changes in goblet and Paneth cells number were also determined. Goblet cells synthesize and secret mucins to form a mucus layer lining the gastrointestinal tract, preventing microorganism and noxious substances from reaching the epithelium. Increased mucus production has been demonstrated to mediate IL-22-induced amelioration of intestinal inflammation [325]. Thus, the increased goblet cell number in HFD-fed B6129 mice may represent a compensatory mechanism against HFD-induced colonic inflammation. Paneth cells reside at the bottom of the small intestine crypts and produce large amounts of antimicrobial peptides and proteins. The increased Paneth cell number in HN B6129

mice may contribute to decreased abundance of hemolytic bacteria in these mice by increasing the secretion of antimicrobial substance.

Conclusions

In conclusion, HFD and niacin had minor impact on gut microbiota composition, colon length, Paneth and goblet cell number in B6 mice. However, B6129 mice that were fed a HFD displayed disrupted gut microbiota composition with increased proportion of hemolytic bacteria and abnormal number of goblet cell, all of which were improved by niacin treatment. In addition, niacin supplementation increased colon length and Paneth cell number in HFD-fed B6129 mice. Therefore, B6 mice were more resistant to HFD and niacin-induced changes in gut microbiota composition and small intestine histology than B6129 mice.

Conclusions and Future Directions

As a wild type control, B6 mice have been extensively studied in various metabolic studies. However, compared with B6 mice, B6129 mice are better approximate controls for those genetically engineered strains that maintained on a mixed B6;129 background due to prevailing occurrence of passenger mutations in the regions flanking the target gene. Nevertheless, a limited number of studies have characterized the physiological and metabolic phenotype of B6129 mice under nutritional challenge. Therefore, the current study employed the classic HFD containing 60% fat to induce obesity in B6 and B6129 mice and comparatively studied the differences in metabolic responses in adipose tissue, liver, and gastrointestinal tract between these two strains of mice. In addition to HFD, the effects of niacin on these metabolic parameters were also studied in B6 and B6129 mice. Previous work from our lab and other labs have demonstrated that pharmacological doses of niacin increase serum adiponectin concentrations, inhibit obesity-induced adipose tissue inflammation, prevent triglyceride accumulation in NAFLD and suppress colonic inflammation in colitis and colorectal cancer. All of the above studies were done in either B6 mice or rats. However, the pharmacological effects of niacin in B6129 mice are unknown.

Upon HFD feeding, B6 and B6129 mice had similar weight gain and developed insulin resistance. However, niacin significantly decreased weight gain in HFD-fed B6 but not B6129 mice. Both strains of mice developed adipose tissue inflammation, but it was more advanced in B6 mice. Niacin decreased adipose tissue inflammation in B6129 but not B6 mice. Even with

similar increases in NAFLD histological score, B6129 had lower normalized liver weight than B6 mice. Unexpectedly, niacin potentiated the development of NAFLD in B6129 mice by increasing normalized liver weight, hepatic triglyceride content and NAFLD histological score. In contrast, niacin had no impact on any of these parameters in B6 mice. Metabolomics and lipidomics analysis revealed that HFD and niacin resulted in different metabolite and lipid profiles in B6 and B6129 mice. A total of 21 and 26 metabolites were identified as different between chow and HFD group in B6 and B6129 mice, respectively. In B6 mice, only 6 metabolites were identified as different with niacin treatment and no specific pathways appeared to be impacted. In contrast, in B6129 mice, 16 metabolites and 5 pathways were impacted by niacin during HFD feeding. Of the metabolites that were changed in these pathways, 4-HPP did not change with HFD feeding but significantly decreased with niacin treatment. The decreased 4-HPP has been indicated to be associated with impaired β-oxidation. Lipidomics analysis identified that the abundance of PC was not altered in B6 mice, but decreased in HFD-fed B6129 mice. Mechanistically, long-term high doses of niacin deplete the methyl-pool in hepatocytes, preventing other methylation reactions, such as the conversion of PC from PE. The involvement of PC in VLDL triglyceride production and secretion suggests that niacin-induced fatty liver in HFD-fed B6129 mice may be partly due to decreased secretion of triglycerides. The different effects of niacin in the livers of B6 and B6129 mice may be associated with their genetic background. Individuals that have metabolic disturbances similar to B6129 mice are potentially predisposed to the adverse effects of niacin or other methyl-consumers (e.g. alcohol). In addition, HFD and niacin had minor impact on gut microbiota composition, colon length, Paneth and goblet cell number in B6 mice. However, B6129 mice that were fed a HFD displayed disrupted gut microbiota composition with increased proportion of hemolytic bacteria and

decreased proportion of *Bifidobacterium* and *Bacteroides* and abnormal number of goblet cell, all of which were improved by niacin treatment. Therefore, B6 mice are more resistant to HFD and niacin-induced changes in gut microbiota composition and small intestine histology than B6129 mice. Researchers should be aware of these metabolic differences between B6 and B6129 mice when considering choosing appropriate controls for their study design.

Studies in this dissertation described for the first time important metabolomic difference between B6 and B6129 mice. However, these studies have also posed additional questions. Niacin decreased body weight gain in HFD-fed B6 but not B6129 mice without changing food intake. Therefore, the mechanism by which niacin affects energy expenditure need to be further investigated, including the possible role of brown adipose tissue. In addition, further studies are needed to examine the effect of HFD and niacin on colon function and its relationship with gut microbiota composition. Since the gut-adipose-liver axis has been proposed to play an important role in the development of metabolic syndrome, the cross talk among these tissues should be studied as well.

References

1. Huang, T. and F.B. Hu, *Gene-environment interactions and obesity: recent developments and future directions.* BMC Med Genomics, 2015. **8 Suppl 1**: p. S2.

2. Ng, M., et al., *Global, regional, and national prevalence of overweight and obesity in children and adults during 1980-2013: a systematic analysis for the Global Burden of Disease Study 2013.* Lancet, 2014. **384**(9945): p. 766-81.

3. Gallagher, E.J. and D. LeRoith, *Obesity and Diabetes: The Increased Risk of Cancer and Cancer-Related Mortality.* Physiol Rev, 2015. **95**(3): p. 727-48.

4. Van Gaal, L.F., I.L. Mertens, and C.E. De Block, *Mechanisms linking obesity with cardiovascular disease.* Nature, 2006. **444**(7121): p. 875-80.

5. Woo Baidal, J.A. and J.E. Lavine, *The intersection of nonalcoholic fatty liver disease and obesity.* Sci Transl Med, 2016. **8**(323): p. 323rv1.

6. Scherer, P.E., *Adipose tissue: from lipid storage compartment to endocrine organ.* Diabetes, 2006. **55**(6): p. 1537-45.

7. Halaas, J.L., et al., *Weight-reducing effects of the plasma protein encoded by the obese gene.* Science, 1995. **269**(5223): p. 543-6.

8. Maffei, M., et al., *Leptin levels in human and rodent: measurement of plasma leptin and ob RNA in obese and weight-reduced subjects.* Nat Med, 1995. **1**(11): p. 1155-61.

9. Lee, G.H., et al., *Abnormal splicing of the leptin receptor in diabetic mice.* Nature, 1996. **379**(6566): p. 632-5.

10. Chua, S.C., Jr., et al., *Phenotypes of mouse diabetes and rat fatty due to mutations in the OB (leptin) receptor.* Science, 1996. **271**(5251): p. 994-6.

11. Considine, R.V., et al., *Serum immunoreactive-leptin concentrations in normal-weight and obese humans.* N Engl J Med, 1996. **334**(5): p. 292-5.

12. Leon-Cabrera, S., et al., *Hyperleptinemia is associated with parameters of low-grade systemic inflammation and metabolic dysfunction in obese human beings.* Front Integr Neurosci, 2013. **7**: p. 62.

13. Janik, J.E., et al., *Interleukin 1 alpha increases serum leptin concentrations in humans.* J Clin Endocrinol Metab, 1997. **82**(9): p. 3084-6.

14. Sarraf, P., et al., *Multiple cytokines and acute inflammation raise mouse leptin levels: potential role in inflammatory anorexia.* J Exp Med, 1997. **185**(1): p. 171-5.

15. Finck, B.N., et al., *In vivo and in vitro evidence for the involvement of tumor necrosis factor-alpha in the induction of leptin by lipopolysaccharide.* Endocrinology, 1998. **139**(5): p. 2278-83.

16. Scherer, P.E., et al., *A novel serum protein similar to C1q, produced exclusively in adipocytes.* J Biol Chem, 1995. **270**(45): p. 26746-9.

17. Berg, A.H., T.P. Combs, and P.E. Scherer, *ACRP30/adiponectin: an adipokine regulating glucose and lipid metabolism.* Trends Endocrinol Metab, 2002. **13**(2): p. 84-9.

18. Wozniak, S.E., et al., *Adipose tissue: the new endocrine organ? A review article.* Dig Dis Sci, 2009. **54**(9): p. 1847-56.

19. Hotta, K., et al., *Circulating concentrations of the adipocyte protein adiponectin are decreased in parallel with reduced insulin sensitivity during the progression to type 2 diabetes in rhesus monkeys.* Diabetes, 2001. **50**(5): p. 1126-33.

20. Pyrzak, B., et al., *Adiponectin as a biomarker of the metabolic syndrome in children and adolescents.* Eur J Med Res, 2010. **15 Suppl 2**: p. 147-51.

21. Yamauchi, T., et al., *Cloning of adiponectin receptors that mediate antidiabetic metabolic effects.* Nature, 2003. **423**(6941): p. 762-9.

22. Hug, C., et al., *T-cadherin is a receptor for hexameric and high-molecular-weight forms of Acrp30/adiponectin.* Proc Natl Acad Sci U S A, 2004. **101**(28): p. 10308-13.

23. Denzel, M.S., et al., *T-cadherin is critical for adiponectin-mediated cardioprotection in mice.* J Clin Invest, 2010. **120**(12): p. 4342-52.

24. Gray, S.L. and A.J. Vidal-Puig, *Adipose tissue expandability in the maintenance of metabolic homeostasis.* Nutr Rev, 2007. **65**(6 Pt 2): p. S7-12.

25. Haczeyni, F., K.S. Bell-Anderson, and G.C. Farrell, *Causes and mechanisms of adipocyte enlargement and adipose expansion.* Obes Rev, 2018. **19**(3): p. 406-420.

26. Wang, Q.A. and P.E. Scherer, *The AdipoChaser mouse: A model tracking adipogenesis in vivo.* Adipocyte, 2014. **3**(2): p. 146-50.

27. Samocha-Bonet, D., et al., *Metabolically healthy and unhealthy obese--the 2013 Stock Conference report.* Obes Rev, 2014. **15**(9): p. 697-708.

28. Thorne, A., et al., *A pilot study of long-term effects of a novel obesity treatment: omentectomy in connection with adjustable gastric banding.* Int J Obes Relat Metab Disord, 2002. **26**(2): p. 193-9.

29. Klein, S., et al., *Absence of an effect of liposuction on insulin action and risk factors for coronary heart disease.* N Engl J Med, 2004. **350**(25): p. 2549-57.

30. Lackey, D.E. and J.M. Olefsky, *Regulation of metabolism by the innate immune system.* Nat Rev Endocrinol, 2016. **12**(1): p. 15-28.

31. Weisberg, S.P., et al., *Obesity is associated with macrophage accumulation in adipose tissue.* J Clin Invest, 2003. **112**(12): p. 1796-808.

32. Murano, I., et al., *Dead adipocytes, detected as crown-like structures, are prevalent in visceral fat depots of genetically obese mice.* J Lipid Res, 2008. **49**(7): p. 1562-8.

33. Yuan, M., et al., *Reversal of obesity- and diet-induced insulin resistance with salicylates or targeted disruption of Ikkbeta.* Science, 2001. **293**(5535): p. 1673-7.

34. Arkan, M.C., et al., *IKK-beta links inflammation to obesity-induced insulin resistance.* Nat Med, 2005. **11**(2): p. 191-8.

35. Dinarello, C.A., et al., *Interleukin-18 and IL-18 binding protein.* Front Immunol, 2013. **4**: p. 289.

36. de Luca, C. and J.M. Olefsky, *Stressed out about obesity and insulin resistance.* Nat Med, 2006. **12**(1): p. 41-2; discussion 42.

37. De Lorenzo, A., et al., *Normal-weight obese syndrome: early inflammation?* Am J Clin Nutr, 2007. **85**(1): p. 40-5.

38. van Exel, E., et al., *Low production capacity of interleukin-10 associates with the metabolic syndrome and type 2 diabetes : the Leiden 85-Plus Study.* Diabetes, 2002. **51**(4): p. 1088-92.

39. Cancello, R., et al., *Reduction of macrophage infiltration and chemoattractant gene expression changes in white adipose tissue of morbidly obese subjects after surgery-induced weight loss.* Diabetes, 2005. **54**(8): p. 2277-86.

40. Farrell, G.C. and C.Z. Larter, *Nonalcoholic fatty liver disease: from steatosis to cirrhosis.* Hepatology, 2006. **43**(2 Suppl 1): p. S99-S112.

41. Perumpail, B.J., et al., *Clinical epidemiology and disease burden of nonalcoholic fatty liver disease.* World J Gastroenterol, 2017. **23**(47): p. 8263-8276.

42. Bellentani, S., et al., *Epidemiology of non-alcoholic fatty liver disease.* Dig Dis, 2010. **28**(1): p. 155-61.

43. Buzzetti, E., M. Pinzani, and E.A. Tsochatzis, *The multiple-hit pathogenesis of non-alcoholic fatty liver disease (NAFLD).* Metabolism, 2016. **65**(8): p. 1038-48.

44. Donnelly, K.L., et al., *Sources of fatty acids stored in liver and secreted via lipoproteins in patients with nonalcoholic fatty liver disease.* J Clin Invest, 2005. **115**(5): p. 1343-51.

45. Simard, J.R., B.K. Pillai, and J.A. Hamilton, *Fatty acid flip-flop in a model membrane is faster than desorption into the aqueous phase.* Biochemistry, 2008. **47**(35): p. 9081-9.

46. Ehehalt, R., et al., *Translocation of long chain fatty acids across the plasma membrane--lipid rafts and fatty acid transport proteins.* Mol Cell Biochem, 2006. **284**(1-2): p. 135-40.

47. Bradbury, M.W., *Lipid metabolism and liver inflammation. I. Hepatic fatty acid uptake: possible role in steatosis.* Am J Physiol Gastrointest Liver Physiol, 2006. **290**(2): p. G194-8.

48. Harmon, C.M. and N.A. Abumrad, *Binding of sulfosuccinimidyl fatty acids to adipocyte membrane proteins: isolation and amino-terminal sequence of an 88-kD protein implicated in transport of long-chain fatty acids.* J Membr Biol, 1993. **133**(1): p. 43-9.

49. Hajri, T. and N.A. Abumrad, *Fatty acid transport across membranes: relevance to nutrition and metabolic pathology.* Annu Rev Nutr, 2002. **22**: p. 383-415.

50. Buque, X., et al., *A subset of dysregulated metabolic and survival genes is associated with severity of hepatic steatosis in obese Zucker rats.* J Lipid Res, 2010. **51**(3): p. 500-13.

51. Miquilena-Colina, M.E., et al., *Hepatic fatty acid translocase CD36 upregulation is associated with insulin resistance, hyperinsulinaemia and increased steatosis in non-alcoholic steatohepatitis and chronic hepatitis C.* Gut, 2011. **60**(10): p. 1394-402.

52. Greco, D., et al., *Gene expression in human NAFLD.* Am J Physiol Gastrointest Liver Physiol, 2008. **294**(5): p. G1281-7.

53. Wilson, C.G., et al., *Hepatocyte-Specific Disruption of CD36 Attenuates Fatty Liver and Improves Insulin Sensitivity in HFD-Fed Mice.* Endocrinology, 2016. **157**(2): p. 570-85.

54. Zhou, J., et al., *A novel pregnane X receptor-mediated and sterol regulatory element-binding protein-independent lipogenic pathway.* J Biol Chem, 2006. **281**(21): p. 15013-20.

55. Zhou, J., et al., *Hepatic fatty acid transporter Cd36 is a common target of LXR, PXR, and PPARgamma in promoting steatosis.* Gastroenterology, 2008. **134**(2): p. 556-67.

56. Chmurzynska, A., *The multigene family of fatty acid-binding proteins (FABPs): function, structure and polymorphism.* J Appl Genet, 2006. **47**(1): p. 39-48.

57. Furuhashi, M. and G.S. Hotamisligil, *Fatty acid-binding proteins: role in metabolic diseases and potential as drug targets.* Nat Rev Drug Discov, 2008. **7**(6): p. 489-503.

58. Memon, R.A., et al., *Regulation of putative fatty acid transporters and Acyl-CoA synthetase in liver and adipose tissue in ob/ob mice.* Diabetes, 1999. **48**(1): p. 121-7.

59. Falcon, A., et al., *FATP2 is a hepatic fatty acid transporter and peroxisomal very long-chain acyl-CoA synthetase.* Am J Physiol Endocrinol Metab, 2010. **299**(3): p. E384-93.

60. Doege, H., et al., *Targeted deletion of FATP5 reveals multiple functions in liver metabolism: alterations in hepatic lipid homeostasis.* Gastroenterology, 2006. **130**(4): p. 1245-58.

61. Krammer, J., et al., *Overexpression of CD36 and acyl-CoA synthetases FATP2, FATP4 and ACSL1 increases fatty acid uptake in human hepatoma cells.* Int J Med Sci, 2011. **8**(7): p. 599-614.

62. Doege, H., et al., *Silencing of hepatic fatty acid transporter protein 5 in vivo reverses diet-induced non-alcoholic fatty liver disease and improves hyperglycemia.* J Biol Chem, 2008. **283**(32): p. 22186-92.

63. Stahl, A., et al., *Fatty acid transport proteins: a current view of a growing family.* Trends Endocrinol Metab, 2001. **12**(6): p. 266-73.

64. Seessle, J., et al., *Palmitate activation by fatty acid transport protein 4 as a model system for hepatocellular apoptosis and steatosis.* Biochim Biophys Acta, 2015. **1851**(5): p. 549-65.

65. Musso, G., R. Gambino, and M. Cassader, *Recent insights into hepatic lipid metabolism in non-alcoholic fatty liver disease (NAFLD).* Prog Lipid Res, 2009. **48**(1): p. 1-26.

66. Kreuz, S., et al., *Acetyl-CoA carboxylases 1 and 2 show distinct expression patterns in rats and humans and alterations in obesity and diabetes.* Diabetes Metab Res Rev, 2009. **25**(6): p. 577-86.

67. Mao, J., et al., *Liver-specific deletion of acetyl-CoA carboxylase 1 reduces hepatic triglyceride accumulation without affecting glucose homeostasis.* Proc Natl Acad Sci U S A, 2006. **103**(22): p. 8552-7.

68. Abu-Elheiga, L., et al., *Mutant mice lacking acetyl-CoA carboxylase 1 are embryonically lethal.* Proc Natl Acad Sci U S A, 2005. **102**(34): p. 12011-6.

69. Abu-Elheiga, L., et al., *Continuous fatty acid oxidation and reduced fat storage in mice lacking acetyl-CoA carboxylase 2.* Science, 2001. **291**(5513): p. 2613-6.

70. Abu-Elheiga, L., et al., *Acetyl-CoA carboxylase 2 mutant mice are protected against obesity and diabetes induced by high-fat/high-carbohydrate diets.* Proc Natl Acad Sci U S A, 2003. **100**(18): p. 10207-12.

71. Savage, D.B., et al., *Reversal of diet-induced hepatic steatosis and hepatic insulin resistance by antisense oligonucleotide inhibitors of acetyl-CoA carboxylases 1 and 2.* J Clin Invest, 2006. **116**(3): p. 817-24.

72. Stiede, K., et al., *Acetyl-coenzyme A carboxylase inhibition reduces de novo lipogenesis in overweight male subjects: A randomized, double-blind, crossover study.* Hepatology, 2017. **66**(2): p. 324-334.

73. Chirala, S.S., et al., *Fatty acid synthesis is essential in embryonic development: fatty acid synthase null mutants and most of the heterozygotes die in utero.* Proc Natl Acad Sci U S A, 2003. **100**(11): p. 6358-63.

74. Chakravarthy, M.V., et al., *"New" hepatic fat activates PPARalpha to maintain glucose, lipid, and cholesterol homeostasis.* Cell Metab, 2005. **1**(5): p. 309-22.

75. Iizuka, K., B. Miller, and K. Uyeda, *Deficiency of carbohydrate-activated transcription factor ChREBP prevents obesity and improves plasma glucose control in leptin-deficient (ob/ob) mice.* Am J Physiol Endocrinol Metab, 2006. **291**(2): p. E358-64.

76. Fiebig, R.G., et al., *Training down-regulates fatty acid synthase and body fat in obese Zucker rats.* Med Sci Sports Exerc, 2002. **34**(7): p. 1106-14.

77. Popeijus, H.E., W.H. Saris, and R.P. Mensink, *Role of stearoyl-CoA desaturases in obesity and the metabolic syndrome.* Int J Obes (Lond), 2008. **32**(7): p. 1076-82.

78. Ntambi, J.M., et al., *Loss of stearoyl-CoA desaturase-1 function protects mice against adiposity.* Proc Natl Acad Sci U S A, 2002. **99**(17): p. 11482-6.

79. Cohen, P., et al., *Role for stearoyl-CoA desaturase-1 in leptin-mediated weight loss.* Science, 2002. **297**(5579): p. 240-3.

80. Flowers, J.B., et al., *Loss of stearoyl-CoA desaturase-1 improves insulin sensitivity in lean mice but worsens diabetes in leptin-deficient obese mice.* Diabetes, 2007. **56**(5): p. 1228-39.

81. Jiang, G., et al., *Prevention of obesity in mice by antisense oligonucleotide inhibitors of stearoyl-CoA desaturase-1.* J Clin Invest, 2005. **115**(4): p. 1030-8.

82. Miyazaki, M., et al., *Hepatic stearoyl-CoA desaturase-1 deficiency protects mice from carbohydrate-induced adiposity and hepatic steatosis.* Cell Metab, 2007. **6**(6): p. 484-96.

83. Hu, C.C., K. Qing, and Y. Chen, *Diet-induced changes in stearoyl-CoA desaturase 1 expression in obesity-prone and -resistant mice.* Obes Res, 2004. **12**(8): p. 1264-70.

84. Stefan, N., et al., *Low hepatic stearoyl-CoA desaturase 1 activity is associated with fatty liver and insulin resistance in obese humans.* Diabetologia, 2008. **51**(4): p. 648-56.

85. Cases, S., et al., *Cloning of DGAT2, a second mammalian diacylglycerol acyltransferase, and related family members.* J Biol Chem, 2001. **276**(42): p. 38870-6.

86. Oelkers, P., et al., *Characterization of two human genes encoding acyl coenzyme A:cholesterol acyltransferase-related enzymes.* J Biol Chem, 1998. **273**(41): p. 26765-71.

87. Smith, S.J., et al., *Obesity resistance and multiple mechanisms of triglyceride synthesis in mice lacking Dgat.* Nat Genet, 2000. **25**(1): p. 87-90.

88. Chen, H.C., et al., *Increased insulin and leptin sensitivity in mice lacking acyl CoA:diacylglycerol acyltransferase 1.* J Clin Invest, 2002. **109**(8): p. 1049-55.

89. Stone, S.J., et al., *Lipopenia and skin barrier abnormalities in DGAT2-deficient mice.* J Biol Chem, 2004. **279**(12): p. 11767-76.

90. Choi, C.S., et al., *Suppression of diacylglycerol acyltransferase-2 (DGAT2), but not DGAT1, with antisense oligonucleotides reverses diet-induced hepatic steatosis and insulin resistance.* J Biol Chem, 2007. **282**(31): p. 22678-88.

91. Yu, X.X., et al., *Antisense oligonucleotide reduction of DGAT2 expression improves hepatic steatosis and hyperlipidemia in obese mice.* Hepatology, 2005. **42**(2): p. 362-71.

92. Naik, R., et al., *Therapeutic strategies for metabolic diseases: Small-molecule diacylglycerol acyltransferase (DGAT) inhibitors.* ChemMedChem, 2014. **9**(11): p. 2410-24.

93. Monetti, M., et al., *Dissociation of hepatic steatosis and insulin resistance in mice overexpressing DGAT in the liver.* Cell Metab, 2007. **6**(1): p. 69-78.

94. McLaren, D.G., et al., *DGAT2 Inhibition Alters Aspects of Triglyceride Metabolism in Rodents but Not in Non-human Primates.* Cell Metab, 2018. **27**(6): p. 1236-1248 e6.

95. Shimano, H. and R. Sato, *SREBP-regulated lipid metabolism: convergent physiology - divergent pathophysiology.* Nat Rev Endocrinol, 2017. **13**(12): p. 710-730.

96. Eberle, D., et al., *SREBP transcription factors: master regulators of lipid homeostasis.* Biochimie, 2004. **86**(11): p. 839-48.

97. Shimano, H., et al., *Isoform 1c of sterol regulatory element binding protein is less active than isoform 1a in livers of transgenic mice and in cultured cells.* J Clin Invest, 1997. **99**(5): p. 846-54.

98. Liang, G., et al., *Diminished hepatic response to fasting/refeeding and liver X receptor agonists in mice with selective deficiency of sterol regulatory element-binding protein-1c.* J Biol Chem, 2002. **277**(11): p. 9520-8.

99. Shimomura, I., Y. Bashmakov, and J.D. Horton, *Increased levels of nuclear SREBP-1c associated with fatty livers in two mouse models of diabetes mellitus.* J Biol Chem, 1999. **274**(42): p. 30028-32.

100. Kohjima, M., et al., *SREBP-1c, regulated by the insulin and AMPK signaling pathways, plays a role in nonalcoholic fatty liver disease.* Int J Mol Med, 2008. **21**(4): p. 507-11.

101. Moon, Y.A., et al., *The Scap/SREBP pathway is essential for developing diabetic fatty liver and carbohydrate-induced hypertriglyceridemia in animals.* Cell Metab, 2012. **15**(2): p. 240-6.

102. Yahagi, N., et al., *Absence of sterol regulatory element-binding protein-1 (SREBP-1) ameliorates fatty livers but not obesity or insulin resistance in Lep(ob)/Lep(ob) mice.* J Biol Chem, 2002. **277**(22): p. 19353-7.

103. Iizuka, K., et al., *Deficiency of carbohydrate response element-binding protein (ChREBP) reduces lipogenesis as well as glycolysis.* Proc Natl Acad Sci U S A, 2004. **101**(19): p. 7281-6.

104. Dentin, R., et al., *Liver-specific inhibition of ChREBP improves hepatic steatosis and insulin resistance in ob/ob mice.* Diabetes, 2006. **55**(8): p. 2159-70.

105. Benhamed, F., et al., *The lipogenic transcription factor ChREBP dissociates hepatic steatosis from insulin resistance in mice and humans.* J Clin Invest, 2012. **122**(6): p. 2176-94.

106. Repa, J.J., et al., *Regulation of mouse sterol regulatory element-binding protein-1c gene (SREBP-1c) by oxysterol receptors, LXRalpha and LXRbeta.* Genes Dev, 2000. **14**(22): p. 2819-30.

107. Joseph, S.B., et al., *Direct and indirect mechanisms for regulation of fatty acid synthase gene expression by liver X receptors.* J Biol Chem, 2002. **277**(13): p. 11019-25.

108. Zelcer, N. and P. Tontonoz, *Liver X receptors as integrators of metabolic and inflammatory signaling.* J Clin Invest, 2006. **116**(3): p. 607-14.

109. Kalaany, N.Y., et al., *LXRs regulate the balance between fat storage and oxidation.* Cell Metab, 2005. **1**(4): p. 231-44.

110. Grefhorst, A., et al., *Stimulation of lipogenesis by pharmacological activation of the liver X receptor leads to production of large, triglyceride-rich very low density lipoprotein particles.* J Biol Chem, 2002. **277**(37): p. 34182-90.

111. Sinal, C.J., et al., *Targeted disruption of the nuclear receptor FXR/BAR impairs bile acid and lipid homeostasis.* Cell, 2000. **102**(6): p. 731-44.

112. Kalaany, N.Y. and D.J. Mangelsdorf, *LXRS and FXR: the yin and yang of cholesterol and fat metabolism.* Annu Rev Physiol, 2006. **68**: p. 159-91.

113. Diraison, F., P. Moulin, and M. Beylot, *Contribution of hepatic de novo lipogenesis and reesterification of plasma non esterified fatty acids to plasma triglyceride synthesis during non-alcoholic fatty liver disease.* Diabetes Metab, 2003. **29**(5): p. 478-85.

114. Petersen, K.F., et al., *The role of skeletal muscle insulin resistance in the pathogenesis of the metabolic syndrome.* Proc Natl Acad Sci U S A, 2007. **104**(31): p. 12587-94.

115. Schreurs, M., F. Kuipers, and F.R. van der Leij, *Regulatory enzymes of mitochondrial beta-oxidation as targets for treatment of the metabolic syndrome.* Obes Rev, 2010. **11**(5): p. 380-8.

116. Tolwani, R.J., et al., *Medium-chain acyl-CoA dehydrogenase deficiency in gene-targeted mice.* PLoS Genet, 2005. **1**(2): p. e23.

117. Zhang, D., et al., *Mitochondrial dysfunction due to long-chain Acyl-CoA dehydrogenase deficiency causes hepatic steatosis and hepatic insulin resistance.* Proc Natl Acad Sci U S A, 2007. **104**(43): p. 17075-80.

118. Stefanovic-Racic, M., et al., *A moderate increase in carnitine palmitoyltransferase 1a activity is sufficient to substantially reduce hepatic triglyceride levels.* Am J Physiol Endocrinol Metab, 2008. **294**(5): p. E969-77.

119. Miele, L., et al., *Hepatic mitochondrial beta-oxidation in patients with nonalcoholic steatohepatitis assessed by 13C-octanoate breath test.* Am J Gastroenterol, 2003. **98**(10): p. 2335-6.

120. Iozzo, P., et al., *Fatty acid metabolism in the liver, measured by positron emission tomography, is increased in obese individuals.* Gastroenterology, 2010. **139**(3): p. 846-56, 856 e1-6.

121. Petersen, K.F., et al., *Assessment of Hepatic Mitochondrial Oxidation and Pyruvate Cycling in NAFLD by (13)C Magnetic Resonance Spectroscopy.* Cell Metab, 2016. **24**(1): p. 167-71.

122. Hussain, M.M., J. Shi, and P. Dreizen, *Microsomal triglyceride transfer protein and its role in apoB-lipoprotein assembly.* J Lipid Res, 2003. **44**(1): p. 22-32.

123. Raabe, M., et al., *Analysis of the role of microsomal triglyceride transfer protein in the liver of tissue-specific knockout mice.* J Clin Invest, 1999. **103**(9): p. 1287-98.

124. Cuchel, M., et al., *Inhibition of microsomal triglyceride transfer protein in familial hypercholesterolemia.* N Engl J Med, 2007. **356**(2): p. 148-56.

125. Walkey, C.J., et al., *Biochemical and evolutionary significance of phospholipid methylation.* J Biol Chem, 1998. **273**(42): p. 27043-6.

126. Zhu, X., et al., *Phosphatidylethanolamine N-methyltransferase (PEMT) knockout mice have hepatic steatosis and abnormal hepatic choline metabolite concentrations despite ingesting a recommended dietary intake of choline.* Biochem J, 2003. **370**(Pt 3): p. 987-93.

127. van der Veen, J.N., et al., *Pioglitazone attenuates hepatic inflammation and fibrosis in phosphatidylethanolamine N-methyltransferase-deficient mice.* Am J Physiol Gastrointest Liver Physiol, 2016. **310**(7): p. G526-38.

128. Cano, A., et al., *Methionine adenosyltransferase 1A gene deletion disrupts hepatic very low-density lipoprotein assembly in mice.* Hepatology, 2011. **54**(6): p. 1975-86.

129. Leonardi, R., et al., *Elimination of the CDP-ethanolamine pathway disrupts hepatic lipid homeostasis.* J Biol Chem, 2009. **284**(40): p. 27077-89.

130. Hamilton, R.L. and P.E. Fielding, *Nascent very low density lipoproteins from rat hepatocytic Golgi fractions are enriched in phosphatidylethanolamine.* Biochem Biophys Res Commun, 1989. **160**(1): p. 162-73.

131. Agren, J.J., J.P. Kurvinen, and A. Kuksis, *Isolation of very low density lipoprotein phospholipids enriched in ethanolamine phospholipids from rats injected with Triton WR 1339.* Biochim Biophys Acta, 2005. **1734**(1): p. 34-43.

132. Fu, S., et al., *Aberrant lipid metabolism disrupts calcium homeostasis causing liver endoplasmic reticulum stress in obesity.* Nature, 2011. **473**(7348): p. 528-31.

133. Ling, J., et al., *Hepatic ratio of phosphatidylcholine to phosphatidylethanolamine predicts survival after partial hepatectomy in mice.* Hepatology, 2012. **55**(4): p. 1094-102.

134. Li, Z., et al., *The ratio of phosphatidylcholine to phosphatidylethanolamine influences membrane integrity and steatohepatitis.* Cell Metab, 2006. **3**(5): p. 321-31.

135. Fabbrini, E., S. Sullivan, and S. Klein, *Obesity and nonalcoholic fatty liver disease: biochemical, metabolic, and clinical implications.* Hepatology, 2010. **51**(2): p. 679-89.

136. Fabbrini, E., et al., *Alterations in adipose tissue and hepatic lipid kinetics in obese men and women with nonalcoholic fatty liver disease.* Gastroenterology, 2008. **134**(2): p. 424-31.

137. Baffy, G., *Kupffer cells in non-alcoholic fatty liver disease: the emerging view.* J Hepatol, 2009. **51**(1): p. 212-23.

138. Cai, D., et al., *Local and systemic insulin resistance resulting from hepatic activation of IKK-beta and NF-kappaB.* Nat Med, 2005. **11**(2): p. 183-90.

139. Lanthier, N., et al., *Kupffer cell activation is a causal factor for hepatic insulin resistance.* Am J Physiol Gastrointest Liver Physiol, 2010. **298**(1): p. G107-16.

140. Tomita, K., et al., *Tumour necrosis factor alpha signalling through activation of Kupffer cells plays an essential role in liver fibrosis of non-alcoholic steatohepatitis in mice.* Gut, 2006. **55**(3): p. 415-24.

141. Gordon, S., *Alternative activation of macrophages.* Nat Rev Immunol, 2003. **3**(1): p. 23-35.

142. Shoelson, S.E., J. Lee, and A.B. Goldfine, *Inflammation and insulin resistance.* J Clin Invest, 2006. **116**(7): p. 1793-801.

143. Ribeiro, P.S., et al., *Hepatocyte apoptosis, expression of death receptors, and activation of NF-kappaB in the liver of nonalcoholic and alcoholic steatohepatitis patients.* Am J Gastroenterol, 2004. **99**(9): p. 1708-17.

144. Sender, R., S. Fuchs, and R. Milo, *Are We Really Vastly Outnumbered? Revisiting the Ratio of Bacterial to Host Cells in Humans.* Cell, 2016. **164**(3): p. 337-40.

145. Arumugam, M., et al., *Enterotypes of the human gut microbiome.* Nature, 2011. **473**(7346): p. 174-80.

146. Jandhyala, S.M., et al., *Role of the normal gut microbiota.* World J Gastroenterol, 2015. **21**(29): p. 8787-803.

147. Blumberg, R. and F. Powrie, *Microbiota, disease, and back to health: a metastable journey.* Sci Transl Med, 2012. **4**(137): p. 137rv7.

148. Biasucci, G., et al., *Mode of delivery affects the bacterial community in the newborn gut.* Early Hum Dev, 2010. **86 Suppl 1**: p. 13-5.

149. Makino, H., et al., *Mother-to-infant transmission of intestinal bifidobacterial strains has an impact on the early development of vaginally delivered infant's microbiota.* PLoS One, 2013. **8**(11): p. e78331.

150. Munyaka, P.M., E. Khafipour, and J.E. Ghia, *External influence of early childhood establishment of gut microbiota and subsequent health implications.* Front Pediatr, 2014. **2**: p. 109.

151. Baothman, O.A., et al., *The role of Gut Microbiota in the development of obesity and Diabetes.* Lipids Health Dis, 2016. **15**: p. 108.

152. Zhang, C., et al., *Structural resilience of the gut microbiota in adult mice under high-fat dietary perturbations.* ISME J, 2012. **6**(10): p. 1848-57.

153. Ley, R.E., et al., *Obesity alters gut microbial ecology.* Proc Natl Acad Sci U S A, 2005. **102**(31): p. 11070-5.

154. Ley, R.E., et al., *Microbial ecology: human gut microbes associated with obesity.* Nature, 2006. **444**(7122): p. 1022-3.

155. Higashimura, Y., et al., *Protective effect of agaro-oligosaccharides on gut dysbiosis and colon tumorigenesis in high-fat diet-fed mice.* Am J Physiol Gastrointest Liver Physiol, 2016. **310**(6): p. G367-75.

156. Backhed, F., et al., *Mechanisms underlying the resistance to diet-induced obesity in germ-free mice.* Proc Natl Acad Sci U S A, 2007. **104**(3): p. 979-84.

157. Backhed, F., et al., *The gut microbiota as an environmental factor that regulates fat storage.* Proc Natl Acad Sci U S A, 2004. **101**(44): p. 15718-23.

158. Turnbaugh, P.J., et al., *An obesity-associated gut microbiome with increased capacity for energy harvest.* Nature, 2006. **444**(7122): p. 1027-31.

159. Schwiertz, A., et al., *Microbiota and SCFA in lean and overweight healthy subjects.* Obesity (Silver Spring), 2010. **18**(1): p. 190-5.

160. Payne, A.N., et al., *The metabolic activity of gut microbiota in obese children is increased compared with normal-weight children and exhibits more exhaustive substrate utilization.* Nutr Diabetes, 2011. **1**: p. e12.

161. Nishimura, S., I. Manabe, and R. Nagai, *Adipose tissue inflammation in obesity and metabolic syndrome.* Discov Med, 2009. **8**(41): p. 55-60.

162. Cani, P.D., et al., *Metabolic endotoxemia initiates obesity and insulin resistance.* Diabetes, 2007. **56**(7): p. 1761-72.

163. Gulhane, M., et al., *High Fat Diets Induce Colonic Epithelial Cell Stress and Inflammation that is Reversed by IL-22.* Sci Rep, 2016. **6**: p. 28990.

164. Kim, K.A., et al., *High fat diet-induced gut microbiota exacerbates inflammation and obesity in mice via the TLR4 signaling pathway.* PLoS One, 2012. **7**(10): p. e47713.

165. Amar, J., et al., *Intestinal mucosal adherence and translocation of commensal bacteria at the early onset of type 2 diabetes: molecular mechanisms and probiotic treatment.* EMBO Mol Med, 2011. **3**(9): p. 559-72.

166. Cani, P.D., et al., *Changes in gut microbiota control metabolic endotoxemia-induced inflammation in high-fat diet-induced obesity and diabetes in mice.* Diabetes, 2008. **57**(6): p. 1470-81.

167. Dinh, C.H., et al., *Bardoxolone Methyl Prevents High-Fat Diet-Induced Colon Inflammation in Mice.* J Histochem Cytochem, 2016. **64**(4): p. 237-55.

168. Chassaing, B., et al., *Lack of soluble fiber drives diet-induced adiposity in mice.* Am J Physiol Gastrointest Liver Physiol, 2015. **309**(7): p. G528-41.

169. Yin, Y.N., et al., *Effects of four Bifidobacteria on obesity in high-fat diet induced rats.* World J Gastroenterol, 2010. **16**(27): p. 3394-401.

170. An, H.M., et al., *Antiobesity and lipid-lowering effects of Bifidobacterium spp. in high fat diet-induced obese rats.* Lipids Health Dis, 2011. **10**: p. 116.

171. Chen, J., et al., *Bifidobacterium adolescentis supplementation ameliorates visceral fat accumulation and insulin sensitivity in an experimental model of the metabolic syndrome.* Br J Nutr, 2012. **107**(10): p. 1429-34.

172. Kim, S.W., et al., *Lactobacillus rhamnosus GG improves insulin sensitivity and reduces adiposity in high-fat diet-fed mice through enhancement of adiponectin production.* Biochem Biophys Res Commun, 2013. **431**(2): p. 258-63.

173. Everard, A., et al., *Responses of gut microbiota and glucose and lipid metabolism to prebiotics in genetic obese and diet-induced leptin-resistant mice.* Diabetes, 2011. **60**(11): p. 2775-86.

174. Dewulf, E.M., et al., *Insight into the prebiotic concept: lessons from an exploratory, double blind intervention study with inulin-type fructans in obese women.* Gut, 2013. **62**(8): p. 1112-21.

175. Genta, S., et al., *Yacon syrup: beneficial effects on obesity and insulin resistance in humans.* Clin Nutr, 2009. **28**(2): p. 182-7.

176. Parnell, J.A. and R.A. Reimer, *Weight loss during oligofructose supplementation is associated with decreased ghrelin and increased peptide YY in overweight and obese adults.* Am J Clin Nutr, 2009. **89**(6): p. 1751-9.

177. Kassam, Z., et al., *Fecal microbiota transplantation for Clostridium difficile infection: systematic review and meta-analysis.* Am J Gastroenterol, 2013. **108**(4): p. 500-8.

178. Altschul, R., A. Hoffer, and J.D. Stephen, *Influence of nicotinic acid on serum cholesterol in man.* Arch Biochem Biophys, 1955. **54**(2): p. 558-9.

179. Meyers, C.D., V.S. Kamanna, and M.L. Kashyap, *Niacin therapy in atherosclerosis.* Curr Opin Lipidol, 2004. **15**(6): p. 659-65.

180. Carlson, L.A., *Nicotinic acid: the broad-spectrum lipid drug. A 50th anniversary review.* J Intern Med, 2005. **258**(2): p. 94-114.

181. Morgan, J.M., et al., *Effects of extended-release niacin on lipoprotein subclass distribution.* Am J Cardiol, 2003. **91**(12): p. 1432-6.

182. Pieper, J.A., *Overview of niacin formulations: differences in pharmacokinetics, efficacy, and safety.* Am J Health Syst Pharm, 2003. **60**(13 Suppl 2): p. S9-14; quiz S25.

183. Cooper, D.L., et al., *Effects of formulation design on niacin therapeutics: mechanism of action, metabolism, and drug delivery.* Int J Pharm, 2015. **490**(1-2): p. 55-64.

184. Piepho, R.W., *The pharmacokinetics and pharmacodynamics of agents proven to raise high-density lipoprotein cholesterol.* Am J Cardiol, 2000. **86**(12A): p. 35L-40L.

185. Knopp, R.H., et al., *Equivalent efficacy of a time-release form of niacin (Niaspan) given once-a-night versus plain niacin in the management of hyperlipidemia.* Metabolism, 1998. **47**(9): p. 1097-104.

186. Berns, J.S., *Niacin and related compounds for treating hyperphosphatemia in dialysis patients.* Semin Dial, 2008. **21**(3): p. 203-5.

187. Soga, T., et al., *Molecular identification of nicotinic acid receptor.* Biochem Biophys Res Commun, 2003. **303**(1): p. 364-9.

188. Tunaru, S., et al., *PUMA-G and HM74 are receptors for nicotinic acid and mediate its anti-lipolytic effect.* Nat Med, 2003. **9**(3): p. 352-5.

189. Wise, A., et al., *Molecular identification of high and low affinity receptors for nicotinic acid.* J Biol Chem, 2003. **278**(11): p. 9869-74.

190. Graff, E.C., et al., *Anti-inflammatory effects of the hydroxycarboxylic acid receptor 2.* Metabolism, 2016. **65**(2): p. 102-13.

191. Gille, A., et al., *Nicotinic acid: pharmacological effects and mechanisms of action.* Annu Rev Pharmacol Toxicol, 2008. **48**: p. 79-106.

192. Mandrika, I., et al., *Hydroxycarboxylic Acid Receptor Ligands Modulate Proinflammatory Cytokine Expression in Human Macrophages and Adipocytes without Affecting Adipose Differentiation.* Biol Pharm Bull, 2018. **41**(10): p. 1574-1580.

193. Wanders, D., et al., *Niacin increases adiponectin and decreases adipose tissue inflammation in high fat diet-fed mice.* PLoS One, 2013. **8**(8): p. e71285.

194. Lauring, B., et al., *Niacin lipid efficacy is independent of both the niacin receptor GPR109A and free fatty acid suppression.* Sci Transl Med, 2012. **4**(148): p. 148ra115.

195. van der Hoorn, J.W., et al., *Niacin increases HDL by reducing hepatic expression and plasma levels of cholesteryl ester transfer protein in APOE*3Leiden.CETP mice.* Arterioscler Thromb Vasc Biol, 2008. **28**(11): p. 2016-22.

196. Lukasova, M., et al., *Nicotinic acid inhibits progression of atherosclerosis in mice through its receptor GPR109A expressed by immune cells.* J Clin Invest, 2011. **121**(3): p. 1163-73.

197. Wu, B.J., et al., *Evidence that niacin inhibits acute vascular inflammation and improves endothelial dysfunction independent of changes in plasma lipids.* Arterioscler Thromb Vasc Biol, 2010. **30**(5): p. 968-75.

198. Moore, K.J. and I. Tabas, *Macrophages in the pathogenesis of atherosclerosis.* Cell, 2011. **145**(3): p. 341-55.

199. Wu, B.J., et al., *Niacin inhibits vascular inflammation via the induction of heme oxygenase-1.* Circulation, 2012. **125**(1): p. 150-8.

200. Zandi-Nejad, K., et al., *The role of HCA2 (GPR109A) in regulating macrophage function.* FASEB J, 2013. **27**(11): p. 4366-74.

201. Digby, J.E., et al., *Anti-inflammatory effects of nicotinic acid in adipocytes demonstrated by suppression of fractalkine, RANTES, and MCP-1 and upregulation of adiponectin.* Atherosclerosis, 2010. **209**(1): p. 89-95.

202. Plaisance, E.P., et al., *Niacin stimulates adiponectin secretion through the GPR109A receptor.* Am J Physiol Endocrinol Metab, 2009. **296**(3): p. E549-58.

203. Fraterrigo, G., et al., *Relationship between Changes in Plasma Adiponectin Concentration and Insulin Sensitivity after Niacin Therapy.* Cardiorenal Med, 2012. **2**(3): p. 211-217.

204. Fang, H. and R.L. Judd, *Adiponectin Regulation and Function.* Compr Physiol, 2018. **8**(3): p. 1031-1063.

205. Ouchi, N., et al., *Adipocyte-derived plasma protein, adiponectin, suppresses lipid accumulation and class A scavenger receptor expression in human monocyte-derived macrophages.* Circulation, 2001. **103**(8): p. 1057-63.

206. Okamoto, Y., et al., *Adiponectin reduces atherosclerosis in apolipoprotein E-deficient mice.* Circulation, 2002. **106**(22): p. 2767-70.

207. Wang, X., et al., *Adiponectin abates atherosclerosis by reducing oxidative stress.* Med Sci Monit, 2014. **20**: p. 1792-800.

208. Wang, X., et al., *Adiponectin improves NF-kappaB-mediated inflammation and abates atherosclerosis progression in apolipoprotein E-deficient mice.* Lipids Health Dis, 2016. **15**: p. 33.

209. Fujishima, Y., et al., *Adiponectin association with T-cadherin protects against neointima proliferation and atherosclerosis.* FASEB J, 2017. **31**(4): p. 1571-1583.

210. Carlson, L.A., L. Oro, and J. Ostman, *Effect of a single dose of nicotinic acid on plasma lipids in patients with hyperlipoproteinemia.* Acta Med Scand, 1968. **183**(5): p. 457-65.

211. Jin, F.Y., V.S. Kamanna, and M.L. Kashyap, *Niacin accelerates intracellular ApoB degradation by inhibiting triacylglycerol synthesis in human hepatoblastoma (HepG2) cells.* Arterioscler Thromb Vasc Biol, 1999. **19**(4): p. 1051-9.

212. Ganji, S.H., et al., *Niacin noncompetitively inhibits DGAT2 but not DGAT1 activity in HepG2 cells.* J Lipid Res, 2004. **45**(10): p. 1835-45.

213. Ganji, S.H., M.L. Kashyap, and V.S. Kamanna, *Niacin inhibits fat accumulation, oxidative stress, and inflammatory cytokine IL-8 in cultured hepatocytes: Impact on non-alcoholic fatty liver disease.* Metabolism, 2015. **64**(9): p. 982-90.

214. Hernandez, M., S.D. Wright, and T.Q. Cai, *Critical role of cholesterol ester transfer protein in nicotinic acid-mediated HDL elevation in mice.* Biochem Biophys Res Commun, 2007. **355**(4): p. 1075-80.

215. Rubic, T., M. Trottmann, and R.L. Lorenz, *Stimulation of CD36 and the key effector of reverse cholesterol transport ATP-binding cassette A1 in monocytoid cells by niacin.* Biochem Pharmacol, 2004. **67**(3): p. 411-9.

216. Knowles, H.J., et al., *Niacin induces PPARgamma expression and transcriptional activation in macrophages via HM74 and HM74a-mediated induction of prostaglandin synthesis pathways.* Biochem Pharmacol, 2006. **71**(5): p. 646-56.

217. Ganji, S.H., et al., *Therapeutic role of niacin in the prevention and regression of hepatic steatosis in rat model of nonalcoholic fatty liver disease.* Am J Physiol Gastrointest Liver Physiol, 2014. **306**(4): p. G320-7.

218. Hu, M., et al., *Liver fat reduction with niacin is influenced by DGAT-2 polymorphisms in hypertriglyceridemic patients.* J Lipid Res, 2012. **53**(4): p. 802-9.

219. Arauz, J., et al., *Nicotinic acid prevents experimental liver fibrosis by attenuating the prooxidant process.* Int Immunopharmacol, 2015. **28**(1): p. 244-51.

220. Li, Q., et al., *Dietary nicotinic acid supplementation ameliorates chronic alcohol-induced fatty liver in rats.* Alcohol Clin Exp Res, 2014. **38**(7): p. 1982-92.

221. Jadeja, R.N., et al., *Loss of GPR109A/HCAR2 induces aging-associated hepatic steatosis.* Aging (Albany NY), 2019. **11**(2): p. 386-400.

222. Ye, L., et al., *Niacin fine-tunes energy homeostasis through canonical GPR109A signaling.* FASEB J, 2019. **33**(4): p. 4765-4779.

223. Dalton, T.A. and R.S. Berry, *Hepatotoxicity associated with sustained-release niacin.* Am J Med, 1992. **93**(1): p. 102-4.

224. Schaffellner, S., et al., *Niacin-Associated Acute Hepatotoxicity Leading to Emergency Liver Transplantation.* Am J Gastroenterol, 2017. **112**(8): p. 1345-1346.

225. Rader, J.I., R.J. Calvert, and J.N. Hathcock, *Hepatic toxicity of unmodified and time-release preparations of niacin.* Am J Med, 1992. **92**(1): p. 77-81.

226. Durham, S.H., E.W. Covington, and K.J. Clemmons, *Hepatotoxicity upon using niacin to pass a drug test: A case report.* J Am Pharm Assoc (2003), 2018. **58**(5): p. 564-567.

227. Coppola, A., P.G. Brady, and H.J. Nord, *Niacin-induced hepatotoxicity: unusual presentations.* South Med J, 1994. **87**(1): p. 30-2.

228. Leung, K., et al., *Niacin-Induced Anicteric Microvesicular Steatotic Acute Liver Failure.* Hepatol Commun, 2018. **2**(11): p. 1293-1298.

229. Bhardwaj, S.S. and N. Chalasani, *Lipid-lowering agents that cause drug-induced hepatotoxicity.* Clin Liver Dis, 2007. **11**(3): p. 597-613, vii.

230. Gray, D.R., et al., *Efficacy and safety of controlled-release niacin in dyslipoproteinemic veterans.* Ann Intern Med, 1994. **121**(4): p. 252-8.

231. Rikans, L.L., D. Arata, and D.C. Cederquist, *Fatty Livers Produced in Albino Rats by Excess Niacin in High Fat Diets. I. Alterations in Enzyme and Coenzyme Systems Induced by Supplementing 40 Percent Fat Diets with O.1 Percent of Niacin.* J Nutr, 1964. **82**: p. 83-7.

232. Rikans, L.L., D. Arata, and D.C. Cederquist, *Fatty Livers Produced in Albino Rats by Excess Niacin in High Fat Diets. Ii. Effect of Choline Supplements.* J Nutr, 1965. **85**: p. 107-12.

233. Kang-Lee, Y.A., et al., *Metabolic effects of nicotinamide administration in rats.* J Nutr, 1983. **113**(2): p. 215-21.

234. Zhou, S.S., et al., *Dietary methyl-consuming compounds and metabolic syndrome.* Hypertens Res, 2011. **34**(12): p. 1239-45.

235. Thangaraju, M., et al., *GPR109A is a G-protein-coupled receptor for the bacterial fermentation product butyrate and functions as a tumor suppressor in colon.* Cancer Res, 2009. **69**(7): p. 2826-32.

236. Elangovan, S., et al., *The niacin/butyrate receptor GPR109A suppresses mammary tumorigenesis by inhibiting cell survival.* Cancer Res, 2014. **74**(4): p. 1166-78.

237. Singh, N., et al., *Activation of Gpr109a, receptor for niacin and the commensal metabolite butyrate, suppresses colonic inflammation and carcinogenesis.* Immunity, 2014. **40**(1): p. 128-39.

238. Salem, H.A. and W. Wadie, *Effect of Niacin on Inflammation and Angiogenesis in a Murine Model of Ulcerative Colitis.* Sci Rep, 2017. **7**(1): p. 7139.

239. Fangmann, D., et al., *Targeted Microbiome Intervention by Microencapsulated Delayed-Release Niacin Beneficially Affects Insulin Sensitivity in Humans.* Diabetes Care, 2018. **41**(3): p. 398-405.

240. Hankes, L.V., et al., *Effect of Huntington's and Alzheimer's diseases on the transport of nicotinic acid or nicotinamide across the human blood-brain barrier.* Adv Exp Med Biol, 1991. **294**: p. 675-8.

241. Alisky, J.M., *Niacin improved rigidity and bradykinesia in a Parkinson's disease patient but also caused unacceptable nightmares and skin rash--a case report.* Nutr Neurosci, 2005. **8**(5-6): p. 327-9.

242. Wakade, C., et al., *Low-dose niacin supplementation modulates GPR109A, niacin index and ameliorates Parkinson's disease symptoms without side effects.* Clin Case Rep, 2015. **3**(7): p. 635-7.

243. Wakade, C., et al., *Upregulation of GPR109A in Parkinson's disease.* PLoS One, 2014. **9**(10): p. e109818.

244. Wakade, C., et al., *Niacin modulates macrophage polarization in Parkinson's disease.* J Neuroimmunol, 2018. **320**: p. 76-79.

245. Chen, J., et al., *Niaspan treatment increases tumor necrosis factor-alpha-converting enzyme and promotes arteriogenesis after stroke.* J Cereb Blood Flow Metab, 2009. **29**(5): p. 911-20.

246. Chen, J., et al., *Niaspan increases angiogenesis and improves functional recovery after stroke.* Ann Neurol, 2007. **62**(1): p. 49-58.

247. Cui, X., et al., *Niacin treatment of stroke increases synaptic plasticity and axon growth in rats.* Stroke, 2010. **41**(9): p. 2044-9.

248. Shehadah, A., et al., *Niaspan treatment induces neuroprotection after stroke.* Neurobiol Dis, 2010. **40**(1): p. 277-83.

249. Rahman, M., et al., *The beta-hydroxybutyrate receptor HCA2 activates a neuroprotective subset of macrophages.* Nat Commun, 2014. **5**: p. 3944.

250. Gambhir, D., et al., *GPR109A as an anti-inflammatory receptor in retinal pigment epithelial cells and its relevance to diabetic retinopathy.* Invest Ophthalmol Vis Sci, 2012. **53**(4): p. 2208-17.

251. Yu, A.L., et al., *Constitutive expression of HCA(2) in human retina and primary human retinal pigment epithelial cells.* Curr Eye Res, 2014. **39**(5): p. 487-92.

252. Wang, Y. and H. Yan, *MicroRNA-126 contributes to Niaspan treatment induced vascular restoration after diabetic retinopathy.* Sci Rep, 2016. **6**: p. 26909.

253. Cho, K.H., et al., *Niacin ameliorates oxidative stress, inflammation, proteinuria, and hypertension in rats with chronic renal failure.* Am J Physiol Renal Physiol, 2009. **297**(1): p. F106-13.

254. Cho, K.H., et al., *Niacin improves renal lipid metabolism and slows progression in chronic kidney disease.* Biochim Biophys Acta, 2010. **1800**(1): p. 6-15.

255. Kwon, W.Y., et al., *Niacin attenuates lung inflammation and improves survival during sepsis by downregulating the nuclear factor-kappaB pathway.* Crit Care Med, 2011. **39**(2): p. 328-34.

256. Kwon, W.Y., et al., *Niacin and Selenium Attenuate Sepsis-Induced Lung Injury by Up-Regulating Nuclear Factor Erythroid 2-Related Factor 2 Signaling.* Crit Care Med, 2016. **44**(6): p. e370-82.

257. Jeong, K.Y., et al., *The therapeutic effect and mechanism of niacin on acute lung injury in a rat model of hemorrhagic shock: Down-regulation of the reactive oxygen species-dependent nuclear factor kappaB pathway.* J Trauma Acute Care Surg, 2015. **79**(2): p. 247-55.

258. Subramani, K., et al., *Deficiency of metabolite sensing receptor HCA2 impairs the salutary effect of niacin in hemorrhagic shock.* Biochim Biophys Acta Mol Basis Dis, 2019. **1865**(3): p. 688-695.

259. Coleman, D.L. and K.P. Hummel, *The influence of genetic background on the expression of the obese (Ob) gene in the mouse.* Diabetologia, 1973. **9**(4): p. 287-93.

260. Simpson, E.M., et al., *Genetic variation among 129 substrains and its importance for targeted mutagenesis in mice.* Nat Genet, 1997. **16**(1): p. 19-27.

261. Lusis, A.J., J. Yu, and S.S. Wang, *The problem of passenger genes in transgenic mice.* Arterioscler Thromb Vasc Biol, 2007. **27**(10): p. 2100-3.

262. Vanden Berghe, T., et al., *Passenger Mutations Confound Interpretation of All Genetically Modified Congenic Mice.* Immunity, 2015. **43**(1): p. 200-9.

263. Uz, T., et al., *5-lipoxygenase (5LOX)-deficient mice express reduced anxiety-like behavior.* Restor Neurol Neurosci, 2002. **20**(1-2): p. 15-20.

264. Yu, P., et al., *Lack of interleukin-1 signaling results in perturbed early vein graft wall adaptations.* Surgery, 2013. **153**(1): p. 63-9.

265. Schmidt, C., et al., *Proinflammatory cytokines cause down-regulation of renal chloride entry pathways during sepsis.* Crit Care Med, 2007. **35**(9): p. 2110-9.

266. Wang, M., et al., *Mechanisms of sex differences in TNFR2-mediated cardioprotection.* Circulation, 2008. **118**(14 Suppl): p. S38-45.

267. Baracchi, F. and M.R. Opp, *Sleep-wake behavior and responses to sleep deprivation of mice lacking both interleukin-1 beta receptor 1 and tumor necrosis factor-alpha receptor 1.* Brain Behav Immun, 2008. **22**(6): p. 982-93.

268. Sharma, P., et al., *Epithelium-dependent modulation of responsiveness of airways from caveolin-1 knockout mice is mediated through cyclooxygenase-2 and 5-lipoxygenase.* Br J Pharmacol, 2012. **167**(3): p. 548-60.

269. Park, B.N., et al., *In vivo tracking of intravenously injected mesenchymal stem cells in an Alzheimer's animal model.* Cell Transplant, 2018. **27**(8): p. 1203-1209.

270. Stevens, L.M. and R.E. Brown, *Reference and working memory deficits in the 3xTg-AD mouse between 2 and 15-months of age: a cross-sectional study.* Behav Brain Res, 2015. **278**: p. 496-505.

271. Habib, A., et al., *LISPRO mitigates beta-amyloid and associated pathologies in Alzheimer's mice.* Cell Death Dis, 2017. **8**(6): p. e2880.

272. Ishimori, N., et al., *Quantitative trait loci analysis for plasma HDL-cholesterol concentrations and atherosclerosis susceptibility between inbred mouse strains C57BL/6J and 129S1/SvImJ.* Arterioscler Thromb Vasc Biol, 2004. **24**(1): p. 161-6.

273. Ishimori, N., et al., *Quantitative trait loci that determine plasma lipids and obesity in C57BL/6J and 129S1/SvImJ inbred mice.* J Lipid Res, 2004. **45**(9): p. 1624-32.

274. Su, Z., et al., *Candidate genes for obesity revealed from a C57BL/6J x 129S1/SvImJ intercross.* Int J Obes (Lond), 2008. **32**(7): p. 1180-9.

275. Bock, P.M., et al., *Oral supplementations with L-glutamine or L-alanyl-L-glutamine do not change metabolic alterations induced by long-term high-fat diet in the B6.129F2/J mouse model of insulin resistance.* Mol Cell Biochem, 2016. **411**(1-2): p. 351-62.

276. Asgharpour, A., et al., *A diet-induced animal model of non-alcoholic fatty liver disease and hepatocellular cancer.* J Hepatol, 2016. **65**(3): p. 579-88.

277. Konrad, D. and S. Wueest, *The gut-adipose-liver axis in the metabolic syndrome.* Physiology (Bethesda), 2014. **29**(5): p. 304-13.

278. Sun, K., C.M. Kusminski, and P.E. Scherer, *Adipose tissue remodeling and obesity.* J Clin Invest, 2011. **121**(6): p. 2094-101.

279. Crewe, C., Y.A. An, and P.E. Scherer, *The ominous triad of adipose tissue dysfunction: inflammation, fibrosis, and impaired angiogenesis.* J Clin Invest, 2017. **127**(1): p. 74-82.

280. Liu, Q., S. Bengmark, and S. Qu, *The role of hepatic fat accumulation in pathogenesis of non-alcoholic fatty liver disease (NAFLD).* Lipids Health Dis, 2010. **9**: p. 42.

281. Parsons, W.B., Jr., et al., *Changes in concentration of blood lipids following prolonged administration of large doses of nicotinic acid to persons with hypercholesterolemia: preliminary observations.* Proc Staff Meet Mayo Clin, 1956. **31**(13): p. 377-90.

282. Grundy, S.M., et al., *Influence of nicotinic acid on metabolism of cholesterol and triglycerides in man.* J Lipid Res, 1981. **22**(1): p. 24-36.

283. Plaisance, E.P., et al., *Increased total and high-molecular weight adiponectin after extended-release niacin.* Metabolism, 2008. **57**(3): p. 404-9.

284. Almind, K. and C.R. Kahn, *Genetic determinants of energy expenditure and insulin resistance in diet-induced obesity in mice.* Diabetes, 2004. **53**(12): p. 3274-85.

285. Ishimori, N., et al., *Quantitative trait loci that determine BMD in C57BL/6J and 129S1/SvlmJ inbred mice.* Journal of Bone and Mineral Research, 2006. **21**(1): p. 105-112.

286. Pfaffl, M.W., *A new mathematical model for relative quantification in real-time RT–PCR.* Nucleic Acids Research, 2001. **29**(9): p. e45.

287. Liang, W., et al., *Establishment of a general NAFLD scoring system for rodent models and comparison to human liver pathology.* PLoS One, 2014. **9**(12): p. e115922.

288. van Beek, L., et al., *The limited storage capacity of gonadal adipose tissue directs the development of metabolic disorders in male C57Bl/6J mice.* Diabetologia, 2015. **58**(7): p. 1601-9.

289. Strissel, K.J., et al., *Adipocyte death, adipose tissue remodeling, and obesity complications.* Diabetes, 2007. **56**(12): p. 2910-8.

290. Fjaere, E., et al., *Indomethacin treatment prevents high fat diet-induced obesity and insulin resistance but not glucose intolerance in C57BL/6J mice.* J Biol Chem, 2014. **289**(23): p. 16032-45.

291. Bullen, J.W., Jr., et al., *Regulation of adiponectin and its receptors in response to development of diet-induced obesity in mice.* Am J Physiol Endocrinol Metab, 2007. **292**(4): p. E1079-86.

292. Menon, R.M., et al., *Effect of the rate of niacin administration on the plasma and urine pharmacokinetics of niacin and its metabolites.* J Clin Pharmacol, 2007. **47**(6): p. 681-8.

293. Zheng, Y., et al., *B Vitamins Can Reduce Body Weight Gain by Increasing Metabolism-related Enzyme Activities in Rats Fed on a High-Fat Diet.* Curr Med Sci, 2018. **38**(1): p. 174-183.

294. Graff, E.C., et al., *Anti-inflammatory effects of the hydroxycarboxylic acid receptor 2.* Metabolism, 2016. **65**(2): p. 102-113.

295. Jaus, H., et al., *Metabolic effects and liver damage after prolonged administration of high doses of nicotinamide to rats.* Nutr Metab, 1977. **21 Suppl 1**: p. 38-41.

296. Knip, M., et al., *Safety of high-dose nicotinamide: a review.* Diabetologia, 2000. **43**(11): p. 1337-45.

297. Tryndyak, V., et al., *Interstrain differences in the severity of liver injury induced by a choline- and folate-deficient diet in mice are associated with dysregulation of genes involved in lipid metabolism.* FASEB J, 2012. **26**(11): p. 4592-602.

298. Pogribny, I.P., et al., *Strain-dependent dysregulation of one-carbon metabolism in male mice is associated with choline- and folate-deficient diet-induced liver injury.* FASEB J, 2013. **27**(6): p. 2233-43.

299. Folch, J., M. Lees, and G.H. Sloane Stanley, *A simple method for the isolation and purification of total lipides from animal tissues.* J Biol Chem, 1957. **226**(1): p. 497-509.

300. Bligh, E.G. and W.J. Dyer, *A rapid method of total lipid extraction and purification.* Can J Biochem Physiol, 1959. **37**(8): p. 911-7.

301. Matyash, V., et al., *Lipid extraction by methyl-tert-butyl ether for high-throughput lipidomics.* J Lipid Res, 2008. **49**(5): p. 1137-46.

302. Yuan, M., et al., *A positive/negative ion-switching, targeted mass spectrometry-based metabolomics platform for bodily fluids, cells, and fresh and fixed tissue.* Nat Protoc, 2012. **7**(5): p. 872-81.

303. Breitkopf, S.B., et al., *A relative quantitative positive/negative ion switching method for untargeted lipidomics via high resolution LC-MS/MS from any biological source.* Metabolomics, 2017. **13**(3).

304. Cotoia, A., et al., *p-Hydroxyphenylpyruvate, an intermediate of the Phe/Tyr catabolism, improves mitochondrial oxidative metabolism under stressing conditions and prolongs survival in rats subjected to profound hemorrhagic shock.* PLoS One, 2014. **9**(3): p. e90917.

305. Jobgen, W., et al., *High fat feeding and dietary L-arginine supplementation differentially regulate gene expression in rat white adipose tissue.* Amino Acids, 2009. **37**(1): p. 187-98.

306. Jobgen, W., et al., *Dietary L-arginine supplementation reduces white fat gain and enhances skeletal muscle and brown fat masses in diet-induced obese rats.* J Nutr, 2009. **139**(2): p. 230-7.

307. Dunn, M.F., *Key roles of microsymbiont amino acid metabolism in rhizobia-legume interactions.* Crit Rev Microbiol, 2015. **41**(4): p. 411-51.

308. Wang, Y. and S. Hekimi, *Understanding Ubiquinone.* Trends Cell Biol, 2016. **26**(5): p. 367-378.

309. Puri, P., et al., *A lipidomic analysis of nonalcoholic fatty liver disease.* Hepatology, 2007. **46**(4): p. 1081-90.

310. Ter Horst, K.W., et al., *Hepatic Diacylglycerol-Associated Protein Kinase Cepsilon Translocation Links Hepatic Steatosis to Hepatic Insulin Resistance in Humans.* Cell Rep, 2017. **19**(10): p. 1997-2004.

311. Julius, U., *Niacin as antidyslipidemic drug.* Can J Physiol Pharmacol, 2015. **93**(12): p. 1043-54.

312. Fengler, V.H., et al., *Susceptibility of Different Mouse Wild Type Strains to Develop Diet-Induced NAFLD/AFLD-Associated Liver Disease.* PLoS One, 2016. **11**(5): p. e0155163.

313. Wu, G.D., et al., *Linking long-term dietary patterns with gut microbial enterotypes.* Science, 2011. **334**(6052): p. 105-8.

314. Jiang, T., et al., *Apple-Derived Pectin Modulates Gut Microbiota, Improves Gut Barrier Function, and Attenuates Metabolic Endotoxemia in Rats with Diet-Induced Obesity.* Nutrients, 2016. **8**(3): p. 126.

315. Hegyi, J., R.A. Schwartz, and V. Hegyi, *Pellagra: dermatitis, dementia, and diarrhea.* Int J Dermatol, 2004. **43**(1): p. 1-5.

316. Jobin, C., *GPR109a: the missing link between microbiome and good health?* Immunity, 2014. **40**(1): p. 8-10.

317. Nishino, R., et al., *Commensal microbiota modulate murine behaviors in a strictly contamination-free environment confirmed by culture-based methods.* Neurogastroenterol Motil, 2013. **25**(6): p. 521-8.

318. Sudo, N., et al., *Postnatal microbial colonization programs the hypothalamic-pituitary-adrenal system for stress response in mice.* J Physiol, 2004. **558**(Pt 1): p. 263-75.

319. Benno, Y. and T. Mitsuoka, *Impact of Bifidobacterium longum on human fecal microflora.* Microbiol Immunol, 1992. **36**(7): p. 683-94.

320. Trevizan, A.R., et al., *Kinetics of acute infection with Toxoplasma gondii and histopathological changes in the duodenum of rats.* Exp Parasitol, 2016. **165**: p. 22-9.

321. Di Sabatino, A., et al., *Distribution, proliferation, and function of Paneth cells in uncomplicated and complicated adult celiac disease.* Am J Clin Pathol, 2008. **130**(1): p. 34-42.

322. Vainrub, A., O. Pustovyy, and V. Vodyanoy, *Resolution of 90 nm (lambda/5) in an optical transmission microscope with an annular condenser.* Opt Lett, 2006. **31**(19): p. 2855-7.

323. Eun, C.S., et al., *Induction of bacterial antigen-specific colitis by a simplified human microbiota consortium in gnotobiotic interleukin-10-/- mice.* Infect Immun, 2014. **82**(6): p. 2239-46.

324. Armougom, F., et al., *Monitoring bacterial community of human gut microbiota reveals an increase in Lactobacillus in obese patients and Methanogens in anorexic patients.* PLoS One, 2009. **4**(9): p. e7125.

325. Sugimoto, K., et al., *IL-22 ameliorates intestinal inflammation in a mouse model of ulcerative colitis.* J Clin Invest, 2008. **118**(2): p. 534-44.